QATAR UNIVERSITY

COLLEGE OF ARTS AND SCIENCES

FABRICATION OF NANO-COMPOSITE MEMBRANE FOR FO DESALINATION

BY

HAMMADUR RAHMAN SIDDIQUI

A Thesis Submitted to

the College of Arts and Sciences

in Partial Fulfillment of the Requirements for the Degree of

Master of Science in Material Science and Technology

June 2021

COMMITTEE PAGE

The members of the Committee approve the Thesis of
Hammadur Rahman Siddiqui defended on 17/04/2020

Prof. Igor Krupa
Thesis/Dissertation Supervisor

Prof. Syed Javaid Zaidi
Thesis Co-Supervisor

Dr. Alaa Alhawari
Committee Member

Approved:

Ibrahim AlKaabi, Dean, College of Arts and Sciences

ABSTRACT

SIDDIQUI, HAMMAD .R, Masters : June : 2021, Material Science and Technology

Title: Fabrication of Nano-composite membrane for FO desalination

Supervisor of Thesis: Prof. Igor Krupa; Thesis Co-Supervisor: Prof. Syed Javaid Zaidi.

The aim of this work is to solve the current issues experienced in forward osmosis (FO) membranes such as low water flux, membrane fouling, and high reverse solute flux (RSF). We also propose a novel technique to eradicate the problems faced with electrospinning technique for the fabrication of nanofibers (NFB). Polysulfone (PSF) and polyethersulfone (PES) are used to fabricate highly porous FO NFB membrane with enhanced water flux and minimal RSF value. In this study, NFB are produced by a novel solution blow spinning (SBS) technique. These fabricated NFB are tested for the FO process and further modified by interfacial polymerization (IP) technique to deposit polyamide (PA) layer incorporating nanomaterial (graphene oxide)

The structure and morphology of the NFB are characterized using (SEM), (AFM), Contact angle measurement, (FTIR) and (XRD) studies. These techniques confirmed the changes in the membrane morphology, formation of PA layer and presence of graphene oxide (GO) in it.

The novelty of this work is the use of solution blown spinning technique for the NFB membrane production, which has not been reported for use in membrane-based desalination. NFB formed using this technique showed considerable enhancement in water flux and decreased RSF. In addition, the prepared NFB membrane after the heat-pressing post treatment exhibited good mechanical strength with an improvement in young's modulus almost three to four times. The FO performance of the nanofiber membrane showed a significant increase in flux of almost two-fold, while having minimal RSF values below 0.2 g/m^2h.

DEDICATION

This Thesis is Dedicated to my father Dr. Siddiqui Ataur Rahman for unprecedented support he provided and to encouraging me to believe in my self.

ACKNOWLEDGMENTS

My sincere gratitude goes first to my supervisors Prof .Syed Javaid Zaidi and Prof. Igor Krupa for their support and guidance throughout my graduate education and thesis work. I would also like to thank my other committee member Dr. Alaa Alhawari their advice and assistance provided.

I would like to thank my colleagues and lab technicians at the Center for Advanced Materials, for their genuine kindness, constant encouragement, lighting my passion for research and for constant support during trouble shooting the experimental setup.

In addition My deep sincere thanks goes to Mrs. Haleema Saleem for her help and utmost support during my thesis work. I am also thankful to Nada AbouNahia for help in experimental data collection. I also thank the faculty members of Material Science and Technology program at Qatar University for building my understanding of materials and expanding my knowledge in the field ,which significantly helped me build and trouble shoot experimental lab setup

Finally, I am grateful to my parents for their constant encouragement, love and unconditional support throughout my.

TABLE OF CONTENTS

LIST OF TABLES

LIST OF FIGURES

CHAPTER 1: INTRODUCTION.

1.1 Global water scarcity

The most persistent problem affecting almost one-third of the world's total population (7.9 billion) is inadequate access to clean water. Clean drinking water and sanitation are considered to be fundamental to the realization of human rights. Access to clean water for all is key towards the sustainable development. There is nothing more essential than water to life on earth. There is a scarcity of safe water even in countries possessing enough natural resources. While nearly 70 % of the world is covered by water, just 2.5 % of it is fresh. The remaining is saline as well as ocean-based. Moreover, just 1 % of the freshwater is simply accessible, with much of it trapped in snowfields and glaciers. The major water resource, i.e., seawater (approximately 97%) is not fit for human consumption because of the high salinity. In recent years, water crisis has become a serious global problem due to fast population growth, rapid industrialization, global warming, and damage to available freshwater resources. The foretasted factors will make water sources such as surface water and some subsurface water harder to access for the people. The rate of water consumption will continue to rise in the coming decades. More than one-third of the population currently faces the challenge of water scarcity. According to a report by the United Nations (UN) and the World Health Organization(WHO) in 2017, about 2.6 billion people from the global population (7.5 billion) have no access to clean drinking water, and almost 1.7 million people are sick every year because of diarrheal diseases due to drinking unclean water (World Health Organization, 2018). This population number will likely double by the year 2025 [1]. Additionally, 66% of the global population faces extreme water scarcity for a minimum of one month per year [2]. Statistics illustrate that conventional water sources such as rain, snowmelt, and groundwater are no longer adequate in water-

stressed regions. Credible predictions say that the global water supply will grow almost 40% in the amount that is currently available by 2030, which means a notable rise in demand [3]. Although substantial progress has been made, there are still many ways to improve, water status, sanitation and hygiene for the current global population. Scarcity of fresh water and rising water needs are stressing the development of low-cost and environmentally friendly technologies.

1.2 Desalination

Saline water desalination is the process of removing salts from seawater to meet the requirements for human uses. Desalination has become a popular in both arid and humid regions of the world because of increased water stress around the globe. Seawater desalination provides a "unlimited climate-independent and steady supply of high-quality water". Desalination and water reuse can increase the water supply while not negatively affecting the freshwater ecosystems. As per the present desalination estimates, there are almost 1,590 desalination plants operational, located in 177 countries and territories across all major regions of the world. Currently, the amount of water desalination has been reported to have reached 95 million m^3d^{-1} of which the Middle East and Africa (MENA) region contributes to a 48 percent share of global water production [4].

Desalination basically means separation of the salts from sea water to get two streams one with high concentration of salts and other pure water fit for domestic and industrial use. To achieve the separation of sea water into two stream some form of energy is required for separation. A variety of technologies are available to achieve the separation depending upon the type of feed water intake and salinity of water. Desalination can be done either in seawater or inland brackish water. Since it is still the same level of salinity, desalination of seawater supplies a dependable and sufficient source of high-quality water. The salinity of the Arabian Sea varies widely, being

between 40,000 and 50,000 parts per million (ppm). As governments in GCC countries have abundant fossil fuel resources, about 97% of the water demand is fulfilled by desalination. The most successful desalination processes used commercially in the GCC region are multi stage flash distillation and reverse osmosis. Initially multi-stage flash distillation (MSF) was used due the availability of low cost fuel and high salinity of feed water of the region. Recently reverse osmosis is replacing the MSF due to lower cost of production, simple design, environment friendly, ease of maintenance and modular nature.

1.2.1Forward Osmosis

Forward osmosis (FO) is known to be a normal physical process and is the transport of water through a selectively permeable membrane forced by osmotic pressure variation over a membrane. Forward osmosis happens naturally by the physical process of diffusion through semipermeable membrane. This method works when two liquids of different concentrations are on either side of the semipermeable membrane which permits passage of water molecules leaving the salt behind. As there is difference of concentration separated by membrane, it causes a distinctive osmotic pressure which forces flow from higher concentration (draw solution) to the region of low concentration (feed concentration). This flow continues till the concentration on either side of the membrane becomes equal. The FO membrane allows only water molecules to pass through it, while at the same time discarding the movement of other molecules or ions.

Over the last few years, FO has gained popularity for a number of potential applications in industries like power generation, wastewater treatment and a stand-alone process for desalination of seawater with a promising future [9].

1.3 RESEARCH QUESTIONS AND WORKING HYPOTHESIS

1.3.1 RESEARCH OBJECTIVES:

The main goal of the proposed thesis is to identify the benefit of using nanomaterial on the FO membrane for FO seawater desalination. This can be achieved by improving the membrane properties by enhancing its strength to withstand fouling and improving the salt rejection with specific salt rejection capabilities depending on the feed water. The thesis aims to effectively produce new modified/fabricated membrane with enhanced permeability, salt rejection properties. This will subsequently help to increase the life of the membrane. Some of the nanomaterials will be synthesized and some commercially available nanoparticles will be used after proper optimization. Modifications will be done on a support layer, which is a polysulfone sheet, and also on commercially available membranes by using electrospinning and interfacial polymerization techniques.

However, the proposed FO membrane have not been fabricated using the Solution blow spining technique with addition of nanoparticle, adding a layer of novelty through fabrication and studying the effect of nanoparticles on the membrane over time. Hence it will also be first study using this technique and will be a unique study for using with high TDS condition for Qatar seawater. The following are the research objectives of the thesis:

- To design and fabricate a nanocomposite membrane for FO desalination process.
- To optimize and select the ideal conditions for each of the nanofiber membranes used and for modifying the commercial membrane and fabricate membrane using the polysulfide as support layer by changing the process

- Characterization of membrane to study and compare the effect of modification on the membrane surface through studying the molecular and structural parameters of the membrane, including membrane functional groups, surface roughness, contact angle, and morphology.

- Study the mechanical properties of these membranes using and Tensile testing to study the strength of pure nano fiber and after modification also

- Bench scale experiments are performed on these membranes to mainly study the performance under the different operating conditions.

- To study the effect of various parameters, such as flow rate and conductivity, on the performance of membranes.

- Study the power consumption shift in running an experimental batch on each membrane set

1.4 Thesis Structure

The first part of this dissertation focuses on giving a general overview of water scarcity issues its importance. This chapter also briefly discusses on water purification techniques, current membrane-based desalination technologies available which are in use around the world and lastly focus on reverse osmosis and the shift to forward osmosis, along with its challenges which will be addressed in this research study. The second chapter discuss on the Qatar and its global presence in water desalination and shows its past present and future. This chapter also shows the current trends around the GCC and show various trends that highlight the shift from more energy intensive thermal-based technologies to more green membrane-based technologies. In the third chapter, a comprehensive review of forward osmosis and the related issues, along with different membrane fabrication techniques are presented. This chapter also explains the overall use of nanomaterials in the polymer-based FO membranes. The fourth chapter in this thesis explains about methods and materials that were used to successfully set up the FO bench and test the system. Testing procedures and characterization techniques on various membranes are discussed. In chapter 5, the results of each system; and various membranes and its related performances are explained in depth and relationships are drawn to give a full picture of the water quality obtained by using solution blow spinning and hot pressed membranes. Lastly, conclusions on the work are presented with recommendations for future work.

Chapter 2: Qatar Seawater Desalination past present and future

This is part is a Published Article.

2.1 Abstract

The world depends on water to sustain life and cater to development. Gulf region is among the most arid environments of the world with no natural water resource, minimum to no rainfall. Complete water requirement is fulfilled by seawater desalination. With increasing urbanization, population growth and increase in standard of living increases the requirement of clean water dramatically. In this paper review the current status and shift of trend in seawater desalination will be discussed about Qatar with reference to the Gulf countries. Qatar is blessed with unprecedented natural gas and oil reserves and the least amount of water available per capita and highest per capita CO2 emission . Water desalination and clean water has been identified as one of the major challenges in Vison 2030. As Qatar economy is based on seawater desalination to overcome the water shortages, reduce the carbon footprint, preparation for 2022 FIFA world cup while achieving the goal of vision 2030 Qatar is shifting from the energy-intensive convention thermal desalination process to a much cleaner greener membrane process for seawater desalination

Keywords:-Thermal desalination, reverse osmosis, shift of trend in desalination , seawater desalination , Qatar water problem ,Qatar vison 2030, Qatar

2.2 Introduction

The most pervasive problem afflicting almost one third of the world's 7 billion population is inadequate access to clean water. The rate of water consumption will continue to rise in the coming decades. Having access to clean water is a global problem even in countries, which are rich in natural water resources. With current unstable price of crude oil the cost of clean water is also on the rise. Clean water is much more

important than all other natural resources. water is essential element to sustain life and cater advancement of a country. Oceans are the most abundant resource of water as earth's surface covering almost 75% area. Out of which 97% is unfit for drinking due to high salinity. In the remaining 3% almost 70 % is frozen in ice glaciers, the remaining 28% of the tiny 3 % is fresh deep underground water which is not accessible or not feasible in some cases. All the fresh water aquifers, lakes, rivers make up 2% of tiny 3 %. Water is the commodity that governs the life of people and sustainability, advancement that can be achieved by a community, this is proved by a fact that all major civilization were developed within 100 km of large water bodies. Majority of those still face water scarcity today in some form depending upon the topographical location, population and environment . In the Asian countries it is mainly due to the misuse of water resources, improper recycling of wastewater, government polices etc.. Where as in the Gulf cooperation council (GCC) consisting of six countries " Qatar, Oman, Kuwait, Bahrain, Saudi, UAE" it is due to the fact that this region is an arid desert land with little to no natural clean water .The whole Gulf region has little to no underground water resources. There are few water resources that concentrated in Oman and south cost of Saudia.[10] Gulf region has an average rainfall of 75 ppm with an evaporation rate of over 3000 ppm which offset the requirement. The salinity of seawater of the Arabian peninsula is significantly higher than other parts of the world with total dissolved solids (TDS) ranging from 40000 to50000 ppm[11].Due to this alarming level of water scarcity the governments of GCC countries with rich reserve of fosil fuels have turned toward desalination of seawater [12] to fulfil their water needs. Most of the water requirement in the gulf region, almost 99%, is fulfilled by sea water desalination. The Gulf region accounts for more than 60 % of the global desalination capacity. The desalination in gulf region is mainly based upon thermal and reverse

osmosis technologies.

The ease of access of saline water through Arabian sea for desalination of sea water prompted the gulf countries setting up water desalination industries along the coast of the Arabian gulf. As a resulted all the desalination plants are located in close proximity to each other, which has increased water salinity of the region due to brine disposal and lead to various environmental problems. The location of desalination plants in the Arabian Peninsula are depicted in Figure 1.

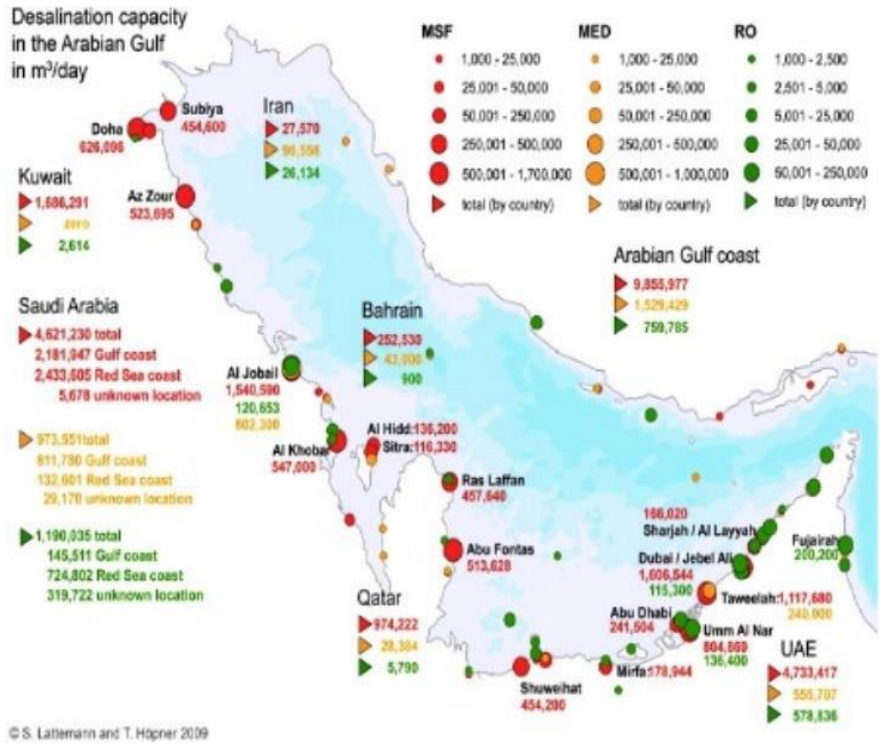

Figure 1 desalination plants in the Arabian gulf[13]

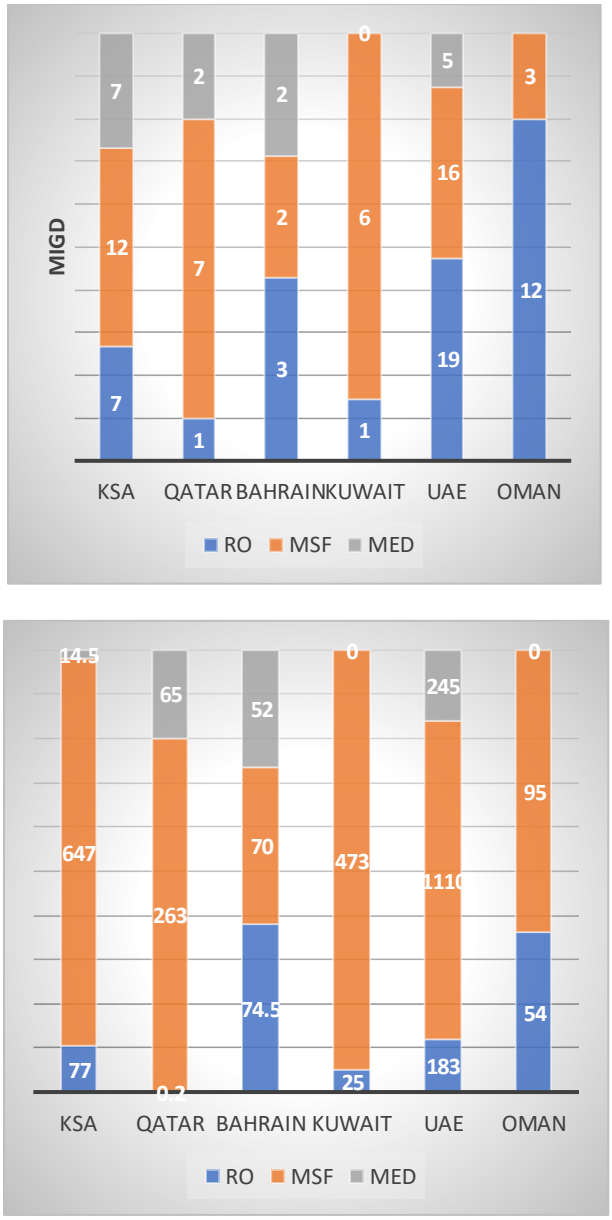

Figure 2 (a) Number of Desalination Plants in the Gulf (b)Desalination capacity of existing plants

Desalination of seawater was first introduced in the year 1950s in Kuwait followed by Qatar in 1955. In the early years of seawater desalination the plants setup and installed were completely based on the thermal desalination process untill1970 [14].figure 2 shows the total number of major desalination plants in GCC and their overall production capacity . Qatar population in the early 2000s was around 0.5 million and by the end

of 2012 the population increased more than three times reaching 2 million and has crossed 2.6 million by June of 2018 and is predicted to reach 4 million by the year 2030. This exponential increase in population increases the requirement for clean water for domestic and industrial use. Moreover, the massive infrastructure developments in Qatar and higher standards of living are increasing the demands of clean water. Also, environmental concerns of CO2 emissions as a result of use of hydrocarbon resources in the thermal desalination process and their cost effectiveness make the thermal desalination process not an ideal one. Taking these factors into account the GCC governments are shifting to reverse osmosis seawater desalination [15-17]

This paper reviews the past present and future of Qatar's sea water desalination technology. The two important commercial processes, which are used to desalinate seawater for water supply in Qatar are based on thermal process, such as multi stage flash (MSF) distillation and multi-effect distillation (MED), and membrane based process such as reverse osmosis technology

2.3 Technologies

Desalination basically means separation of the salts from sea water to get two streams one with high concentration of salts and other pure water fit for domestic and industrial use. To achieve the separation of sea water into two stream some form of energy is required for separation. A variety of technologies are available to achieve the separation depending upon the type of feed water intake and salinity of water like MSF, MED ,RO. The most successful desalination processes used commercially in the GCC region are multi stage flash distillation and reverse osmosis. Initially MSF was used due the availability of low cost fuel and high salinity of feed water of the region . Recently reverse osmosis is replacing the MSF due to lower cost of production, simple design, environment friendly, ease of maintenance and modular nature. Both the technologies are presently used in Qatar and are explained below.

2.3 Multi stage flash distillation

The first flash evaporation system was built in 1957 in Kuwait with a capacity of 1 MIGD followed by Qatar in1960 with a capacity 1.5 MIGD in 1962 . First plant of other GCC countries are summarized in table 1.

Table 1 MSF plant start date in GCC[5]

Country	Date	Plant name	Capacity MIGD
Qatar	1962	Ras Abu Abood	1.5
Oman	1976	Al Ghabra Massira	5
Kuwait	1960	Shuwaika E1 & E2	2
Bahrain	1975	Sitgra a & b	5
UAE	1977	Abu Dhabi vapour plant	15
KSA	1967	Al Dhaba	0.8

The multi-stage flash distillation desalination system involves phase change. It works by the phenomenon of boiling sea water under pressure lower than the atmospheric pressure. The steam from the boiled water is pure which is condensed to get pure drinking water. This boiling of seawater under 100^{o}C is known as flashing technique used in multi stage flash distillation columns[11, 18]. The MSF process is made economical by using it simultaneously with power generation plants, the MSF process consist of heat input, heat recovery and heat rejection units.

Sea water is heated under low-pressure brine heater in which steam is externally supplied. seawater flows on the tube side of the heat exchanger. The heated sea water then flows into the flash evaporator section containing multiple stages with temperature ranging from 90-120^{o} C depending upon the feed water quality and type of pre-treatment done. Operating plant at 120^{o} C increases efficiency but it also increases

corrosion and chances of scale formation. At each stage the vacuum is increased making more pure water evaporate at lower temperature. The water evaporated comes in contact with cold condenser tubes, which condenses and forms pure water. At each stage the concentration of brine is increased as the water is being vaporised. At the end concentrated brine is discharged from the process .

2.4 Reverse osmosis

Reverse osmosis desalination is a physical process which work on the movement of water from area of high level of concentration to a area with low concentration. It is the reverse of the osmosis process. This movement happens through a special type of barrier called semi preamble membrane, which allows the flow of water and restricts the salts. Under the influence of a pressure higher than the osmotic pressure to the side with higher salinity.In this process there is no need for phase sepration or heating. The energy required in this process is only used to power the high-pressure centrifugal pumps. The amount of pressure required depends on the salinity of the feed water, temperature,. Major component of reverse osmosis sea water desalination process are as follows

- pre-treatment
- high pressure pumps
- membrane separation
- post treatment .

Raw sea water is intillay fileterd travelling through screens to remove large derbis. Further the sea water is taken in to multi media gravity filter media which has slica, sand and granite as media. This helps to remove the suspended solid in the sea water intake. In Qatar dissolved air folatiatiion is used to increse contact time by dispersion of bubbles to enhances removal of algae ,oil ,other polymerics substances of low

density that float and cannot be seperated by sedmentation. Finally the sea water is drwan into cartige filter which remove particels that are larger than 10 miconrs .

Pretreatmment is needed to eliminate the undersiralbe constitunets in sea water which will lead to membrane fouling. This is required to clear the feed water of possible foulant or scalant causing minerals and make it suitable for membrane filtration. The type of pre-treatment used directly depends upon the quality feed water intake.

High pressure pumps are used to pump the pre-treated seawater up to the required pressure by reverse osmosis membrane to achieve the desired separation of feed water into pure water and concentrated brine streams. For this application, centrifugal pumps are used, which operate in the range of 50-80 bar. The membrane modules are arranged in spiral wound configuration. As the process operates at ambient temperature and the material of construction of membrane is non corrosive. the scale formation is close to zero in reverse osmosis process.[19]

In the last section after the membrane filtration units, water goes for post treatment. To normalize water for domestic use by stabilizing the alkalinity by adding calcium hydroxide with 30-40 ppm chlorine is added to safeguard water from microorganism during storage and transportation. Finally water flows through decarbonization system to maintain the PH of water [18, 20]

Table 2First RO plants in Gulf**[14]**

Country	**Date**
Qatar	1982
Oman	1982
Kuwait	1987
Bahrain	1984
UAE	1977
KSA	1968

2.5 SHIFT OF TREND IN DESALINATION

The size of thermal plants are quite large with its main material of construction as steel which is prone to corrosion under heating and low pressure conditions continuously. Scales are formed as Mg and Ca salts and forms layer on the inner walls of the heat exchangers, which reduces plant efficiency significantly. The MSF plant consumes a huge amount of energy with total consumed equivalent mechanical energy of 20 kwh/m^3 of desalinated water . The Average estimated cost of 1kwh of mechanical work estimated to 0.11 dollars, then the energy cost to produce 1m^3 of desalinated water is equal to 2.2 dollars for MSF system .which is excepted to increase as the fuel prices are increasing globally.

Apart from the cost, large size of the plant ,troubleshooting problems , plant operation shutdown, cleaning and maintenance ,harmful CO^2 emissions ,high temperature of concentrated brine discharged into the sea, disrupting the marine eco system[21], all of them make the plant more costly[22]. Due to these factors most of the new plants commissioned or planned for sea water desalination in the recent years in Qatar and the Gulf region are based on reverse osmosis process technology as the total energy equivalent required in terms of mechanical energy is equal to 5 kwh/m^3 . Cost of which is equal to 0.55 dollar per m^3 (estimated 1 kwh work equals 0.11 dollar) of desalinated water, which is significantly less as compared to MSF plant and Reverse osmosis plant pre 2000 of similar desalinated water capacity[23]. The reason behind such huge price gap is SWRO doesn't require heating and condensing , the only main energy consumption is by the pump and over the years due to the development of highly efficient membranes that can operate longer duration before a need of cleaning and replacement , the centrifugal pumps used today use significantly less energy while having higher output then before and use of energy recovery devices which are attached

to the outlet of concentrated brine stream which is coming from the membrane unit .The brine only losses the applied pressure very slightly (1-4 bar of the applied pressure from the high pressure pump). this high pressure brine stream is directed to a turbine and which rotates to produce power used in powering the pre-treatment process [17]

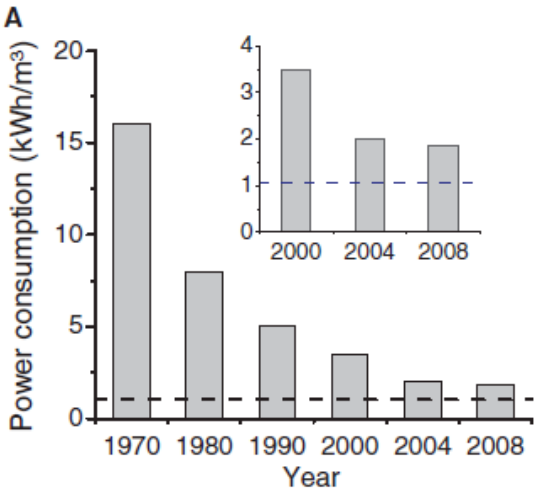

Figure 3 (a) change in power consumption Ro stage of SWRO plants from 1970 to 2008.

The dashed lines is theoretical minimum energy required for desalination at 50 % recovery (values excluding energy required for intake, pre-treatment and post treatment) (a) change in power consumption Ro stage of SWRO plants from 1970 to 2008.the dashed lines is theoretical minimum energy required for desalination at 50 % recovery (values excluding energy required for intake, pre-treatment and post treatment)the size of a typical RO plant is almost 70% percent smaller than a typical MSF plant of same capacity. The reverse osmosis plant has a modular design in the form of horizontal or vertical stack of membrane called as RO trains attached in series or parallel which are generally made up of a material which is non corrosive to sea water due to which it requires very less shutdown and maintenance operation can be

done while the plant is online, the only energy consumed in RO is by the pump with all the above factors reducing the cost of setting up and operation of plant has turned QATAR and other GCC countries government to shift to reverse osmosis plant for its new projects [14]

2.6 QATAR PAST PRESENT AND FUTURE

The first sea water desalination plant in Qatar was established in the year 1953 based on submerged tube process with a capacity of 682 m^3/day. The second plant was set up in the year 1962 at Ras abu Abood based upon the commercially successful multi stage flash distillation process (MSF) with a capacity of 1.5 MIGD .The third plant was established in 1977 at Ras Abu Fantas which was also based upon MSF .The fourth plant was built at Abu Samra in the year 1982 based on a new reverse osmosis technology with a capacity of 909 m^3 per day .The fifth major desalination plant was set up in the year 2016 at Ras AbuFantas based upon the reverse osmosis

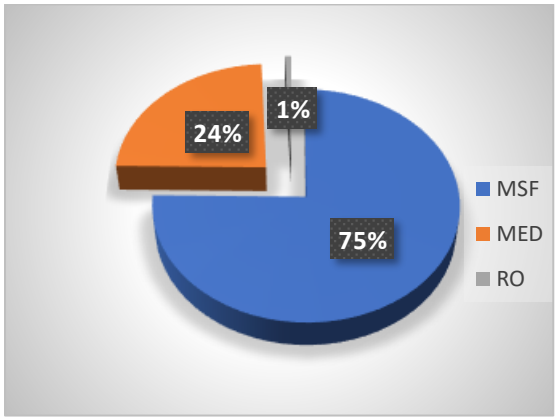

Figure 4 Overall capacity of Qatar sea water desalination up to 2010,

sea water desalination. The sixth and the latest plant is set up at Umm Al Houl with a capacity of 136 MIGD, Out if which 60 MIGD is achieved using reverse osmosis process and the remaining 76 MIGD is achieved by a hybrid MSF co power

generation plant . Commissioning of all the desalination plant in Qatar along with the capacity and technology used are summarized in table 3 and figure 4 shows the overall percent share of each desalination technology used in Qatar .

Table 3 Desalinization plants of Qatar [14]

Plant	**Capacity (MIGD)**	**Technology**	**Commissioning year**
Ras Abu Fantas	55	MSF	(1997-1983)(1994)
Ras Abu Fantas b	33	MSF	1977-1998
Ras Laffana	40	MSF	2003-2004
Ras Laffan-b Qatar power	60	MSF	2006-2008
Abu Samra	0.2	RO	1982
Qaeedat al Shamal	0.2	MSF	1993
Ras Abu Fantas A1	45	MSF	2010
Ras Abu Fantas B2	30	MSF	2008
Ras Qertas	63	MED	2010-2011
Dukan	2	MED	1997
Ras Abu Fantas A3	36	RO	2016
Umm al houl	60	RO	2016-2017
	76	MSF	
Total	500		

As reported by Qatar statistics authority the population of Qatar as of June 2018 was 2.6 million. This compared to 1.15 million population in 2008 ,which is more than 2 times in the last 10 years and this compared to 0.5 million population in the year 2000 which has almost increased by 4 times the last 18 years .which is represented in figure 5.

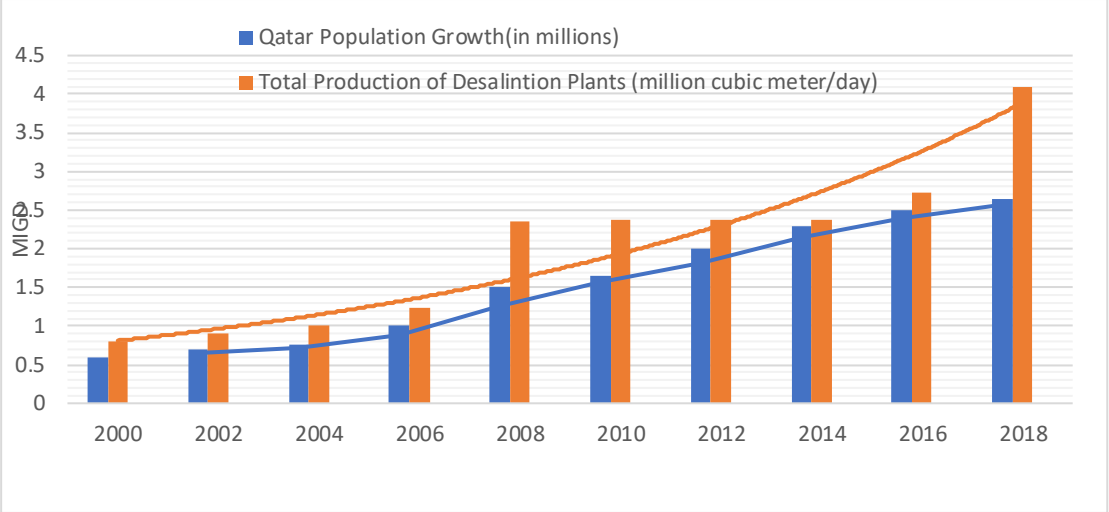

Figure 5 increase in water demand with respect to Qatar population growth

The prime goal of Qatar vison 2030 is to have a sustainable development in the present to have a better tomorrow for future generations. Which can be achieved by reducing the use of hydrocarbon by shifting to energy efficient processes with less CO_2 emissions. while having minimal impact on the environment and marine eco-system. One of the major grand challenge of Qatar vison 2030 is producing and providing safe drinking water while keeping the water production under the guidelines of vison 2030 .Qatar is a an arid country with limited to no underground water with severe lack in rainfall of only 82 mm/year and evaporation rate of 2000mm/year. .As a result of which Qatar falls below the international water poverty line of 1000 m^3 per capita per year .

The fast economic growth, rapid agricultural growth, social development, current fast track licensing and tax free set up for new upcoming industries leading to alluring job opportunities along with a tax free salary, boom in local farming as an outbreak of ongoing illegal siege on the country. Due all these reasons the Qatar population is increasing exponentially and is expected to increase up to 4.4 million by 2030. This increases the water and energy demand and puts pressure on country's water and energy resources due to which the nonconventional production of desalinated water is

to be expanded to support the demand for the current development and be prepared for future requirement due to which two new plant are set up. One in "Rs Abu Fantas 3" with a capacity of 36 MIGD and the second in "Umm Al Houl" plant with a total capacity of 136 MIGD out of which 60 MIGD is based on reverse osmosis sea water desalination and other 73 MIGD is based on thermal plant integrated with power generation technology .With the new RO plant commissioned the overall share of RO has increased drastically as shown in figure 6 .Both of these plants are cost effective as they use way less energy, have zero CO_2 emissions, with easy maintenances, which aligns with the guidelines in achieving of vision 2030 successfully and beyond [10, 18, 23-25].

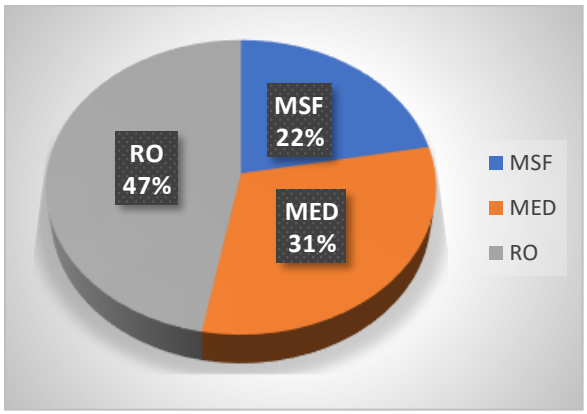

Figure 6 Expected Qatar sweater desalination 2016-2022

2.7 Future Prospects

currently all the GCC countries are in a process to modify their existing plant or completely replace them by Reverse osmosis processes plant. More and more funds are allotted to research and development of sea water desalination technology as the whole region is dependent of desalinated water. As a result of which sea water desalination technology is getting better by various new emerging technologies which can complement, improve the current MSF and RO process, while other emerging

technology can completely replace the existing technologies and reduce the cost of production further figure 7 depicts the overall increases in the number of upcoming major desalination plants in GCC and their overall production capacity.

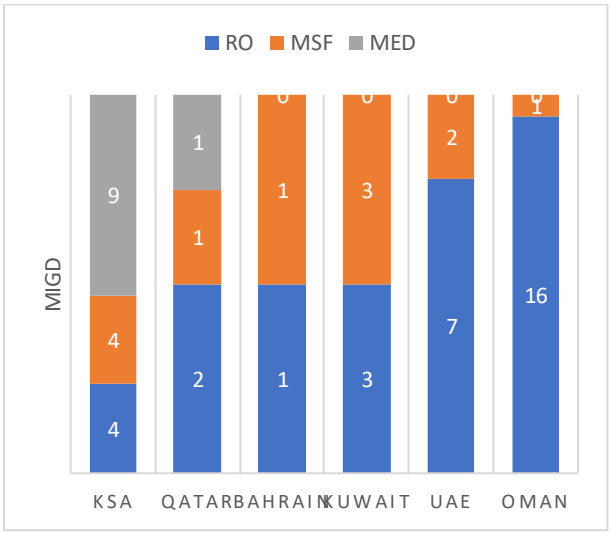

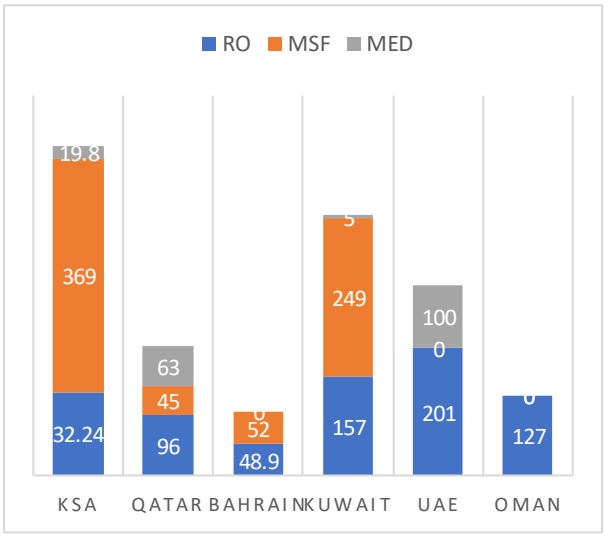

Figure 7 (A) desalination station under construction (b) excepted gulf desalination capacity of plant under construction

2.7.1 Solar energy

Solar distillation in the form of solar still is an ancient but novel method to produce potable water and through modern technology, its various losses can be minimized to

enhance its utility. More R&D on the design of solar stills would provide a range of systems which could be utilized depending upon the situation. The concept of the solar pond, solar collector and the photovoltaic cell can be integrated along with solar stills to produce the best result. [23, 26, 27]

2.7.2Hybrid system

With the expansion in the R&D around the globe, the world is turning toward the hybrid systems to produce the solution for the problems faced currently in present desalination process. .Desalination is be benefited with hybrid systems which use technologies from different disciplines to produce fresh water. Solar PV cell along with wind energy, a combination of nanofiltration and ultrafiltration for pre-treatment, using electro dialysis and reverse osmosis as complementary methods, a plant using forward osmosis integrated with nanofiltration and triple hybrid power-MSF-SWRO are examples which provide an edge over simple systems used in the past [28-31]

2.8 Feed water Pre-treatment

Desalination is an emerging field in the twenty-first century as the boiler technology was at the beginning of the twentieth century. Process modification and various techniques are to be invented so that the system is loss minimized. MSF, MED and pre-treatment of saline water through the various membrane can further simplify the entire process. There is a need for research in this area which can improve plant utilization.

2.8.1 Forward osmosis

Forward osmosis (FO) is a process of extracting sea water from a lower osmotic pressure feed into a higher solution osmotic draw solution across a FO membrane .The FO water can directly desalt sea water as a feed solution by employing higher osmotic pressure draw solution alternatively the FO process can be coupled with and existing

RO to create a lower energy desalination technology. As indirect desalination is achieved by the FO which dilutes the sea water going to the RO ,FO acts as a pre-treatment of the feed water to the RO reducing the required pressure which in turn reduces the required energy consumption.

2.8.3 Membrane distillation

It works by using thermal gradient ,with water vapour transported across a hydrophobic microporous membrane using less temperature and pressure than convention distillation system. The MD process almost uses only 1 bar pressure, MD process is modular and product water quality are insensitive to the feed water salinity up to 200000 ppm, which is its greatest advantage over MSF and RO . It is also less prone to fouling than pressure driven membrane process and requires smaller foot print than the current processes. The product water recovery is close 90 % with recirculation of concentrated brine increasing the reflux .

MD requires energy input in two forms thermal to drive the separation process and electrical to move the feed, product and brine flows of the system .MD can achieve the targeted 1 kwh/m^3 If powered by waste heat to satisfy thermal requirement [29]

2.8.4Nano-filtration/Ultrafiltration

NF is playing a vital role in softening the sea water. An integrated membrane system of nanofiltration and ultrafiltration can be used as the pre-treatment for the seawater to increase the overall efficiency of the SWRO plant. Various factors like operating pressure, cross-flow velocity and feed temperature can be examined to increase the effectiveness of the process. With the advancement of nanomaterials more efficient quality of membranes can be produced to maximize the results.[32, 33]

Chapter 3 LITERATURE REVIEW

3.1 Forward Osmosis Membrane

The membrane separation technology has been extensively used in various industrial, environmental applications, domestic wastewater treatment and desalination. Among the concentration-driven processes, forward osmosis (FO) has recently attracted noticeable attention due to its multiple advantages, including lower energy requirements during operation, ease in cleaning fouled membrane and high water recovery [34-36]. However, FO applications requires further development in key areas such as combating membrane fouling from internal concentration polarization, overcoming lower flux, and its limited performance for reverse salt diffusion [37]. Therefore, recent studies have concentrated their focus on developing new FO membranes with optimized thickness, porosity, and active/support layer that harmonize in order to increase water flux while simultaneously decreasing the internal concentration polarization fouling.

3.2 Introduction to forward osmosis

FO is a technique, which utilizes the natural phenomenon of osmosis based on the movement of the water molecules through a semi-permeable membrane. The driving force behind the movement of the water molecules is the osmotic pressure difference, in opposition to the other membrane based processes that require pressure to transport the water molecules across the membrane. The system set-up requires a concentrated draw solution (DS), which enables the osmotic pressure to draw the water molecules to it from the feed solution (FS), through the semi-permeable membrane. This process is continued through re-concentrating the diluted DS, leading to the production of purified water. The fundamental driving force for the water movement in this process is osmotic pressure, and therefore the need for external energy is negated,

which is an advantage that leads to low fouling of the membrane, and the limited irreversible cake forming, which are considered to be main challenges related to membrane applications, especially in biological treating systems and desalination. On the other hand, FO membranes are not immune to other type of fouling, including the internal concentration polarization, which is caused due to the asymmetrical structure of the FO membranes. Several recent research studies have concentrated on improving the active and support layers of the FO membranes in order to increase its utilization in different applications [38].

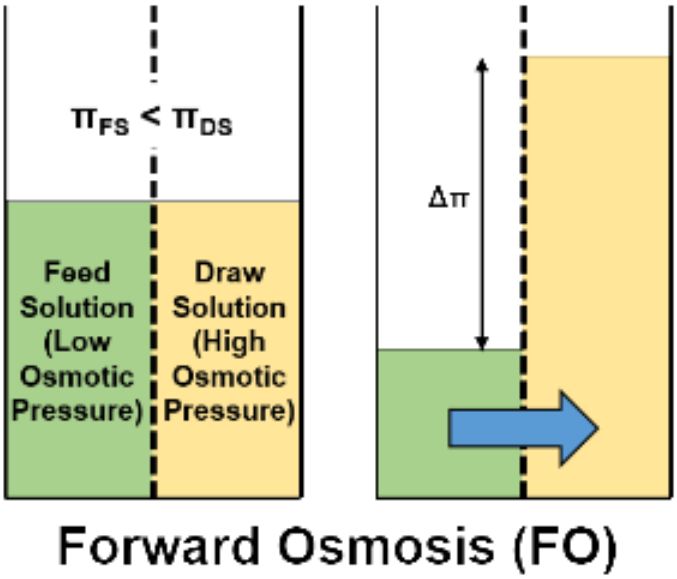

Figure 8 Schematic diagram representing the basics of the forward osmosis technique [39].

The forward osmosis process has a number of significant advantages over the pressure-driven system. The forward osmosis process usually works at a significantly lower pressure compared to the reverse osmosis process. The pressure required in FO is only for the transfer of feed and the drawing of solutions. Since FO operates at a lower pressure, it has lower energy consumption compared to all desalination processes used [40].

Membranes used for FO have high water flux and higher water recovery compared to the reverse osmosis system. This significantly helps in reducing the brine discharge, which is a major issue in the RO process [9, 41-43].With all these properties, forward osmosis when used with RO system decreases the pressure requirements and increases the permeate quality and quantity. The phenomena behind FO is a simple chemical property, and it can be calculated

$$\pi = nMRT \ldots\ldots\ldots\ldots 1$$

Here π is the osmotic pressure, n is Vanhoff factor, M is the molarity R is the ideal gas constant and T is absolute temperature in kelvin.

From the above equation (1) it can be concluded that osmotic pressure is directly proportional to the solute concentration, number of ions and temperature of the water. Performance of the forwards osmosis system can be determined by the output rate of permeate flux. The membrane used for FO also play a major role depending upon various membrane properties. These properties depend on the membrane material such as polysulfone, polyether-sulfone, polyetheramide, CNT, polyacrylonitrile, sulfonated poly etherether ketone etc. These materials are very stable chemically as well as thermally. Selection of material also depends on the draw and feed solution concentration. Membrane used for FO system also need to have high hydrophilicity.

During the modification or fabrication of new FO membrane thickness, porosity of membrane base layer (support layer) and selectivity of the active membrane layer permeability and salt rejection are to be considered. Controlling the membrane properties allows to design an effective FO system. The greatest parameter for membrane performance are

- water permeability
- solute rejection (R)

- solute permeability coefficient (B)
- Structural parameter (S).

Water permeability is based on the ability of a membrane to allow passage of water through the membrane per unit driving force. The capability with which a membrane can partially or completely restrict the solutes, while allowing water molecules to pass through without any hindrance is termed as solute rejection(R). The solute permeability coefficient (B) is described as the transport of a particular solute through the membrane per unit driving force at a given water flux. The structural parameter (S) is a factor that defines the influence of membrane support thickness, porosity and tortuosity on mass transfer in the support layer.

3.3 Comparisons between forward osmosis and conventional membrane processes:

In order to understand the fundamental difference between forward osmosis membranes and the conventional membrane processes, one must overview the membrane technology as a whole. Starting from the eighteenth century, scientists have conducted systematic studies to describe, understand and predict water permeability through a diaphragm. The time frame between the nineteenth and twentieth century witnessed the increase in the usage of membranes in laboratories in order to develop physical/chemical theories, however membranes were yet to be used on an industrial scale. Some notable works on membrane studies includes the measurement of solution osmotic pressures through membranes by Traube and Pfeffer, which was then used by Van't Hoff to improve the limit law and led to the implementation of the Van't Hoff equation. Additionally, Maxwell and others have also used semipermeable membrane in order to develop the fundamental kinetic theories to understand liquids and gases

[44]. The early diaphragms used in membrane studies consisted cattle and fish covers fabricated from animal intestine. However, the consistency of these diaphragms led to the development of nitrocellulose membrane, which was preferred due to their effective reproducibility. The 1950s witnessed the expansion of microfiltration membrane technology based on cellulose acetate polymers. Up until the end of the 20th century, membrane technologies were not vastly used in commercialized application due to being unselective, expensive, slow and unreliable [44]. The first industrial method of membrane technology adopted was the use of defect-free and high-flow reverse osmosis (RO) membranes. These membranes were made of ultra-thin, selective surface, which was deposited on a thicker, permeable microporous base to improve the mechanical strength of the ultra-thin layer. The first membrane was developed by Loeb-Sourirajan and showed a flux that was 10 times higher than any available membrane at that time, which led to the possibility of using these membranes in water desalination. This research advancement is believed to have led to the commercialization of RO techniques and was directly responsible for the development of ultrafiltration and microfiltration membranes. [45]. Reverse osmosis is mainly used to discard salts from seawater; and it is also capable of discarding unwanted organic compounds. It is one of the most common techniques used in desalination, however it also has many disadvantages such as the high amount of water and energy wasted during the process, and higher energy costs related to the reverse osmosis units. Other conventional membrane processes include microfiltration and ultrafiltration, which are mainly used to remove pathogens and particles from fresh water. The most recent type of membrane-based process is the nanofiltration process, which is capable of softening fresh water and remove any undesired products [46].

3.4 Factors influencing the forward osmosis processes:

3.4.1 Feed and draw solution:

As we have mentioned earlier in this chapter, FO is well considered as a technique that requires limited energy for water treatment, and this is due to the usage of smart agents such as the draw solution. However, considering the thermodynamic calculations, it is clear that the FO process is not completely "energy free" [43]. The FO desalination process revolves around two main processes, the first is the dilution of the concentrated DS and the second is the re-concentration of the diluted DS. This results in the use of higher osmotic pressure DS from the feed solution in the first mechanism, which means that the diluted DS can be regenerated to its first level by using different technologies in the second mechanism. Henceforth, the quality of the draw solution plays a critical part in the FO set-up, as it causes some limitations to the rather immature FO technology. These limitations include severe DS leakage, leading to the decrease in the quality of the produced water, and the decrease in the FO effectiveness. DS, as one of the vital factors of the FO process, has a substantial effect on energy consumption. While FO is a common and energy-efficient process without DS recovery, it still needs, in most cases, a secondary step in concentrating DS, which will also directly increase the energy costs involved. The use of the correct DS solution is therefore considered to be of great importance, since it is a significant parameter that affects the usability of the FO technology.

Multiple materials have been considered as DS in the FO process. And they are classified based on their different characteristics, such as their base materials, including inorganic compounds, organic compounds, and functionalized nanoparticles [47-49]. Other classification of DS solutions is based on the type of energy employed in order to regenerate the FO process. These categories of DS utilize the following energy to operate during the FO process: chemical energy, waste heat, electric energy, and solar

energy [50].

3.4.2 Permeability:

Water permeability is based on the ability of the membrane to allow fluid to diffuse through the membrane per unit of driving force. The capacity with which a membrane can allow partially or complete restrict the solutes while allowing water molecules to pass through without any hindrance is termed as solute rejection. The solute permeability coefficient is described as the transport of a particular solute through the membrane per unit driving force at a given water flux. The structural parameter is a factor that influences the membrane thickness, porosity and tortuosity of the membrane on the transfer of mass to the support layer.

3.5 Fabrication of forward osmosis membranes:

The fabrication of membranes for forward osmosis process is an extremely interesting topic in the field of research. And the search for a promising technology capable of addressing both water and energy shortages is extremely crucial in the fabrication of these membranes. This lead to the rise of effective technologies that allow forward osmosis to take place successfully.

As the heart of the forward osmosis process, the forward osmosis membrane permits water molecules to pass as smoothly as possible from the low osmotic pressure solution to the high osmotic pressure solution, in addition of being reusable, durable, sturdy and long-lasting. The two main types of forward osmosis membranes are thin film composite (TFC) and asymmetric cellulose triacetate. The TFC membranes are remarkably popular due to their extreme-selectivity, and ease of optimization through enhancing the support layer with various nanomaterials [51, 52] and in recent years the active layer is also separately modified to improve properties [53, 54]. It is understood

that different fabrication techniques lead to different structures, and hence the fabrication method plays a significant role in the performance of the support layers it produces. In the following section, we discuss about the different support layer fabrication techniques such as electrospinning, phase inversion etc.

3.5.1Electrospinning

Polymer electrospinning has seen growing attention in the last few decades due to its adaptability to a wider polymeric materials and greater consistent fiber quality. Though several methods have been developed to produce nanofibers, electrospinning appears to be the only one which has potential to scale-up to industrial scale. The diameters of fibers produced can range from 40 nm to 2 um. In this technique, electricity is applied to a polymeric solution, and a jet of charged solution breaks the surface tension, flowing to a grounded collector. The high surface to volume ratio of the jet allows for fast evaporation of the solvent, which can result in fine-filament fibers. Solvent-free electrospinning can also work with thermoplastic melts However, polymer solutions may also have greater viscosity, and may have reduced thickness. Electrospinning has the most potential for commercial development, but overall low fiber quality is a limiting factor. Additionally, the solvents available for electrospinning can be dependent on the dielectric constant. This membrane preparation technique is simple and affordable process capable of working under room temperature Additionally, it is capable of generating a wide variety of morphologies, such as nanofibers, nanotubes, and nanorod fibers. This can be seen in Figure 9. However, fabrication in general has several drawbacks, including high voltage requirement, fiber forming, and it is a lengthy process. This technology is only in the research and development stages [55, 56].

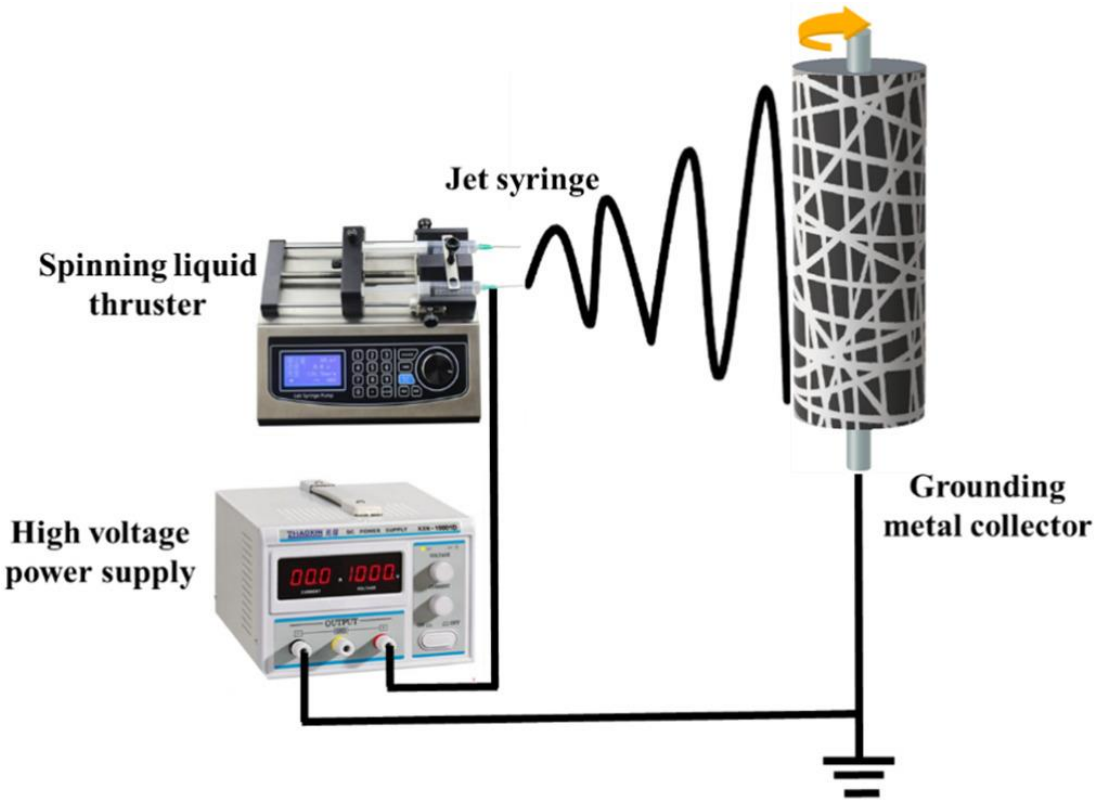

Figure 9 Representation of the electrospinning set up

3.5.2 Phase Inversion

Another widely used technique for the fabrication of FO based membranes both commercially and lab scale is the phase inversion technique, which is capable of forming both asymmetric and symmetric membranes through the precipitation of polymer solution. The phase inversion process involves the precipitation of a polymeric phase solution, to form a homogenous casting solution. The precipitation of the polymer was first done through the precipitation bath, however, newer technologies came along and allowed for the phase inversion process to take place through inhibition of water vapor from a humid atmosphere. The phase inversion process is simply described as the dissolving of a matrix polymer in a mixture of volatile good solvent and an in-volatile poor solvent. Hence when the polymer solution is casted, the good solvent progressively evaporates, causing the precipitation of the polymer host and producing

the required porous structure[57].

The parameters which control the membrane properties and structure can be altered through changing the polymer base, by using good volatile solvent, and the non-volatile solvent, as the thermodynamic and kinetic aspects of the process highly effects the membrane formation. This can be further understood through viewing the ternary phase diagram of the reactant materials used to prepare the membrane, hence the three component phase diagram(Figure.no 10) of the polymer/solvent/precipitant highlights the two main states that the membrane can be casted as, which is either a one phase region which all the components are miscible. And the second state is the two-phase region where the system separates into a polymer rich and polymer poor non-homogenous solution.

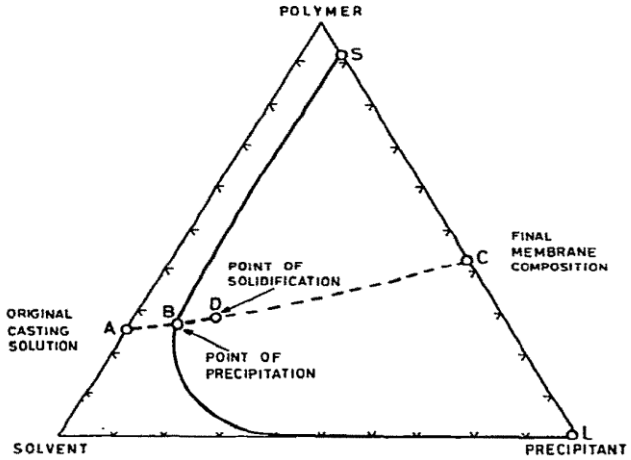

Figure 10 Schematic phase diagram of the system polymer-solvent -precipitant showing precipitation pathway of the casting solution during membrane formation adopted from [57].

3.5.3Pore former agents

Pore formed agents are material that are used in order to prepare and modify forward osmosis based membranes. As the ability to produce a proe, hydrophilic, and

mechanically strong membrane are available, these membranes usually require the production of a good porous structure. Pore formation can be done through multiple method, however the demand for green chemicals in membrane fabrication is higher than ever, due to the concerns from regulatory bodies when assessing environmental impacts and limiting secondary pollutant discharge. Therefore, the preforming materials must have the lowest possible energy needed for production, and also should have the ability to use consist of safe solvents that do not require further treatment and does not produce harm to the environment. Such materials have been produce by Alayande et al. [58] which used biosurfactant, amphiphilic hydroxypropyl-beta-cyclodextrin and polyvinylpyrrolidone (PVP) and used dual pore former to fabricate novel blended polysulfone membranes. These reagents have multiple advantages in their usage, such as their ability to be well dispersed in organic solvents and stably exist in the fabricated membranes. Additionally, these materials have been used as food additive in the past, which highlights its safety in the production of safe and consumable water. Another advantage is the use of bio surfactant with PVP, as it would reduce the interfacial tension between the polymer solution and the water, this directly leads to an enhancement of the interfacial stability in the fabrication and initiation of the macro voids. Such works proves the capability of producing an eco-friendly boosted membrane with higher flux performance without the risk of introducing secondary pollutants. Uses of various possible materials as pore inducing agent also needs to be explored in forward osmosis membranes.

3.5.4 Melt Blowing

Melt blowing is a different technique for generating non-woven webs that has confirmed to be scalable for industrial-scale production. In this method, molten polymer is extruded by way of a narrow orifice and into a stream of higher velocity hot

air. The hot air drag on the polymer melt surface causes the elongation of the polymer, under optimum conditions, into a fiber. This process could be controlled for producing fibers with diameters in the range of 1 to 50 microns[59]. Even though the traditional melt blowing is a cost-effective as well as effective process for the commercial-scale manufacture of non-woven fiber products, this process cannot be used for producing fibers of diameters in similar size range as electrospun fibers, and this technique is appropriate for only the thermoplastic polymers[60].

3.5.5 Solution blow spinning

Solution blow spinning (SBS) is an advanced technique developed recently for the preparation of nanofibers, and it is based on the principle of increased speed air-flow drawing [60]. This method has several benefits such as high production efficiency, lower energy consumption as compared to the electrospinning technique, and this method has been extensively utilized in the fields of filtration materials, membranes, medical dressings, protective materials etc. [61, 62]. This cutting-edge method was developed by combining the elements of both the electrospinning and melt blowing techniques. Moreover, this method can be used to make non-woven webs of microfibers as well as nanofibers with diameters similar to those prepared using the electrospinning technique with the benefit of having production rate of fibers a few times greater and has a higher possibility for industrial scale-up. As compared to the electrospinning process, the SBS process can be carried out at higher injection rates and it does not have any requirement for any high-voltage apparatus or any electrically-conductive collector, however it could be employed for coating any type of material with a wider array of polymer solutions. Further, this technique is not limited to solvents with a higher dielectric constant, and also it does not negatively impact heat-sensitive or

voltage sensitive polymers, like proteins. The SBS device works by delivering the spinning solution to the nozzle at a specific rate, and subsequently the solution is squeezed out of the nozzle for developing a satisfactory flow of the solution[63]. With the impact of the increased speed airflow field, the fine flow is progressively stretched and develops to be thinner, together with the solvent evaporation, and lastly the nanofibers are collected on a particular collection device.[64]

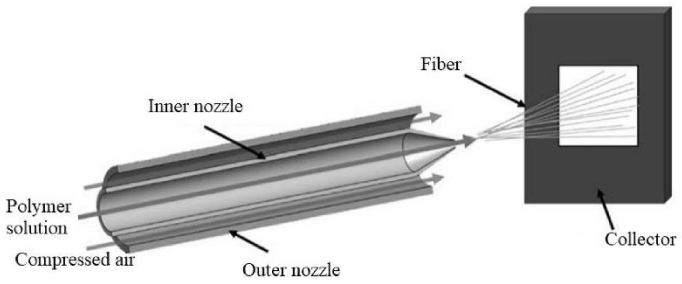

Figure 11 Soultion blow Spining device

3.6 Post Processing Strategies for improving properties of nanofiber membranes

There are different post processing strategies for improving the properties of nanofiber membranes. The most commonly studies post processing strategies are crosslinking, post fabrication drawing/stretching, solvent welding, heat treatment/annealing, and hot pressing of nanofiber membranes. All the membranes and support prepared by the previously mentioned techniques can be further enhanced to a certain degree with additional heat treatment and applied pressure For improving the properties of nanofiber membranes and thereby its applications, some studies were carried out. In a work by You et al.[65], the team heated the electrospun poly(L-lactic acid) (PLLA) nanofibers at temperature 180 C for about 30 to 60 min and attained higher mechanical properties of electrospun poly(L-lactic acid) membranes by thermal inter-fiber bonding. Subsequent to heating at 180C for 30 min, the electrospun poly(L-lactic acid)

membranes demonstrated tensile strength 4.14 MPa and elongation 102.5% relative to tensile strength 3.59 MPa and elongation 12.8% of the unheated poly(L-lactic acid) membrane. In a study by Na et al. [66], an advanced continuous hot-press post-treatment process was used for improving the mechanical properties of the electrospun polyvinylidene fluoride membranes. The scanning electron microscopy results confirmed that there were no remarkable variations in the morphology of the membrane when the hot-press temperature changed from room temperature to 130C, however large pores were developed due to the melting and bonding of fibers under higher temperatures. Tensile tests confirmed that the mechanical properties of the electrospun polyvinylidene fluoride membranes were significantly increased from 25C to 130C, while the porosity as well as the liquid absorption lessened. The hot-press at 130C was optimum for the electrospun polyvinylidene fluoride membranes. The continuous heat-press treatment can be a practicable technique for producing electrospun membranes, not limited to polyvinylidene fluoride, with appropriate mechanical properties and better porosity and liquid absorption for their applications in high-quality filtrations. In a study by Zhang et al. [67], the impacts of temperature, heating time, and heating method on the chemical stability, mechanical properties, and morphology of polysulfone electro spun membrane were examined. The results confirmed that the polysulfone electrospun can accomplish the maximum performance while treated at 190°C for 3 hours with tension heating.

3.7 The enhancement of forward osmosis membranes:

Many solutions have been proposed to limit the problems faced in FO process, such as the application of external forces in the form of low hydraulic pressure (< 10 bar), electrolysis or ultrasound and membrane structure modification [68]. The latter solution captured the interest of many studies due to its effects on the flux and fouling resistance

and selectivity of the process. The addition of nanoparticles to active layer and substrate of thin-film composite membranes is one of the current progresses in this field that efficiently varies the resultant membrane properties. In this chapter, we also discuss about the different polymer-based nanocomposite flat sheet forward osmosis membranes, in which the nanomaterials can be included either in active layer or substrate, or both in the active layer and substrate layer.

3.7.1 Polymer-Based Mixed Matrix Forward Osmosis Membranes:

Several research efforts have been directed towards improving the forward osmosis (FO) membranes properties to prolong their working life and enhance their throughput. These efforts have resulted in the emergence of a new generation of membranes termed as Mixed Matrix Membranes (MMMs). The first version of MMMs was produced in the 1970s to provide interconnected flow paths of high diffusion rate materials, which led to boosting gas separation with membranes [69].

MMMs consists of the continuous phase, which is typically a polymer modified with a dispersed phase (commonly referred to as fillers), which can be organic, inorganic, or biological [70, 71]. The fillers are primarily added to overcome the upper-bound trade-off between the permeability and selectivity [72]. They can also enhance the chemical and physical stability of polymeric membranes. MMMs have a unique nature that combines the strengths and functionalities of the two phases. Figure 12 shows an illustration of the separation capacity of MMMs compared to membranes made of their continuous and dispersed phases separately. There is a range of techniques and a broad spectrum of fillers that are used for synthesizing MMMs. It can be seen from this illustration that MMMs have selectivity more superior than unmodified membranes. The standard techniques and filling materials used specifically for preparing membranes for FO technology will be discussed in the following sections.

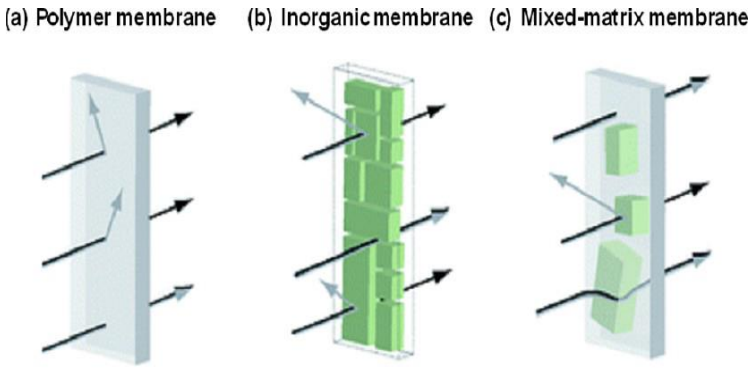

Figure 12 Schematic illustrating three membrane systems: (a) pure polymer membrane, (b) pure inorganic membrane and (c) MMM composed [85]

3.7.2 Polymer-Based Nanocomposite Flat Sheet Forward Osmosis Membranes

Polyamide (PA) thin-film composite (TFC) membranes are now the most widely used membranes for water treatment and desalination in the industry. The schematic representation of the three-layer membrane is shown in Fig. 15. Although the phase inversion technique is the most widely used method for the synthesis of the forward osmosis membrane substrate. Recently, it has been proposed that the electrospinning (ES) technique be applied to the production of the nanofiber polymer substrate instead of the phase inversion technique because it produces more acceptable results with respect to the forward osmosis flux. The ES process uses a higher electrical field for the preparation of dope solution nanofibers.

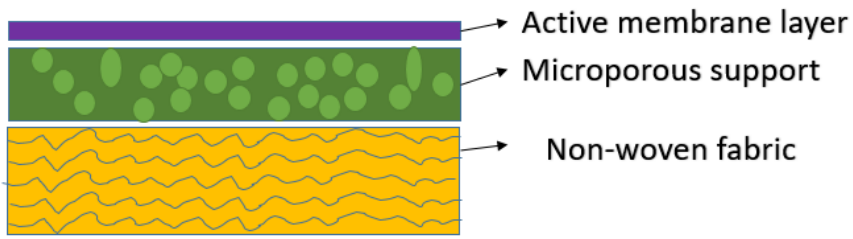

Figure 13 Diagrammatic representation of a thin-film composite membrane

Nanomaterials have recently been found to have significant application in different

fields[73] and their application in desalination and water treatment has been shown to be very significant [60]. The introduction of nanomaterials into the active layer and substrate of thin-film composite membranes is a significant recent development in the forward osmosis desalination sector that effectively varies the resulting membrane properties. This nanomaterial incorporation approach affects the hydrophilicity, permeability, porosity, thickness and roughness of the surface of the substrate. This will also affect the composition of the active layer. The introduction of nanomaterials into either organic or aqueous solutions creates nano-sized pores in the PA selective layer. As a result, the thin-film nanocomposite (TFNC) membranes for forward osmosis applications are normally manufactured in a flat-sheet configuration. In the following section, we explore the integration of nanomaterials into the selective layer and substrate layer of the forward osmosis membranes.

3.7.3 Substrate modified with carbon-based nanomaterials

Due to its exclusive properties, carbon-based nanomaterial graphene oxide (GO) is the ideal material option for the modification of the substrate of thin-film composite forward osmosis membranes due to the existence of abundant oxygen-based functional groups such as hydroxyl, epoxy and carboxyl groups [74]. A two-dimensional (2D) single layer graphene oxide nanosheet is usually one-atom thick. A two-dimensional (2D) single layer graphene oxide nanosheet is usually one-atom thick.

In the analysis, Park et al. [74] examined the manufacture and efficiency of the manufactured thin film composite forward osmosis membranes with graphene oxide-modified substrate. Graphene oxide nanosheets for the production of graphene oxide-polysulfone nanocomposite membrane substrate were included in the polysulfone. The selective polyamide layer was successively prepared on the graphene oxide-polysulfone substrate by an interfacial polymerization process to obtain a thin film of

forward osmosis composite membranes. The test results showed that a graphene oxide-polysulfone nanocomposite membrane substrate with appropriate structural properties, measured in terms of pore size, porosity and thickness, could be generated at an optimum graphene oxide content (0.25 wt percent). The optimal inclusion of graphene oxide in the polysulfone substrate not only significantly increased the permeability of water, but also allowed the successful formation of the polyamide layer compared to that of the pristine polysulfone substrate, which showed an extremely lower water permeability.

Carbon nanotubes (CNTs) are renowned nanomaterials used in membrane-based water treatment due to their improved strength, along with other benefits of nanomaterials.In the study by Tian et al. [75], The team effectively generated an advanced thin-film nanocomposite forward osmosis membrane consisting of a polyetherimide nanofibrous support layer reinforced by functional multi-walled CNTs and an ultra-thin PA selective layer. In addition to the higher interconnected porous structure of the nanofiber support layer, the well-distributed multi-walled CNTs in nanofibers increased the support layer porosity by almost 18.0 per cent and reduced the structural membrane parameter by 30.0 per cent and significantly increased the support layer tensile module by approximately 53.0 per cent. The increased mechanical strength of the built-in functionalized multi-walled CNTs contributed to the additional increase in porosity and pore size of the substrate to mitigate internal concentration polarization.2.5.5 Substrate modified with metal-based nanomaterials.

3.7.4. Substrate modified with metal based nano materials

Titanium dioxide (TiO2) nanoparticles are considered to be one of the most widely used nanomaterials for the preparation of nanocomposite membranes[76]. The extreme hydrophilic surface of the titanium dioxide nanoparticle, along with its

extremely smaller particle size (less than 21 nm), are the main features that are truly considered for the preparation of nanocomposite membranes.

In the work by Emadzadeh et al. [77], titanium dioxide/polysulfone nanocomposite support layers were manufactured by adding different quantities of titanium dioxide nanoparticles (0 to 1 wt percent range) to the polysulfone matrices. Subsequently, the fabricated nanocomposite support layers were distinguished by surface roughness, overall porosity, hydrophilicity and cross-section structure. The team noted that the porosity and hydrophilicity of the support layer increased by the addition of titanium dioxide. In addition, long finger-shaped structures have been prepared by increasing the concentration of titanium dioxide, resulting in an increase in water permeability. An interfacial polymerization of 1,3,5-benzenetricarbonyl trichloride and 1,3-phenylendiamine on the topmost surface of the titanium dioxide/polysulfone nanocomposite support layer was prepared for the manufacture of the nanomaterial integrated thin-film composite membrane for the FO phase. The forward osmosis efficiency evaluation was carried out with a concentration of 0.5 and 2.0 M NaCl in the draw solution, a concentration of 10 mM NaCl in the feed solution and both the active layer facing the draw solution (AL–DS) and the active layer facing the feed solution (AL–FS). The thin-film nanocomposite membrane generated using polysulfone substrate integrated with 0.5 wt per cent titanium dioxide nanoparticles has shown the most favorable results by providing a lower reverse solute flux and higher water permeability.

In addition, a nanocomposite substrate was prepared in a study conducted by Sirinupong et al[78], including a titanium dioxide/graphene oxide hybrid in polysulfone matrices. Before performing the performance review, the fabricated support layer was characterized by surface roughness, surface chemistry and cross-

section structure. The test results indicated that both surface roughness and hydrophilicity polysulfone-based substrates have been improved by the addition of nanomaterials. Titanium dioxide or titanium dioxide/graphene oxide hybrid may be added to support layers with longer finger-shaped voids extended from the top to the bottom. Higher surface hydrophilicity and a satisfactory structure formed are the main factors that cause an increase in the water flow of the supporting nanocomposite sheet. In addition, the water flow of the forward osmosis process using thin-film composite membranes can be improved by using this supporting nanocomposite layer. Compared to the regulation of the thin-film composite membrane, the titanium dioxide substrate membranes and the titanium dioxide/graphene oxide hybrid membranes demonstrated improved water flow with marginal increase in the inverted solute flux. From the results obtained, it can be confirmed that the addition of titanium dioxide and titanium dioxide/graphene oxide hybrids to the supporting polysulfone layer may potentially improve the performance of the thin-film composite membrane for future osmosis applications.

3.7.5Active layer modified with carbon-based nanomaterials

The excellent physical properties of graphene oxide, along with the versatility of chemical functionalization, are attributable to the abundant oxygen-containing functional groups, which make graphene oxide a possible candidate for several applications. In a study conducted by Shen at al. [79], GO nanosheets are prepared as well as incorporated into the active PA layer for the development of advanced TFC membrane for the FO phase. Compared to the control thin-film composite membrane, the graphene oxide-incorporated thin-film composite membranes exhibited improved water flow and suitable solute rejection. The effect of graphene oxide loading on the morphology of the membrane and the forward osmosis performance of the graphene

oxide-incorporated thin-film composite membrane was investigated with respect to the different characterizations as well as the inherent separation performance. In addition, the graphene oxide-incorporated thin-film composite membrane also had a low fouling tendency in the forward osmosis process compared to the graphene oxide-free membrane process..

Shokrgozar et al. [80] investigated the preparation of GO-added PA TFC flat-sheet membranes on the support layer of polysulfone for the FO process. Graphen oxide nanosheets have been introduced into the PA layer using different quantities (ranging from 0.05 to 0.2 wt percent). The test results verified the modification of the PA surface by graphene oxide nanosheets and increased surface hydrophilicity by increasing the concentration of graphene oxide. The results confirmed that the water flux of 0.1 wt per cent graphene oxide included composite membrane was approximately 34.7 L/m2h, showing an increase of 90 per cent relative to TFC, while the salt reverse diffusion decreased to 39 per cent. Fig. 14.4 revealed the forward osmosis fouling test result of the control of the thin-film composite membrane and the graphene oxide-embedded thin-film composite membrane. In addition, it has been noted that the water flow reduction of the graphene oxide-embedded thin-film composite membrane over time is very slow compared to the control of the thin-film composite membrane, indicating a low fouling tendency.

In the case of thin-film composite membranes, carbon-based nanomaterial graphene oxide can be integrated into the thin selective polyamide layer to improve membrane efficiency. The addition of graphene oxide to the selective polyamide layer can increase the internal free volume of the polyamide layer due to the incompatibility of graphene oxide with the polymeric structure and the enhanced surface smoothness as well as the hydrophilicity of the polyamide selective layer generated by the lower

surface tension of the water molecules, improving the transport of water [81].

The outer-selective hollow-fiber TFC membrane has recently been successfully manufactured by Lim et al[82]. The size-controlled GO nanosheets, smaller than 2 μm in size, have been effectively added by Lim et a[83] to the selective PA layer for the preparation of the outer-selective hollow-film thin-film nanocomposite membrane for the FO process by vacuum-assisted interfacial polymerization method. In this study, the team demonstrated, in particular, that the size-controlled GO nanosheets in amine aqueous solution were horizontally aligned as well as stacked on the membrane substrate surface by vacuum suction from outside to inside in vacuum-assisted interfacial polymerization; the size-controlled GO nanosheets were subsequently incorporated into the thin selective poyamide layer with leg. In addition, the successful loading of the size-controlled GO nanosheets inside the polymide layer under vacuum-assisted interfacial polymerization was noted to be more than that under the regular interfacial polymerization process, as there is no concern about particle loss from nitrogen or air blowing to separate excess amine solution. The benefit is that it would be extremely economical to use nanomaterials in the production of thin-film nanocomposite membranes.

3.8 Challenges of the forward osmosis process and how this work aims to address it

Despite the various potentially attractive advantages of the FO process, it is still in nascent stage in comparison to reverse osmosis. The mainchallenges in the forward osmosis process should be resolved before it can become a mainstream commercial process. In addition to this, there is a need of tailoring membranes that will decrease the effect of internal concentration polarization (ICP) which mostly occur in the porous support layer of current forward osmosis membranes and reduces flux .The

performance of the FO process is highly linked to the feed water quality as it is the case in any membrane driven process . There are various salts, organic, inorganic fouling agents and different chemicals which can lead to membrane fouling ,and thereby leading to increase in salt passage and decrease in the quality of the permeate flow. Therefore, the sustainability of membrane permeate flux during FO operation is hugely influenced by feed water composition (foulant type, concentration and physicochemical properties) as well as the feed solution chemistry.

The main challenges faced by FO process is the lack of data for long term study with membrane materials and different draw solution for varying temperatures. Currently, finding the ideal draw solute which is non-toxic in nature, have high solubility, generate high osmotic pressure gradient and be easily available is also a challenge . Presently, during FO membrane filtration process, the draw solution iused needs to be constantly regenerated . With an increase in the number generation cycle, the draw solutions have to be changed completely. Currently there is very little options to select out of the different draw solutes [84, 85].

The FO membranes are not non-fouling membrane, and the membrane do foul significantly. The only difference is the cleaning process is easier compared to other pressure membrane driven process. Fouling in the FO membrane is in the form of easily separable cake type layers. [84, 85]. But after each cleaning 100 % efficiency is not gained and cleaning can only be done for a particular number of times and den the membranes have to eventually be changed [43, 84]

Furthermore, regeneration of draw solute and change of membrane after a certain time adds to the cost and complexity of the overall process. Finding new draw solutes with high osmotic gradient and water flux and there effect in the long run is also very narrowly researched area [86]

The greatest challenge faced by FO process to commercialize on bigger scale is to have membrane with higher flux and maintain the higher flux for a longer time. In order to achieve this there is a need to have better understanding of fouling process in the FO membrane, and to find the steps to mitigate them. There is very little to no data on bio fouling and its effect and growth for using it in FO application in the gulf water with high TDS [87]

The permeate from the FO process also need additional steps to purify before it can be used.There are cases in which when using FO application there is reverse solute diffusion which is mainly due to membrane factors and membrane layers and its orientation. [84] Permeate flux is one performance indicator for a membrane-based process and is primarily dependent on the available osmotic gradient which directly depends on the draw solution . Therefore, the use of ideal draw solution that can generate high osmotic pressure is critical for advancing FO technology. the active layer of the FO membrane should be highly selective to reduce the reverse solute diffusion[49, 88]. This problem can also be overcome by using electrospinng technique for membrane fabrication and modification. There are limited studies showing the use of electrospinning for the FO system. Making membrane with electro spinning to see if it over comes the revere solute diffusion will be a novel study and later studying electron spun membranes for membrane characterization to study how the membrane fouling if any grown on these new membrane and what are the effects of cake layer formation and cleaning of the fouled membranes[84]

Shifting from thermal to membrane technology will not only reduce the cost of desalination but also the environmental impact. Forward Osmosis properties such as reduced membrane fouling, power consumption, cleaning frequency, and chemicals use, draw solution ,membrane , active layer need are to be studied

In a study by Altaee et, the team showed that energy efficiency of FO-RO and RO processes is highly affected by the feed water quality[89]. Thermodynamic analysis results demonstrated that FO-RO outperforms the conventional RO process at low water quality due to membrane fouling which causes considerable reduction in the annual water flux. At 10% water flux decline, FO-RO process was more energy efficient than the RO process particularly at high seawater salinity. The FO-RO process is more competitive to the RO process when feed water quality is low due to high salinity[90].

The main goal of the proposed thesis is to identify the benefit of using nanomaterial on the FO membrane for FO and FO-RO process seawater desalination. This can be achieved by improving the membrane properties by enhancing its strength to withstand fouling, salt rejection with specific salt rejection capabilities depending on the feed water. The thesis aims to effectively produce new modified/fabricated membrane with enhanced salt rejection properties, have better permeate flux and immune to fouling. This will help to increase the life of the membrane. Some of the nanomaterials will be fabricated and others are commercially available nanoparticles which will be used after proper optimization. Furthermore the nanoparticles will be deposited on a support layer which will be a polysulfone sheet and commercially available membranes from DOW and TORAY by using electrospinning and interfacial polymerization

However, the proposed FO membrane have not been fabricated using the electrospinning technique with addition of Nanoparticle, adding a layer of novelty through fabrication and studying the effect of nanoparticles on the membrane over time. hence it will also be first study using this technique and a unique study for using with high TDS condition for Qatar seawater.

Chapter 4: MATERIALS AND METHODS

This chapter discusses the materials used in the preparation of nanofibrous membrane and concentrated solutions used in the experiment. The first section of this chapter outlines the chemicals used, their properties, structures and methods used for the production of samples, including porous support with phase inversion, formation of polyamide (PA) layer and solution blow spinning for the preparation of the final nanofiber membrane. Second section explains feed and draw solution preparation and general setup and experimental procedure. The third section of this chapter explains about equipment and the forward osmosis (FO) bench modeling and fabrication. Lastly, the fourth section will address the characterization techniques used to assess the structural, morphological, thermal, photocatalytic, antibacterial capabilities of the membranes. All chemicals are purchased commercially, unless stated otherwise.

4.1 Materials used

4.1.1 Sodium chloride

In this study, sodium chloride (NaCl) used was commercially purchased from Research Lab India and was used to prepare different concentrations of water.

4.1.2 Polysulfone (PSF)

PSF has a molecular formula of $C(CH_3)_6(C_4(CH_3O)_2)C(4(CH_3)C)4(H_2O)$ Figure 14. This was purchased from Sigma Aldrich. The PSF was used as a substrate layer in the membrane. Toughness and stability at high temperatures are characteristics of these polymers. Polysulfone also has reproducible properties and regulated pore structure of 40 nanometers. Thus this material can be used in applications including hemodialysis, wastewater recovery, and food and beverage processing. [91].

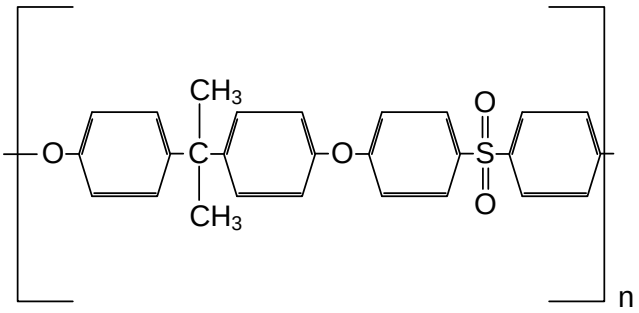

Figure 14 Structure of PSF

4.1.3 Methyl Phenylene Diamine (MPD)

MPD has the formula of CH3NHC6 H4NH2 and is also referred to as IUPAC N-methylbenzene-1,2-diamine. It is one of the monomers used in the preparation of polyamide by interfacial polymerization. It is a water-soluble monomer with a molecular weight of 122,168 g/mol, density of 1,09 g/mL, melting point and boiling point of 22°C and 123,5°C, respectively. The structure is seen in Figure 15

4.1.4Trimesoyl Chloride (TMC)

TMC has formula C6H3(COCl3) and is also referred to as IUPAC benzene-1,3,5-tri carbonyl chloride. It is one of the monomers used in the preparation of polyamide by interfacial polymerization. It has a molecular weight of 265.48 g/mol, a density of 1.487 g/mL, melting point and boiling point of 35°C and 180° C respectively. The structure is seen in Figure 17

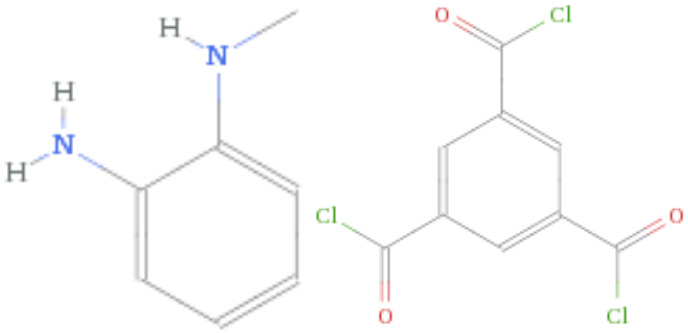

Figure 15MPD and TMC Structure

4.2 Thin Film Composite Polyamide Membrane Preparation

Polysulfone was chosen to make a porous substrate membrane on which the thin polyamide film is formed by in-situ polymerization. The phase inversion preparation is as follows: In 81 ml N-methyl pyrrolidone, 16 wt % of polysulfone and 3 wt % of polyvinyl pyrrolidone is dissolved. The solution is stirred for a few hours until the polymers are fully dissolved. The solution is left over night for degassing, then spread over a non-woven polyester fabric taped through a knife-edge onto a glass plate. The glass plate is then immediately immersed in a bath of deionized water kept at room temperature . After a few minutes, the non-woven support fabric and the polysulfone membrane are separated from the glass plate. The membrane is then washed thoroughly with distilled water and placed in DI water bath until further use.

4.3 Polyamide Thin Layer Preparation.

The support membrane (PSF + nonwoven fabric) held in a mold is immersed in an aqueous solution containing 3.4 wt percent MPD for approximately 2 minutes. The excess MPD solution is separated from the membrane surface by squeszing it via rubber roller on a plain surface. Further membrane is immersed in a solution of 0.15 wt percent of TMC in n hexane for 1 minutes . The membrane is kept at room temperature after the TMC solution has been drained by holding the membrane vertically and patt dry with tissue paper . beyond this it is placed in a 80^{o} C oven for 3 Mins .this is done for In-situ polymerization to take place .Go dissolved liquid is added to DI water and sonicated for 15 mins followed by addition of MPD to the mixture before the IP process. Figure 16 shows the chemical reaction of the same

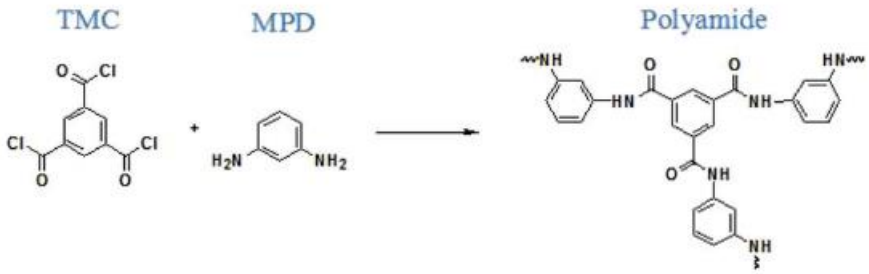

Figure 16 PA layer reaction

4.4 Solution blow spinning nanofiber preparation technique

Poly ether sulfone(PES) and polysulfone (PSF) were selected to be used as base polymers ,as these polymers are widely used in membrane fabrication using phase inversion and electrospinning techniques. Solvents used are N-methyl-2 pyrolidone/tolune in 2:1 ratio to dissolve PES, and N-dimethyl formamide (DMF was used to dissolve PSF. The wt% of polymer and solvent used are summarized in the table 4. The solutions were heated and stirred with a help of a magnetic stirrers until the polymers were completely dissolved , the prepared solution was left for degassing overnight. Then this solution were taken in sterilized medical syringe connected to a inside nozzle of the spinneret. The outer nozzle is attached with an air flow pipe connected to an external compressor. Other details and the samples prepared in our study are summarized below in table 4

Table 4 Membrane parameters

Sample No	Polymer type	Concentration (wt.%)	Solution feeding rate (mL/h)	Air Pressure (bar)	Voltage (kV)	Production time (min)	Thickness (microns)
1	PES	25	8	2	20	10	565
2	PES	25	8	2	20	20	474
3	PSU	10	5	1.5	20	10	500
4	PSU	10	5	1.5	20	20	580
5	PSU	10	5	1.5	20	30	538

4.5 Sample preparation

The sheets of membrane, solution blown nanofibers or phase inversion membranes are cut to exact size as per the Sterlitech cell CF402F. To cut, either template cutter is used in which the membrane is placed in a clean hard surface and template cutter is placed on top if the membrane sheet and a 5 mm thick rubber sheet is placed over it and its gently tapped with a hammer on all four corners to get a clean cut membrane. If the membrane is nanofiber based then the template shaped module is placed on the membrane and a sharp blade cutter is used to cut the membrane. The cut samples are loaded in the cell or stored for later use

4.5.1 Preparation of Feed and Draw solution

As per the desired concentration of required feed, the calculation is done and equal amount of sodium chloride is weighted on a digital weight balance. The weighted salt is transferred to a 500 ml beaker filled with distilled water Purchased from QALCO Qatar and is placed on a magnetic stir plate . Once all the salt is dissolved, this solution is transferred to a can which is filled up to 2 liters. The same procedure is followed to prepare draw solution in a 800 ml beaker which is later transferred to plastic can and

filled until 2 liters with distilled water . Generally, 0.1 M NaCl in 2 Liter was used for feed and 1-1.5 M NaCl was used for draw solutions in all the experiments.

4.5.2 Membranes used in the current research

Various FO membranes are available to be used and many other membrane can be fabricated for using in FO experiment, the membrane used in this research are summarized in the table.no 5 below, other characteristics of cellulose triacetate (CTA) commercial membrane are summarized in table.no\

Table 5 Membrane Used

S.No	Membrane	Technique	Company/ Type
1	CTA	Commercial	FTS
2	8040 TFC	Commercial	Toray (Korea)
3	PES	Solution spinning Blow	Nanofiber membrane prepared in this work
4	PSU	Solution spinning Blow	Nanofiber membrane prepared in this work

4.6 Equipment's

Forward osmosis setup.

The experimental setup built by individual purchasing different components and assembling it in custom built stainless steel bench. The main component of the forwards osmosis process is the Sterlitch Cross flow CF042F cell unit which is purchased from Sterlitech copertaion . The cell dimensions are 12.7 x 8.3 10cm with an internal active area of 4.6 x 9.2 cm with a sloth depth of 0.23 cm . Slot is between the two distinct blocks that make up the cell so feed and draw solution flow on either side of the membrane when sandwiched between the two parts. This gives two distinct section in the cell, top part is feed side and bottom is draw. This cell shown in Fig .no 19 is designed to test various commercial and lab fabricated membrane flat sheet membrane with ease. The pumps and gear drive utilized to circulate flow through the system is purchased from Cole Parmer ,USA.

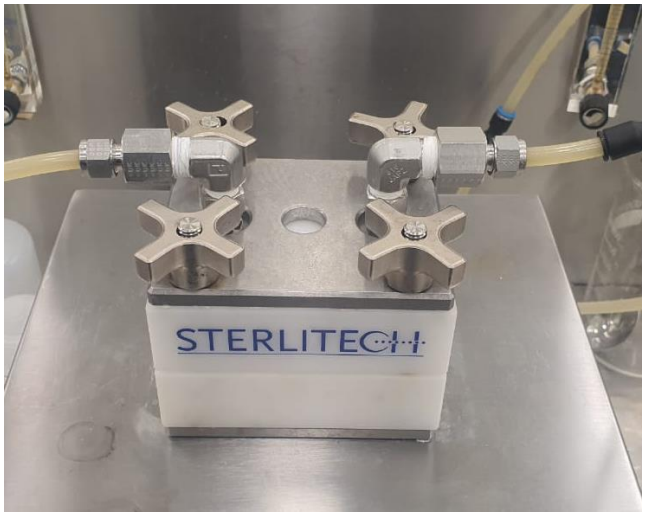

Figure 17 Starlitech Cell

The feed and draw tanks used are plastic cans with 5 liters capacity each. The two flow meters are mounted on the line before entry into the cell to monitor the flow on the feed and draw side. These flow meters are purchased from BROOKS, USA with max flow reading capacity of 3000 ccm/min. These flow meters are used to monitor the flow rate on feed and draw side that can be adjusted accordingly by adjusting the pump speed. Two pressure gauges followed by uni directional control valve from Festo, Germany are also installed on both the line between the cell and return line to main tanks of FS and DS respectively. These are in place to monitor the pressure on each side and control valves are used to pressurize the system, as needed.

In forward osmosis, the main performance is monitored by checking the rate of change of mass with respect to time and change in conductivity. In this system, both the feed and draw side tanks are placed on digital weight balance, custom built from God sun weighing solution, India. The two custom scale have built in data record with date, time interval settings and automated local back up of 10000 entries, both the weight balance can run on battery or electric power as needed. These weight balances are also WIFI enabled which store data directly online in google sheet without the need of any

additional licensed software and external computer.

Pipe network connecting the whole setup together is from Parker, USA purchased locally, and it has 8 mm internal diameter. All the push fittings (Union, T junction and elbows) used in the system are from FESTO, Germany. Fast push connect type are used in the system due to the multiple benefits it provides, and the pipes can be interchanged around the cell to make the system operate in co-current mode or counter current mode (FS and DS flow in parallel or opposite to each other). These fittings also make the systems routine maintenance and service quick and easy. Conductivity and salinity of the system is monitored with a portable multi parameter Mode HQd40, HACH seen in figure 18. This conductivity meter can accurately measure conductivity between 0.00 µS/cm to 3000 mS/cm. It records conductivity automatically also which can be set with respect to time.

Figure 18 Hach multi parameter

The Forward osmosis setup can be completely automated to collect experimental data without constant supervision after startup using the above digital weight balances and Hach HQd40 meter combined.

Figure 19 Forward osmosis set up and FO BENCH

4.7 FO Bench Design, 3D Modeling, Optimization and Fabrication.

The FO bench frame was first designed, modeled, and optimized in solid works once all the features were selected and sized as seen in figure 20. The 304 stainless sheets in 1.5 mm and 3mm thickness were purchased locally and fabricated using combination of both sizes. These steel sheets were marked and were laser cut in a fabrication shop in Doha area and transferred to bigger standardized workshop to properly assemble the cut sheets with features as designed for the FO Process with slots to hold the flow meters, pressure gauge, and FO cell STANDs in the right location. Along with various features, multiple holes of 20 mm diameter were drilled across the bench for ease of cleanly routing the pipes across the setup and safely route electric wires of the pump and weigh balances. This was done to keep the final working area free and open. The base of the bench top is layered with -inch think medium-density fiberboard (MDF)

wood with thin aluminum backing plates. This is done to dampen the benchtop from any vibration . The pump stand are placed under the benchtop to give positive suction head to the variable gear pump and keep the pump induced vibration away from the weight balance and the FO CELL. Double level also serves as added protection to save guard pumps from any leaks that may occur during operation.

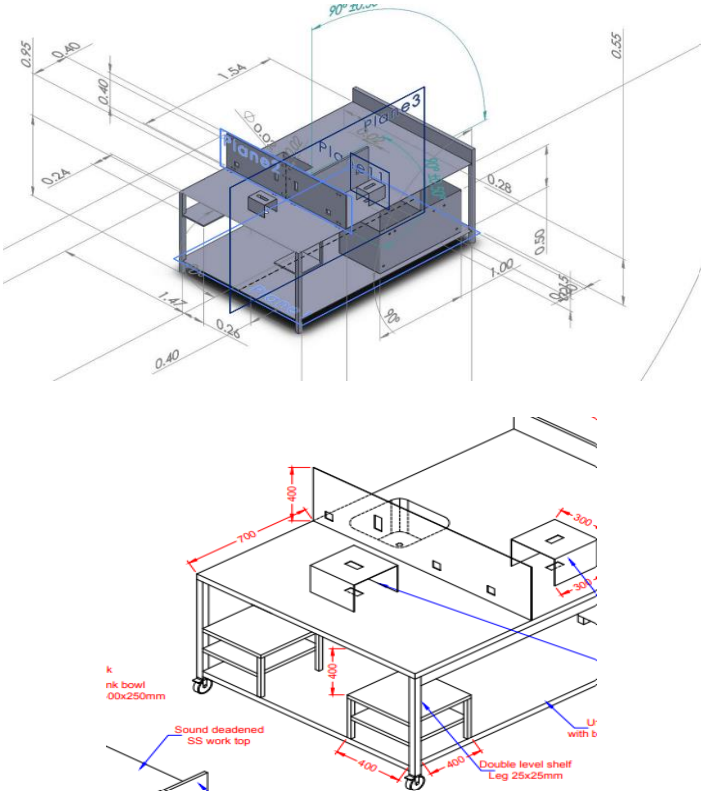

Figure 20 Design and optimization of FO bench in SOLIDWORKS

Pump stands are also incorporated with shelf to store FO membrane samples and hold other spare for the system . To make the system mobile the system is equipped with shock absorbing servo multi directional wheels with breaks. Rigidity and strength in the frame structure is achieved by reinforcing the bench top with c channels running across the width under the benchtop and MDF sheet. The base is fabricated using 3mm 304SS and is reinforced by omega channels across the width.

This system was initially planned for technology readiness level (TRL 3), however,

now the system with automation integration with digital WIFI enabled weight balances along with automated conductive meter can run without any supervision . The system can easily increase water capacity for FS and DS, and this bench can be used to test various FO membranes with ease to gauge their respective performances . The test cell can also be changed from CF042 to SEPA cell or any other easily to run different membrane types and sizes also with ease. This FO-bench is built for 10 years life span and modular nature to be future proof . Currently, the system is at TRL 4-5 .

4.8 Experimental procedure

Precut sample is washed with DI water and mounted directly in the cell for most cases, whereas in some cased the precut membranes are places in DI water for 2 hours for preconditioning prior to placing it in the cell . All FO experiments were run in FO mode as well as PRO mode, where the active layer (AL) is oriented toward the FS and the porous layer (PL) faces DS for FO mode and vice versa for the PRO mode, respectively. To conduct the experiment, the FS and DS side were connected to backwash tank prefilled with 2 L of DI water on each side and worked for maximum of 30 minutes. After this, initial run the main FO experimental runs were carried out with desired FS and DS concentration.. The concentration of FS and the temperature of both solutions were fixed during all FO runs.

Operation conditions of FO runs were conducted under a range of recirculation flow rate in between 800 ccm to 1200 ccm for the feed side and 500 to 800 ccm for the draw side. Change in the flow rate was achieved by adjusting the pump speed of the hydraulic pump. In all runs, the volume of FS and DS was kept at 2L, and in some other cases more volume was kept in the feed side to transfer more water from the feed to draw tank over a long period of time. During the experiments, FO runs were operated at room temperature (22 °C ±2) without any external temperature bath. Flushing by DI water

was performed after each run to overcome fouling and scale formation in the set up. In all the runs, only membranes were changed while all the operational parameters were kept constant.

4.9Measured parameters

4.9.1 Conductivity and TDS

Conductivity measurements were recorded using HQd 40 multiparameter with auto store functionality

4.9.2Weight change

Two weight balances were used to constantly monitor the rate of change of weight in the feed and draw solutions for further calculations.

4.9.3 Water flux (J_w)

Flux, J_w was calculated using the following equation which, is adopted from the literature. Water flux of the membrane refers to the volume of water going through the membrane in unit time per unit area. The unit commonly used is LMH (L m^{-2} h^{-1}).

Jw ¼ DW

qw _ A _ t…….(1)
where ΔW (g) is the water quantity through the area
of A (m^2) within t (h). ρ_w is the density of water
(1000 g m^{-3})

4.9.4 Reverse solute flux

The experimental reverse solute flux (RSF) can be calculated using Eq. (24), mentioned below (put references of papers that used the same) where it measures the amount salt passed through the membrane in unit time (Δh) through the effective area of the membrane

Js ¼

ðCtVt _ C0V0Þ

A _ t (2)

where C_t and C_0 is the concentration of salt in the feed at the t time and the start of experiment, respectively. V_T and V_0 is the volume of the feed solution at the time t and the start of experiment, respectively. The parameter A and t is membrane surface area and the measurement time, respectively.

As for membrane analysis, the membrane was held aside in a small air tight seal box with DI water until analysis. Before analysis the membranes were removed and dried in at room conditions or in a preheat oven at 50°C for a period of 10-15 mins . After drying, small portion of the FO membrane were then cut for characterization before and after experimental run for SEM, Similarly small samples were cut for atomic force microscopy (AFM), contact angle, differential scanning calorimetry (DSC), x-ray photoelectron spectroscopy (XPS), fourier-transform infrared spectroscopy (FTIR), Transmission electron microscopy (TEM), thermogravimetric analysis (TGA), tensile testing (3 samples), and and dynamic mechanical analysis (DMA) . For tensile testing and DMA, samples from the dried membranes were cut with dimensions 5 cm X 1 cm respectively .

4.9.5 Membrane Testing

Both membrane samples with an active membrane surface area of 42 cm^2 were tested using CF042 (Sterlitech Corp.) cross-flow permeation cell (see appendix A for detail description). Feed water consisting of 0.1M sodium chloride was pumped through the entire membrane in FO mode and PRO mode between 0-2 bar on the feed side and 0-0.08 bar on the draw side. The flow rate on both sides was closely monitored and modified if any deviations were detected during service. Conductivity measurements were repeated every 15-20 minutes after the reliability of the device was achieved. In any other case, reading was taken with respect to a variation in the DS weight of 300-400 grams.

4.10 Characterization

4.10.1 Atomic Force Microscope (AFM)

Veeco Metrology Nasoscope IV Scanned Probe Microscope Controller Dimension 3100 SPM is used to examine the surface topography of SA-LbL film on a silicone wafer. To scan the surface topography of the samples using the RTESP tip (Veeco) with a spring constant of 20-80 N/m. In the meantime, the PicoSPM LE (Agilent Corp.) touch mode was used to investigate the surface morphology of SA-LbL film on polysulfone ultrafiltration membrane. AFM scanning probes with a spring constant of 0.02-0.77 N/m were used during characterization. The surface roughness and morphology of the sample size of 20 atoms were taken by 20 atoms and the RMS surface roughness observed in this work is the average value of three different locations.

4.10.2 X-Ray Diffraction (XRD).

X-ray diffraction is a non-destructive, high-resolution analytical technique with a depth of absorption of 10 microns. It studies the effect of different preparation methods on the lattice constant and determines the phase identification of the crystalline material When the incident electromagnetic radiation is in phase with the interatomic distance (d) in the lattice structure, the strongest form of constructive diffraction interference occurs, known as Bragg's law, as shown in Figure .no 21 The Bragg equation is defined by Equation 3, where the radiation wavelength is, the angle between the lattice and the incident beam, and n is the integer number [89].

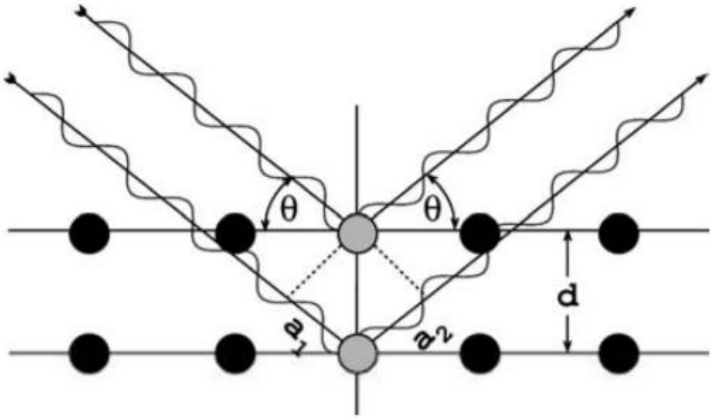

Figure 21 brags law

If a1 + a2 is a positive integer multiplied by a wavelength

Both nanomaterials and nanocomposites were analyzed using XRD technology. As shown in Figure 21, a Analytical Empyrean diffractometer was used to produce X-rays using a copper anode with a K wavelength of 1,54 nm. At a phase scan of 0.013 0 per minute, the scatter angle was measured from 100 to 900. The current of the tube was 40 mA and the applied voltage was 45 V..X-ray diffraction is a non-destructive test to determine the crystalline properties, the crystalline structure of the atomic molecule can be studied and helps to understand the law of Braggs and its relationship to the structure of the crystal, no atoms packed per unit cell, interatomic distance, size and shape of the unit cell for all elements of the periodic table as each element has a distinctive diffraction pattern. Diffraction is the bending of waves around small points and the edges of crystals. Xray is a form of high-energy electromagnetic radiation with a short wavelength of 10-10m. As a beam of x-rays impinges on a solid object, a portion of the beam will be dispersed in all directions by electrons associated with each atom or ion within the beam path. Consider the two parallel planes of atoms with the same h, k, and l Miller indices and separated by the interplanar spacing of the d h k l. Now, as a parallel beam of x-rays of wavelength 5-007 occurs on these two planes at the angle of the

beam. Two rays in this beam are scattered with the atoms P and Q. Constructive

Figure 22: XRD machine

interaction of the scattered rays occurs at an angle to the plane only if the difference in the length of the direction between the two rays is equal to n 5-007=2d. This is the criterion for diffraction under the rule of brags.

4.10.3 XPS

The equipment used in this laboratory is AXIS ultra KARTOS available at the H10 research complex in the Gas Processing Center-F-corridor, Qatar University.

X-ray photoelectron spectroscopy is a sensitive quantitative method used to determine the elementary structure, the empirical formula and the electronic status of the samples. The detection depth of this technique is between 1-10 nm and is triggered by irradiation of X-rays under ultrahigh vacuum conditions. Following the use of the spectrometer as a detector to determine the kinetic energy and the number of excited electrons, the plots are made of the strength signal as a function of the binding energy of the samples [90]. Approximately 5-10 mg of prepared nanomaterial

samples were placed inside the instrument, which was then tested at ultra-high vacuum below 10-8 torr, resulting in a high-resolution spectrum of intensity varying with binding energy (eV), which is why the binding energy is called a finger printing property that is unique to each element.

4.10.4 FTIR

FTIR is an analysis technique that determines the compounds present in a sample of 22

Figure 23 FTIR spectrophotometer model 760 Nicolet

based on an infrared (IR) absorbance range of 4000 – 400 cm-1. The instrument used in this work is the 760 Nicolet FTIR model as shown in Figure 23 , which allowed the identification of organic and inorganic feature groups based on their specific IR frequency.

4.10.5. SEM

Scanning electron microscope is a microscope that uses directed electron beams instead of light, scans the surface of the sample, and generates an image with an extremely high resolution. Electron/sample interaction produces various signal shapes with the most significant signal generated by the backscattered secondary electrons (SE). SE has several characteristics, including surface topography, chemical composition and

morphology.

EDX Energy Dispersive X-ray Spectroscopy is an accessory used in most modern SEMs. Its purpose is to make the inner shell electron of the sample exciting.

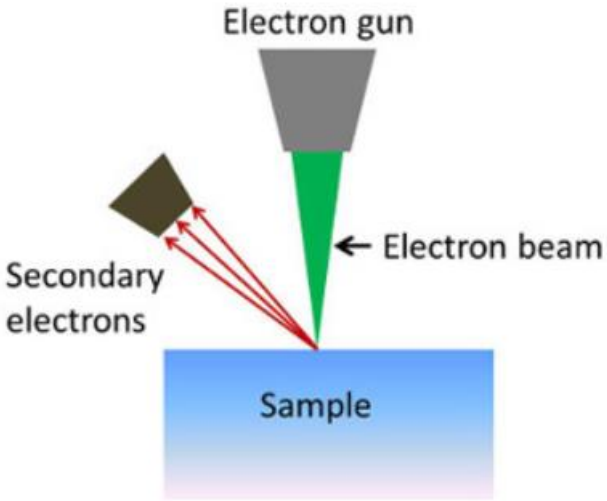

Figure 24 Simplified illustration of the SEM mechanism.

Bombing it with an electron beam as shown in Figure 24 Subsequently, it caused the electron from the higher energy shell to replace the previously-excited electron. EDX is capable of depicting the results in both the spectrum and the map shape, leading to a fingerprint signal generated by an electron moving between the shells [92].

The SEM instrument used in this work was Nova Nano SEM 450 as shown in Figure 25 with a voltage capacity ranging from 200 V to 30 kV. The fiber samples needed pre-treatment, including the spraying of a thin layer of gold particles on the surface, to improve the contact between the beam and the sample.

Figure 25 SEM NOVA

CHAPTER 5: RESULTS AND DISCUSSION

The membrane separation performance depends on the filtration ability of membrane pores, the parameters like pore size, diameter, and thickness of nanofibers [92]. The design principles of nanofiber substrates must satisfy small structural parameters (i.e., high porosity, low curvature, and low thickness), higher hydrophilicity (for accelerating the diffusion of water molecules), and certain mechanical strength (for resisting the cross-flow pressure) [93]. Further, the deposition of an active layer on the nanofiber membrane can enhance the retention effect of the membrane as well as increase the selective permeability[94]. Moreover, for improving the functional characteristics of the thin-film composite membrane more directly, adding different ions or functional nanomaterials to the active layer has also become a research hotspot.

Soheila et al. [95] prepared substrates by electrospinning and phase inversion, and synthesized nanofiber thin film composite FO membrane and normal thin-film composite FO membrane respectively. It was noted that the former has more permeability and reduced salt flux with different salt solutions used as draw solutions. Because the low structure parameter of nanofiber thin-film composite FO membrane decreases the internal concentration polarization (ICP) phenomenon in FO process.

In our study, the solution blown nanofiber membrane samples prepared from polyethersulfone and polysulfone had a thickness in the range of 500-600 microns. It was expected that the solution blown nanofibers could be better fused if the polymer films were heat-pressed for a specific time-period, thereby reducing the thickness, improving both the morphology and characteristics, and the subsequent membrane flux can also be increased. Hence, the samples were hot-pressed at temperatures 150 °C and 175 °C for 10 mins. The original nanofiber samples were named as T1, T2, T3, T4, and T5, as presented in Table 6. The only difference between the polyethersulfone (PES)

based samples T1 and T2 is just in the nanofiber deposition time (T1-10 minutes and T2-20 minutes). Similarly, the only difference between the polysulfone (PSU) based samples T3, T4, and T5 is only in the deposition time (T3-10 minutes, T4-20 minutes, and T5-30 minutes). The corresponding samples hot-pressed at 150 °C temperatures were named as T1-t1, T2-t1, T3-t1, T4-t1 and T5-t1, whereas the samples hot-pressed at 175 °C temperatures were named as T1-t2, T2-t2, T3-t2, T4-t2 and T5-t2. Subsequently, we had selected the best performing samples, and deposited a polyamide (PA) layer on top of this hot-pressed nanofiber membranes. Moreover, graphene oxide (GO) incorporated PA layer were also prepared on top of this hot-pressed nanofiber membranes to know the effect of nanomaterial on the FO membrane performance. The corresponding PA deposited samples are named as T1-t1-PA and T5-t1-PA, and the samples with GO-incorporated PA layer was names as T1-t1-PA-GO and T5-t1-PA-GO.

Table 6 Details of the nanofiber membrane preparation

Sample names	**Polymer type**	**Concentration (wt.%)**	**Solution feeding rate (mL/h)**	**Air Pressure (bar)**	**Voltage (kV)**	**Production time (min)**
T1	PES	25	8	2	20	10
T2	PES	25	8	2	20	20
T3	PSU	10	5	1.5	20	10
T4	PSU	10	5	1.5	20	20
T5	PSU	10	5	1.5	20	30

5.1 FO Experimental Analysis

The water flux of nanofiber membrane samples was analyzed by the cross-flow FO process and results are presented in the following sections. In this experiment, 0.1 M

sodium chloride (NaCl) served as the feed solution and 1.5 M NaCl was considered as the draw solution.

5.1.1 Water flux of original nanofiber membrane samples during FO experiments

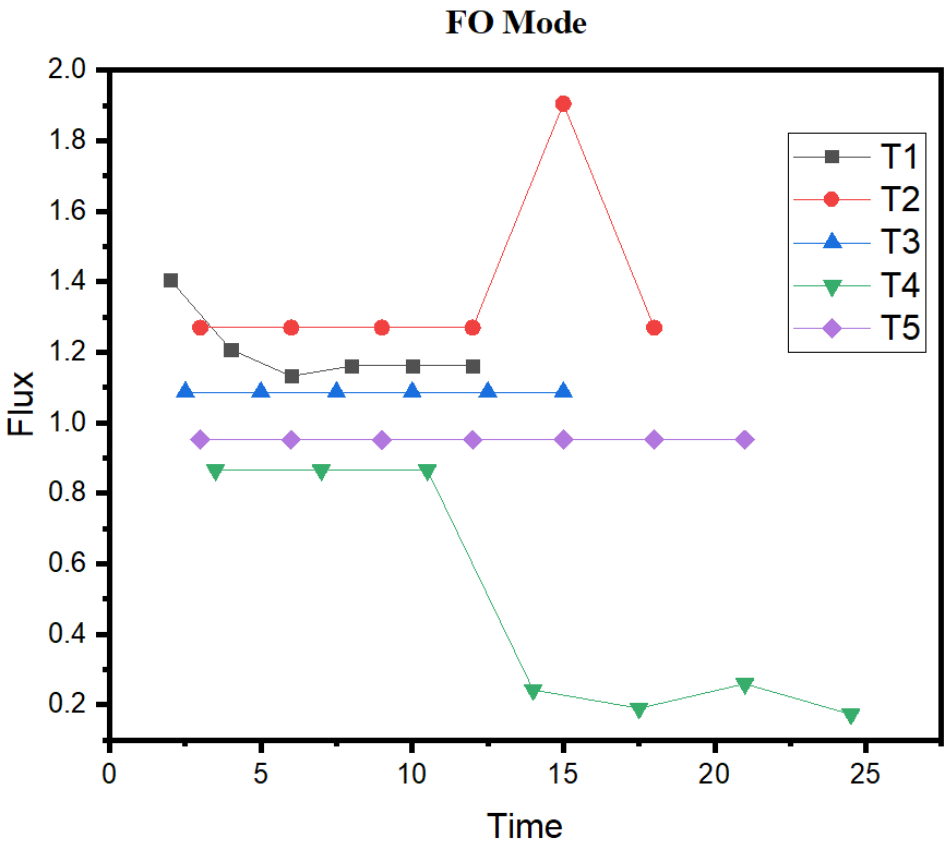

Figure 26 The variation of flux in original nanofiber samples with time.

From Fig. 26 , it can be noted that the polyether sulfone-based samples, i.e., T1 (1.15 L/m^2h) and T2 (1.26 L/m^2h), showed better flux values as compared to other polysufone-based samples. The time-period of the FO process extended from 12 minutes to 25 minutes.

5.1.2 Effect of different heat-press temperatures on the membrane flux

Hot pressing treatment can have an effect on the pore and fiber morphology of the nanofiber membrane [96]. Several studies confirmed that hot pressing had a strong influence on the separation performance of the membrane [97]. Satinderpal et al. [97]also confirmed that hot pressing is an effective technique for reducing the surface roughness as well as fouling tendency. It was established that the hot pressing of the nanofibrous support layer as well as backing material had a remarkable impact on the flux of the membranes along with their mechanical and structural integrity. This consequently effected the separation performance, pressure tolerance as well as the handling ease of the developed membranes. Addition-ally, with an appropriate heat-press post-treatment, the nanofibers heets can be used as self-supported membranes without non-woven support due to its sufficient mechanical strength [98].

In our current study, we are analyzing the variations happening in the flux with time, while using the samples jot-pressed at 150 °C and 175 °C.

5.1.2.1 Heat-press treatment on sample-1

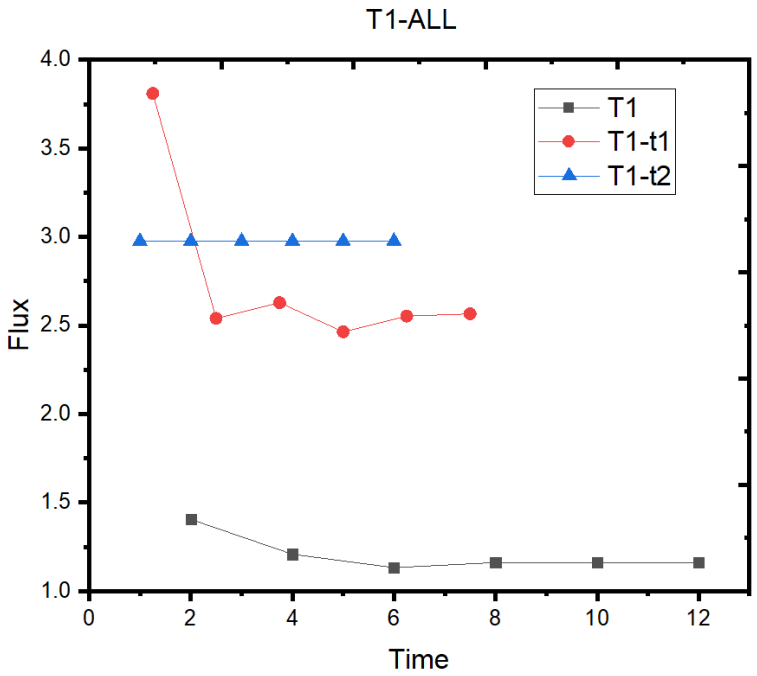

Figure 27 The variation of flux in hot-pressed nanofiber sample-T1 with time.

From Figure 27 , it can be noted that the flux of the PES based sample-T1 increased after the hot-press treatment at 150 °C and 175 °C. The flux of the sample almost doubled (from 1.25 L/m2h to 2.5 L/m2h) after hot-press treatment at 150 °C. Moreover, the flux of the sample reached more than twice (from 1.25 L/m2h to 3.0 L/m2h) subsequent to the hot-press treatment at 175 °C. Some of the fibers will be fused together after heat-press treatment was applied [99]. In the case of original un-pressed samples, the pore sizes were bigger due to its 'loose' fibrous architecture. Thus the water will get exchanged between the two solution (draw and feed), thereby leading to reduced flux. However, the hot pressing affects the pore size distribution of the substrate membranes and thereby its pure water flux [97]. With this hot-press treatment, the pore size of the samples become smaller, and it easily allows the water to pass through the membrane thereby increasing the water flux.

From fig 29, it can also be noted there is no significant difference between the flux generated by T1t1 and T1t2. However, there will be significant energy consumed for heating and cooling the system in 175 C heat treatment and 150 °C heat treatment. Considering this fact, we have carried out the polyamide layer deposition and graphene oxide-incorporated polyamide layer deposition only on top of sample T1t1. This will also avoid the usage of extra energy for heating the system to a much higher temperature of 175 C, and subsequently cooling down the same. Following the same principle, we have carried out just 150 °C heat treatment for other samples T2, T3, T4 and T5 to obtain T2t1, T3t1, T4t1, and T5t1.

5.1.2.2 ***Heat-press treatment on sample-2***

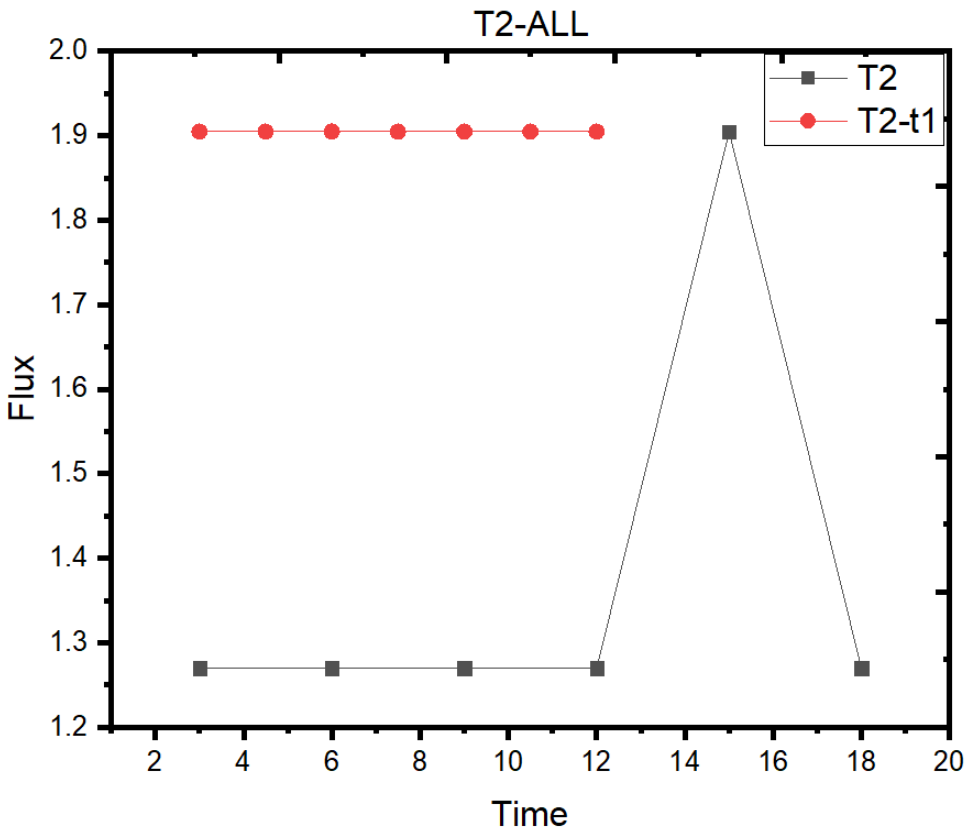

Figure 28 The variation of flux in hot-pressed nanofiber sample-T2 with time.

Similar to the performance of hot pressed sample-T1, the hot-pressed PES-based sample-2 showed a slight improvement in the flux after the hot-press treatment at 150 °C. From fig 29, we could clearly observe that there is no significant difference between the flux generated by T1t1 and T1t2. However, there will be significant energy consumed for heating and cooling the system in 175 °C heat treatment and 150 °C heat treatment. Considering this fact, we have carried out only 150 °C heat treatment in sample T2, in order to avoid the extra energy usage.

The flux of the sample T2-t1 increased (from 1.25 L/m2h to 1.9 L/m2h) after hot-press treatment at 150 °C. However, the flux difference is not very significant as in the case of sample-T1. Moreover, if we correlate this with the non-heat-pressed samples from figure 30, we can observe that there is no significant difference between the flux generated by samples T1 and T2. As stated in the previous section and Table 6, the only difference between both samples is just in the fiber deposition time. The other factors such as concentration, solution feeding rate, air pressure, and voltage in the nanofiber generation are the same for the samples T1 and T2. These results seen in Figure 26 and figure 27 have made the PES based membrane sample-T1 more superior to PES based membrane sample-T2. Moreover, we can confirm the fact that increasing the deposition time is not having any influence on the membrane flux.

Thus, Figure 26 and figure 28 and the explanation provided above clearly stated the main reason behind proceeding with sample T1t1 for additional treatments to improve the water flux. Hence, out of the PES-based samples, we have deposited the polyamide layer and graphene oxide-incorporated polyamide layer only on top of sample T1t1.

5.1.2.3 Heat-press treatment on sample-3

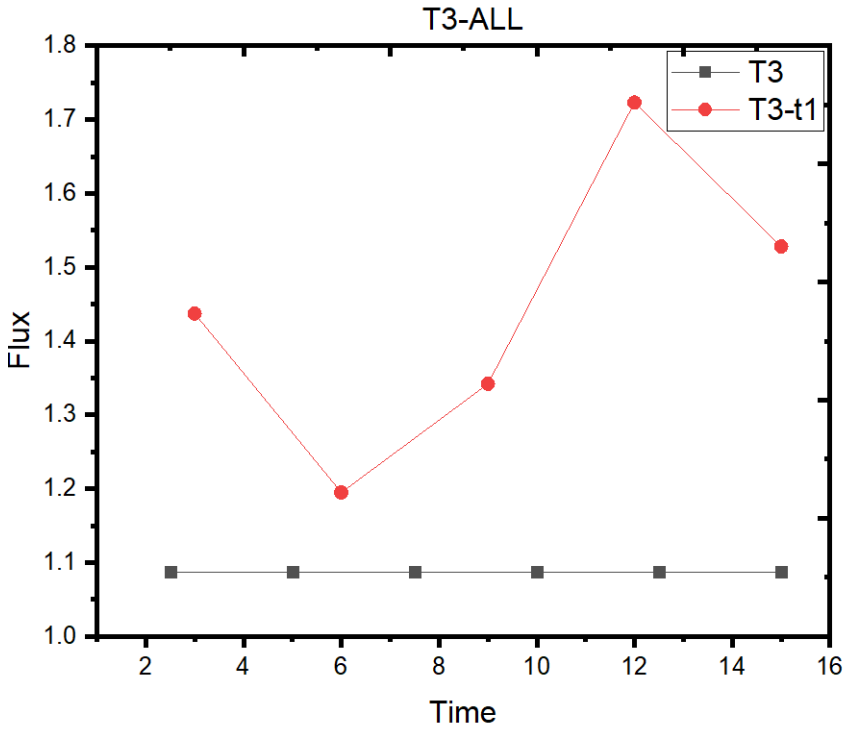

Figure 29 The variation of flux in hot-pressed nanofiber sample-T3 with time.

From Figure 329, it is obvious that the flux of the membrane sample T3-t1 increased from 1.1 L/m2h to 1.45 L/m2h with the 150 °C heat-press treatment. The reason behind this is same as the explanation provided for samples T1-t1 and T2-t1. Further, it can be noted that the FO process continued till a time-period of 15 mins only.

Moreover, from Figure 32, it was observed that the flux of sample T4 dropped during the FO test. The average value of flux of the polysulfone based T4 sample was almost 0.45 L/m2h. This decreased flux was the main reason behind not carrying out the heat-press treatment in this T4 sample.

5.1.2.4 Heat-press treatment on sample-5

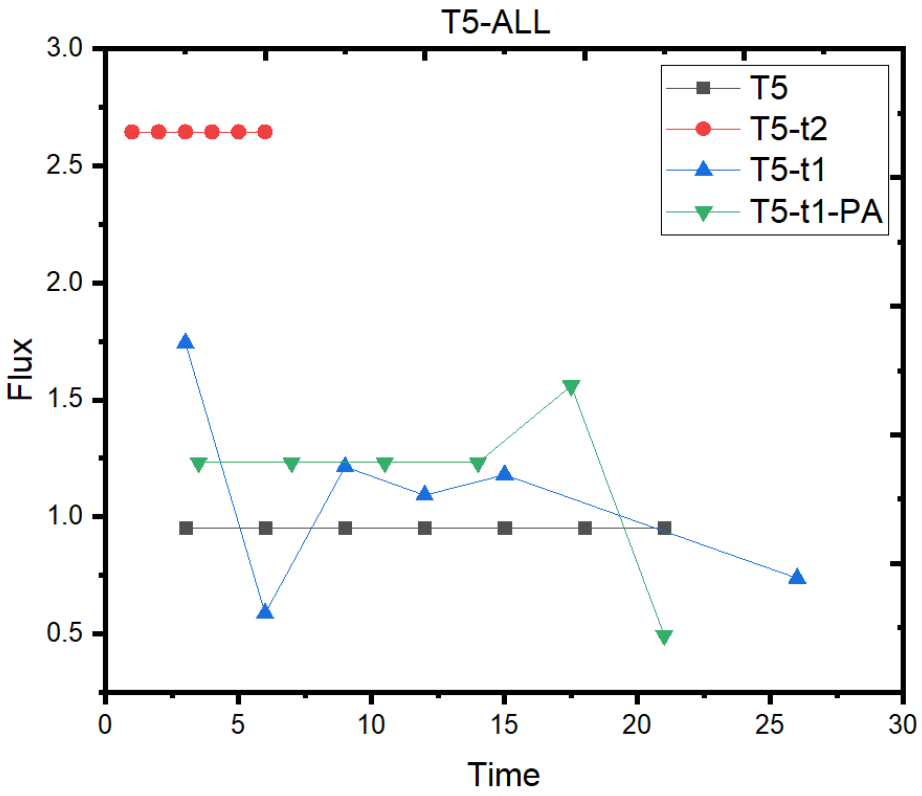

Figure 30 The variation of flux in hot-pressed nanofiber sample-T5 with time

From Figure 30, it can be observed that the flux of the membrane sample T5-t1 increased from 0.9 L/m2h to 1.13 L/m2h (average value) with the 150 °C heat-press treatment. Moreover, we can see that the FO process continued till an extended time-period of 23 mins only. This value is considerably higher, relative to the 15 mins time-period of the T3-t1 sample. Moreover, the T5-t1 sample performance showed similarity to the commercial membrane samples. This is one of the reasons for selecting this sample T5-t1 for the deposition of polyamide layer.

Also, the T5t2 sample showed a very high flux only for a limited period of time. This process will be very difficult to control. Hence, we have not carried out further modifications in sample T5t2.

The prolonged time observed in this case is the main reason behind selecting the T5-t1 sample, instead of T3-t1 sample, for further treatments such as the deposition of the polyamide layer and graphene oxide-incorporated polyamide layer only on top of the sample. Hence, out of the PSU-based samples, we have deposited the polyamide layer and graphene oxide-incorporated polyamide layer only on top of sample T1.

Moreover, the only difference among the three samples, T3, T4, and T5, is just in the fiber deposition time. The other factors such as concentration, solution feeding rate, air pressure, and voltage in the nanofiber generation are the same for the three samples, T3, T4, and T5. These results seen in Figure 28 and Figure 29 have made the PSU based membrane sample-T5 more superior to PSU based membrane samples T3 and T4. Furthermore, we can confirm the fact that increasing the deposition time is not having any influence on the membrane flux.

5.1.2.5 Overall variation of flux in all hot-pressed nanofiber samples with time

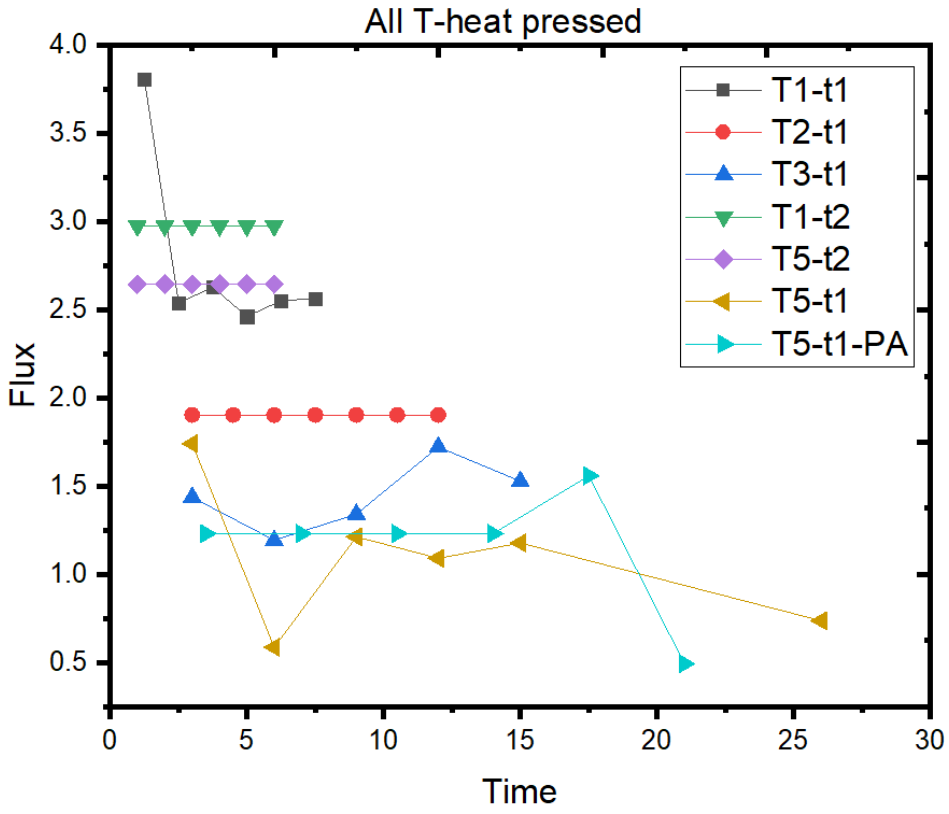

Figure 31 The variation of flux in hot-pressed nanofiber samples with time

From fig. 33, it can be noted that the higher temperature (175 C) pressed samples T1-t2 (3.0 L/m^{2}h), and T5-t2 (2.7 L/m^{2}h) showed better flux values, as compared to the other samples. This is because of the fact that with the hot-press treatment the membrane pore size becomes smaller and the distribution becomes narrower. The interconnected fibrous architecture of the modified substrate membranes with high porosity might have facilitated the mass transfer of water[97]. However, we could observe that the FO process of these high-temperature samples are getting completed within a very short time-period, i.e., 6.5 minutes. This fast process will be uncontrollable and difficult to handle. On the other hands, the nanofiber membrane samples hot-pressed at 150 °C, showed higher flux as compared to the original samples, and also the FO process extended to a longer time frame. The flux values of this 150

°C hot-pressed membranes T1-t1 (2.5 L/m^{2}h extending till 7.5 minutes), T2-t1(1.9 L/m^{2}h extending till 12.5 minutes), T3-t1(1.5 L/m^{2}h extending till 15 minutes), T5-t1(1.25 L/m^{2}h extending till 25 minutes) were definitely better than the original samples.

Moreover, it can be confirmed that the 150 °C temperature hot-pressed samples were noted to have improved time-frame along with reasonable higher flux, relative to the 175 C temperature hot-pressed samples. The flux of T1 samples increased from 1.15 L/m^{2}h to 2.5 L/m^{2}h after 150 °C hot pressing, whereas flux of T5 samples increased from 0.95 L/m^{2}h to 1.25 L/m^{2}h to after 150 °C hot pressing. Thus, 150 °C is considered as the optimal post-treatment temperature in the current study.

5.1.3 Effect of PA deposition on the performance of the hot-pressed T5-t1 nano-fiber membrane

In a study by Phuoc HH et al. [100], an advanced double-skinned FO membrane with a higher water flux was developed for emulsified oil−water treatment. The double-skinned FO membrane consisted of a fully porous sublayer sandwiched between (i) a polyamide layer for salt rejection and (ii) a fairly loose dense skin for emulsified oil particle rejection. The double-skinned membrane developed showed considerably higher water flux and a lower reverse salt transport of using 0.5 M NaCl as the draw solution and DI water as the feed. Moreover, this double-skinned membrane outperformed the single-skinned membrane with much lower fouling propensity for emulsified oil−water separation. Robust membranes with minimized reverse and forward transport of ions are critical for the effective application of the forward osmosis process in treating a variety of source waters.

Thus, in our study, we deposited the polyamide layer on top of the heat-treated nanofiber samples for increasing the water flux and decreasing the reverse solute transport. The nanofiber FO membranes based on the polyether sulfone and polysulfone

has lesser rejection toward NaCl. Hence, it is extremely important to modify the support by the deposition of a thin salt selective layer (polyamide layer) onto the porous support. From Fig. 37, it can be confirmed that the hot-pressed nanofiber sample T5-t1 showed improved performance with respect to flux and extended time. Therefore, the longer time-frame performed hot-pressed membrane, i.e., T5-t1, was selected for the polyamide deposition. Subsequently, it was observed that the PA deposited hot-pressed membrane, T5-t1-PA, showed an improved flux as compared to the T5-t1 sample. Moreover, the fluctuation is less and the FO process time is also reasonable. This confirms the point that the PA deposition on top of the hot-pressed nanofiber membrane showed better performance, as compared to the plain hot-pressed nanofiber samples.

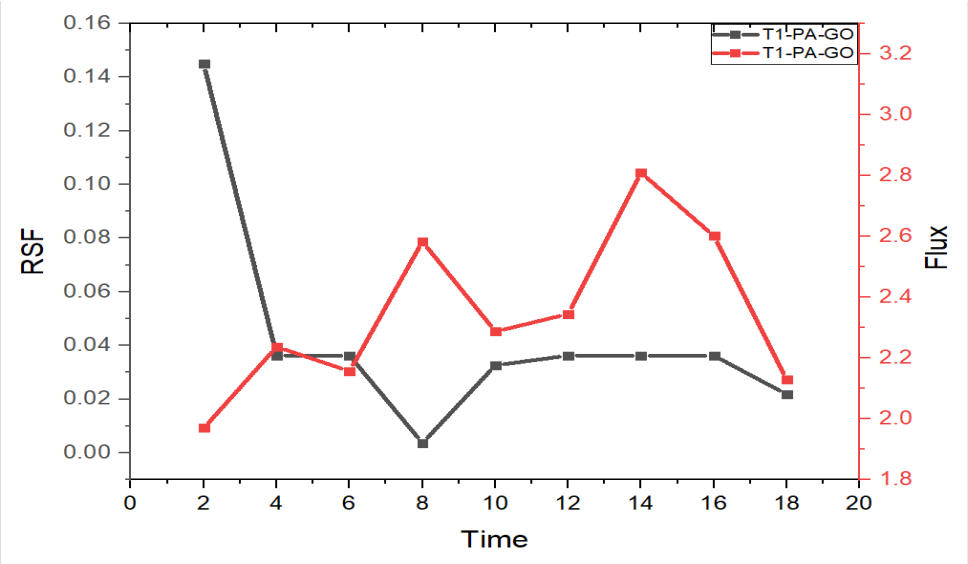

Figure 32 Effect of PA deposition on the performance of the hot-pressed T1-t1-PA nano-fiber membrane

The graph 34 confirms that with the deposition of polyamide on the best performance PES-based hot-pressed nanofiber sample T1-t1, the flux obtained was almost similar to T1-t1. However, the FO process time period considerably extended from 8 minutes to 22 minutes, thereby improving its performance.

Due to these improvements in performance, we had incorporated graphene oxide into the polyamide layer of T1t1PA and T5t1PA for further performance monitoring.

5.1.4 Effect of graphene oxide incorporated PA deposition on the performance of the hot-pressed nano-fiber membranes

When GO is added to the metaphenylene diamine (MPD) in the aqueous solution, it might react with MPD and trimesoyl chloride (TMC) molecules in the course of the interfacial polymerization. The amine groups of metaphenylene diamine might react with graphene oxide to develop new amide bonds and hydrogen bonds at the time of ultra-sonication of the aqueous solution. Subsequently, when the TMC solution contacts the membrane, the interfacial polymerization happens, where acyl chloride groups of TMC will not only react with MPD, but also with GO to form anhydride and ester groups [101].

In some of the previous studies, GO was added to the membrane in the selective layer by chemical crosslinking [102], layer-by-layer self-assembling [103, 104], and accomplished enhanced separation performance with improved water permeability, anti-fouling property or chlorine resistance. On the other hand, those membranes developed by the above-mentioned techniques might may suffer from the water permeability reduction with time as the GO coating layer might interfere with water permeation [105].

In this study, the improved hydrophilicity of GO-incorporated PA deposited nanofiber membrane was confirmed by the water contact angle results. The water contact angle of the membrane increases with the addition of GO into the active layer, confirming that the incorporated GO with oxygen-containing functional groups can improve the hydrophilicity of the membrane remarkably, and thus offer a higher water flux [79].

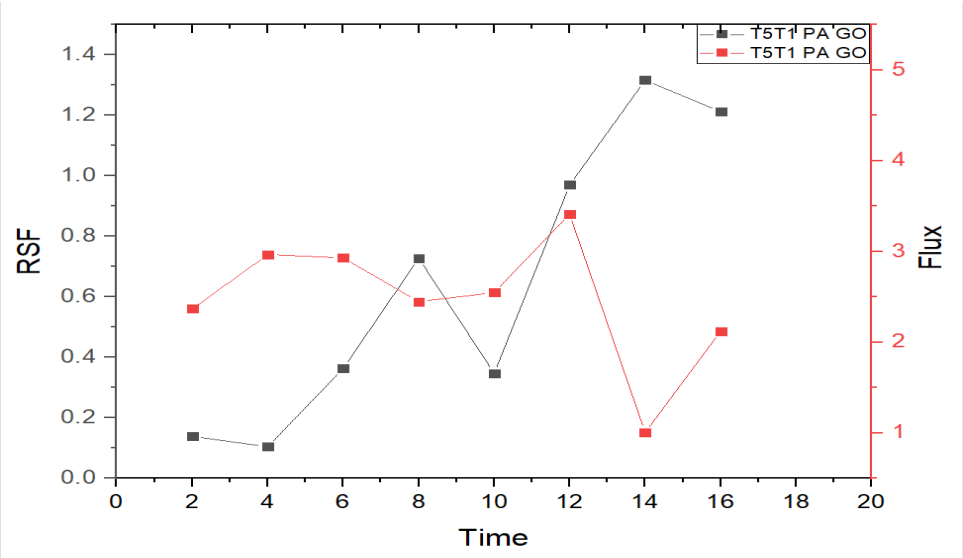

Figure 33 The variation of flux in graphene oxide incorporated PA deposited hot-pressed nanofiber sample T5-t1-PA-GO with time.

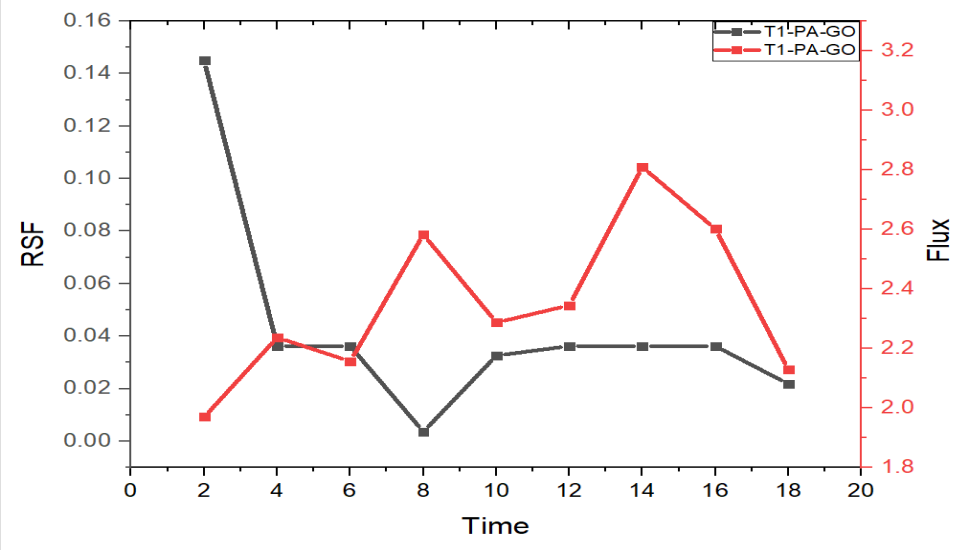

Figure 34 The variation of flux in graphene oxide incorporated PA deposited hot-pressed nanofiber sample T1-t1-PA-GO with time.

From Fig 35 it could be noted that the water flux of the GO-incorporated PA deposited nanofiber membrane T5-t1-PA-GO (2.75 L/m^{2}h average value) showed better flux as compared to the PA deposited nanofiber membrane T5-t1-PA (1.16 L/m2h average

value). The improvement was more than double with a reasonable time-period of 18 minutes. The graph 40 confirms that the sample T1-t1PA-GO shows higher flux as compared to the T1-t1-PA. This confirmed that the water fluxes of the nanofiber membranes will be improved by the deposition of GO-incorporated PA layer. This improvement is due to the combined effect of the additional passages formed, improved hydrophilicity, thinner selective layer etc.

5.1.5 Variation in conductivity versus flux with hot-press treatment

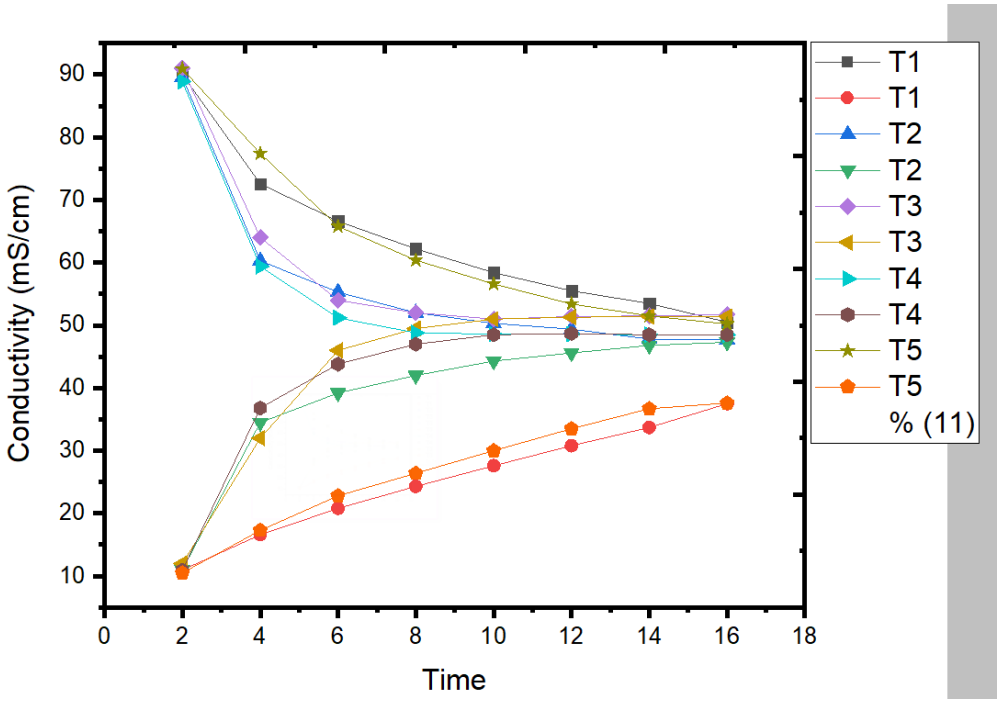

Figure 35 Variation in conductivity versus time for original up-pressed samples

From figure 35, it can be noted that conductivity of draw solution decreasing, and the conductivity of feed solution improving with time. In the case of original un-pressed nanofiber samples, the pore diameter will be large and water will be passing to the draw solution, and subsequently moving back to the feed solution. Here, as time passes, the conductivity of both solutions reach an equilibrium stage, and consequently the

movement of water molecules stops and thereby the FO process. This is due to the fact that concentration difference is essentially required for the osmosis phenomenon to happen. In the original up-pressed nanofiber samples, as the concentration gradient tends to be zero, the FO process will be stopped. Hence, it is extremely important for a post-treatment such as hot-pressing, to reduce the pore size of nanofibers and thus improve the water flux.

5.1.6 Reverse solute flux versus time

Reverse solute flux (RSF) is the back diffusion of the DS across the FO membrane to the FS. RSF must be considered in the FO studies because it might contaminate the FS. Reverse solute flux verses time graphs were plotted for the original nanofiber samples, the best performing PES and PSU samples (T1-t1 and T5-t1), and also PA layer (T1-t1-PA and T5-t1-PA) and GO incorporated PA layer (T1-t1-PA-GO and T5-t1-PA-GO) deposited nanofiber samples.

5.1.6.1 Reverse solute flux versus time in all original nanofiber samples

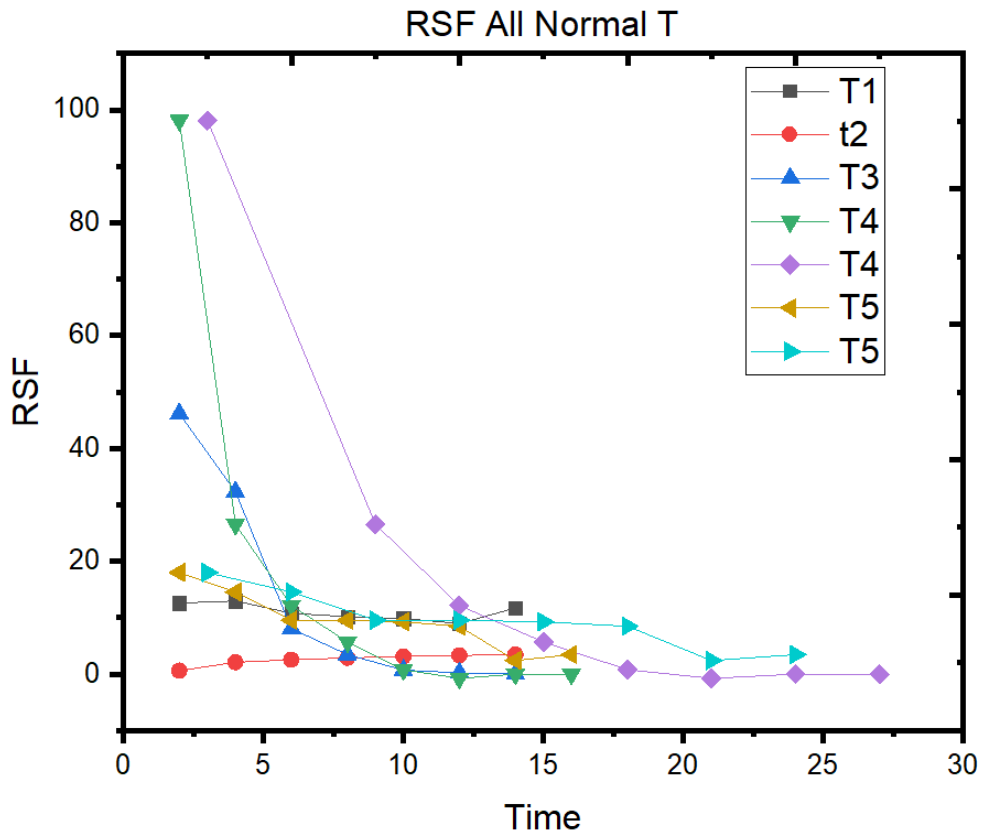

`Figure 36 Reverse solute flux versus time for all original nanofiber samples.

From Fig 38, it can be noted that the initial reverse solute flux (RSF) values of the nanofiber samples were higher initially, and we can see that the RSF value decreasing with time. For the original nanofiber samples, the pore sizes were much higher, allowing the passage of salts, and hence the reverse salt flux was higher initially. The water will be passing to the draw solution, and subsequently moving back to the feed solution. Here, as time passes, the conductivity of both solutions reach an equilibrium stage. Here the salts on the feed side and the draw side will have similar conductivity. Thus the FO process stops and therefor the RSF value attains a zero value as time passes (Figure 36).

This clearly confirms that the original nanofiber samples without any treatment in it

will be difficult to use for the FO process. In the normal un-pressed nanofiber samples (T1, T2, T3, T4 and T5), as time passes, the concentration gradient become zero thereby stopping the FO process. Concentration gradient is extremely needed for the natural osmosis process (FO process) to happen. Hence, it is extremely essential to perform a post-treatment (heat-press treatment) to enable the material to be used for the FO process.

5.1.6.2 Variation in reverse solute flux with hot-press treatment in sample T1

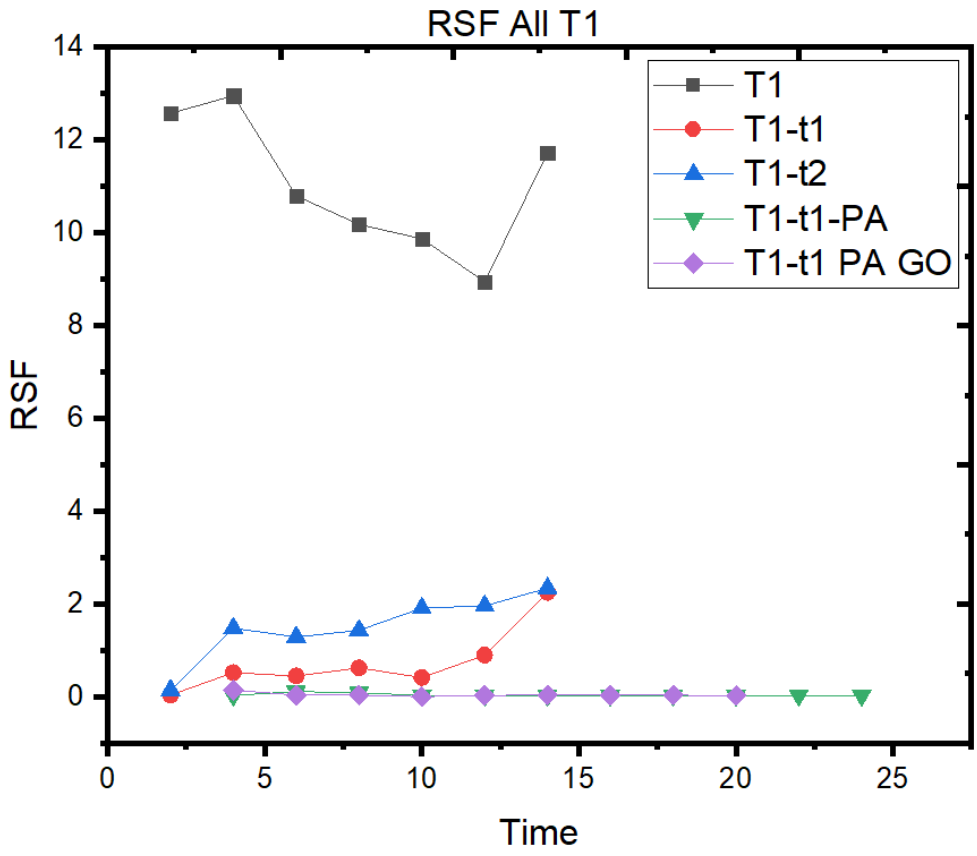

Figure 37 Variation in reverse solute flux with hot-press treatment in sample T1

It can be noted from Figure 37 that the RSF value of the original nanofiber sample T1 was almost 11 g/m2h average value. However, with the hot-press treatment at 150 °C, the RSF value of T1-t1 exponentially reduced to reach values below 2 g/m2h. It was

observed that with the hot-press treatment, the pore size decreases, thereby restricting the passage of salts, and hence exponentially reducing the reverse solute flux. This performance is very similar to the ideal performance, which is close to zero.

Also, from Fig 43 , the RSF performance of T1-t2 can also be noted. It was found that for sample T1-t2, the RSF value was exponentially decreased as compared to the T1 sample, however, the value was slightly higher relative to the sample T1-t1. No added benefit in the RSF value is obtained with higher-temperature heat press treatment.

Thus combining the results from Figure 27 and Figure 35 (the variation of flux in hot-pressed nanofiber sample-T1 with time), it is possible to confirm that the sample T1t1 showed improved flux and lower reverse solute flux value as compared to T1t2. This also confirms the fact that T1-t2 sample with higher-temperature (175 C) hot-press treatment is not having any added benefit with respect to water flux and reverse solute flux, as compared to the T1-t1 sample with 150 °C temperature hot-press treatment. Hence, we have proceeded with the T1-t1 sample for PA deposition as well as GO-incorporated PA layer deposition.

Further, in graph, with the deposition of polyamide layer, the sample T1-t1-PA demonstrated very lesser reverse solute flux, almost close to zero, and also the time-period got extended till 24 minutes. This time period is much higher as compared to the T1-t1 sample (14 minutes). Moreover, with the deposition of GO-incorporated polyamide layer on top of T1-t1, the sample T1-t1-PA-GO demonstrated very lesser reverse solute flux, almost close to zero, and also with extended time-frame.

Therefore, combining the results from Figure 32 , Figure 33.(Effect of PA deposition on the performance of the hot-pressed T1-t1-PA nano-fiber membrane), and Figure 32 (The variation of flux in graphene oxide incorporated PA deposited hot-pressed nanofiber sample T1-t1-PA-GO with time), it is possible to confirm that the sample T1-

t1-PA-GO showed improved flux, extended time-period and very lesser reverse solute flux, almost close to zero. The overall flux value of T1t1-PA-GO is significantly higher than the overall flux value of T1-t1-PA sample.

5.1.6.3 Variation in reverse solute flux with hot-press treatment in sample T5

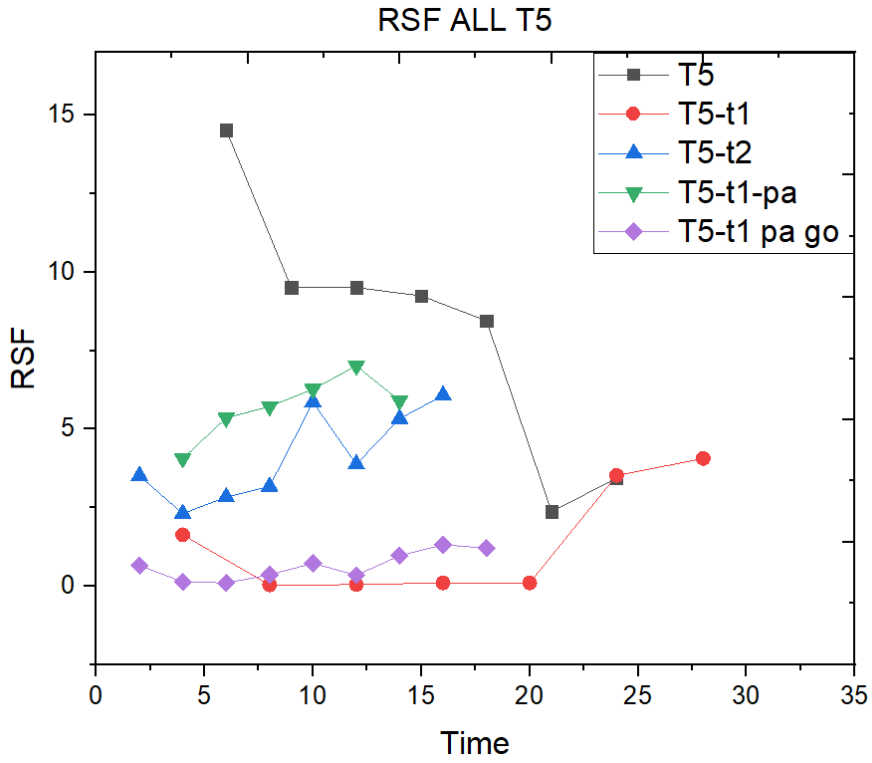

Figure 38 Variation in reverse solute flux with hot-press treatment in sample T5

Same as Figure 37 , it can be noted from Figure 38 that the RSF value of the original nanofiber sample T5 was almost 8.5 g/m^{2}h average value. On the other hand, with the hot-press treatment at 150 °C, the RSF value of T5-t1 exponentially decreased to attain an average value of 1 g/m2h. It was observed that with the hot-press treatment, the pore size reduces, thus restricting the passage of salts, and hence exponentially reducing the reverse solute flux. This performance is same as the ideal performance, which is almost zero.

Moreover, from Fig 41, the RSF performance of T5-t2 can also be observed. It was

found that for sample T5-t2, the RSF value was exponentially decreased as compared to the T5 sample, however, the value was considerably higher as compared to the sample T5t1. No additional benefit in the RSF value was obtained with higher-temperature heat press treatment. Therefore, we have proceeded with the T5-t1 sample for PA deposition as well as GO-incorporated PA layer deposition.

Comparing the RSF values of T5-t1-PA and T5-t1-PA-GO, it can be noted that the RSF value of T5-t1-PA-GO is closer to zero. Hence, combining the results from Figure 33, Figure 26 (The variation of flux in hot-pressed nanofiber samples with time), and Figure 29 (The variation of flux in graphene oxide incorporated PA deposited hot-pressed nanofiber sample T5-t1-PA-GO with time), it is possible to confirm that the sample T5-t1-PA-GO showed improved flux, extended time-period and very lesser reverse solute flux, almost close to zero. Thus, it can be confirmed that the sample T5-t1-PA-GO is attaining ideal FO membrane working conditions.

5.1.6.4 Overall variation in reverse solute flux with 150 °C hot-press treatment in samples T1, T2. T3, and T4

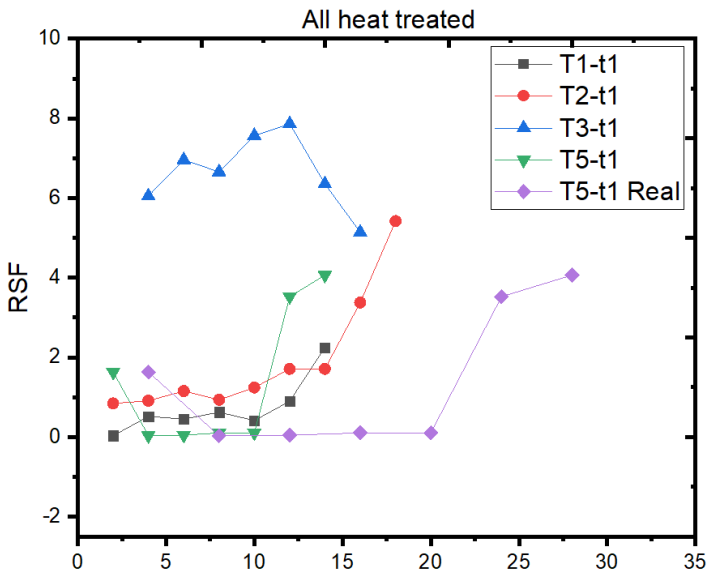

Figure 39 Variation in reverse solute flux with 150 °C hot-press treatment in samples T1, T2, T3, T5.

It can be noted from Figure 39 that the RSF values of the nanofiber samples T1-t1 and T5-t1 was almost close to zero, whereas the RSF values of nanofiber samples T2-t1 and T3-t1 was considerably higher. This Figure 40 also clearly explains the reason for selecting the PES-based T1-t1 sample and PSU-based T5-t1 sample for additional modifications.

5.1.6.4 Reverse solute flux versus time for PA and GO-PA deposited samples

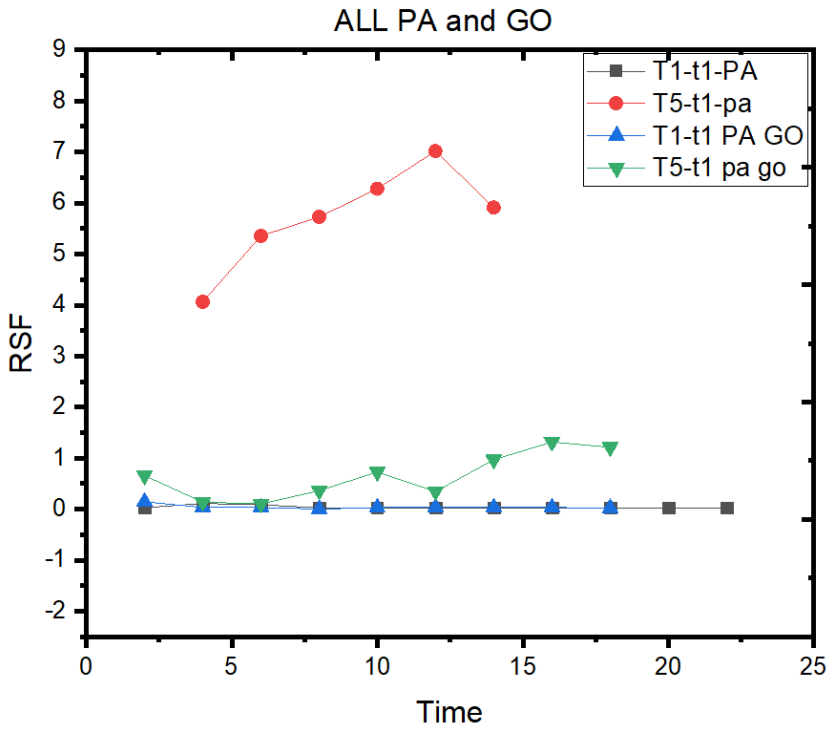

Figure 40 : Reverse solute flux versus time for PA and GO-PA deposited samples (T1-t1-PA, T1-t1-PA-GO, T5-t1-PA, T5-t1-PA-GO)

From fig 42 with the deposition of polyamide layer, the sample T1-t1-PA demonstrated lesser reverse solute flux, almost close to zero, and also the time-period got extended till 24 minutes. This time period is much higher as compared to the T1-t1 sample (14 minutes). Moreover, with the deposition of GO-incorporated polyamide layer on top of T1-t1, the PES-based sample T1-t1-PA-GO demonstrated very lesser reverse solute flux, almost close to zero, and also with extended time-frame.

Comparing the RSF values of T5-t1-PA and T5-t1-PA-GO, it can be noted that the RSF value of T5-t1-PA-GO is extremely closer to zero. Thus overall, we can observe that the PSU-based sample T5-t1-PA-GO showed improved flux, extended time-period and very lesser reverse solute flux, almost close to zero. Thus, it can be confirmed that the sample T5-t1-PA-GO is attaining ideal FO membrane working conditions.

5.2 Effect of varying flow rates

In this study, the effect of increasing recirculation flow rates of both FS and DS on water flux, water recovery %, RSF FO process were investigated applying recirculation flowrates from which are presented in table 7 .The simultaneous increase in the feed and draw solution flow rate varying flow rate experiments were only performed on Heat treated T1 T5 and there respective modified samples with PA and GO . Changing the flow recirculation rate of FS and DS showed limited influence on WF and %Wrecovery Increasing the flow rate of DS and FS as F2 from table resulted in slower water flux and lower values of RSF on all heat treated samples .Further increasing the flow from F2 to F3 resulted in very high water flux and decreased the over all time of the experiment significantly .With limited effect on RSF values .The slight improvement in flux by changing flow rate of DS and FS can be related to the rapid movement of the permeated water through the membrane system leading to increase in the hydraulic shear force across the membrane and decreasing the effect of external concentration polarization (ECP). The following studies also showed similar result [106-108] showed that flux and %recovery were enhanced for pressure driven process at high flow rates and the same trends are also reported in FO processes by lee et al.[106] were they conducted various experiments with different parameters on a hollow fiber membrane. This proves that our nano fiber samples with PA and PA -GO are performing as expected on varying flow rates .

In our experiment we also noted that increasing the feed flow rate keeps the RSF to minimum and water flux slightly increases were as if we increase draw side flow rate the RSF is very significant and sharp drop in membrane flux is also observed.

5.2.1 Varying concentrations and flowrates

After performing various modifications on the nanofiber membrane samples for the FO performance analysis, one of the better performing membranes, i.e., T1-t1-PA, was selected to study the impact of varying concentrations (feed solution and draw solution) with time. Moreover, variation in the FO performance with changing flow rates with each of the concentration on the sample T1-t1-PA was examined. All tests were carried out on the same membrane sample with constant back wash of 20 min on each side in between the experiments. Moreover, the same sample was used to test the membrane if it can withstand varying process parameters like flow rate and concentration in the feed side and the draw side. The experimental flowrates are named as F1, F2 and F3 for the feed side and draw side, and are summarized in the Table.1. For each flow rate, various concentration parameters were tested. For 0. 1M NaCl feed, the draw solution concentration varied from 0.5 M to 2 M NaCl and for pure DI water, the draw solution concentration varied from 0.5 to 2 M NaCl. The details of concentrations and abbreviations used in this chapter are presented in table. 7

Table 7 Variation in the feed side and draw side flow rates

Sl. no	Flow Rate	FEED SIDE (CCM)	DRAW SIDE (CCM
1	F1	900	500
2	F2	1250	1000
3	F3	2000	800
4	F4	1000(+)	1000(-)

Table 8 Variation in the feed side and draw side concentrations

Sl.no	CONCENTRATION	FEED SIDE (M NaCl)	DRAW SIDE (M NaCl)
1	C1	0.1	1
2	C2	0.1	2
3	C3	0.1	0.5
4	C4	0	1
5	C5	0	2
6	C6	0	0.5

The water flux of nanofiber membrane samples was analyzed in a cross-flow mode, and the results obtained are presented in the following sections. In the first experiment, Flow rate F1 was selected and all variations in concentrations C1 to C6 were tested to study the effect of flow rate and concentration.

5.2.1.1 Varying concertation at Flow rate 1

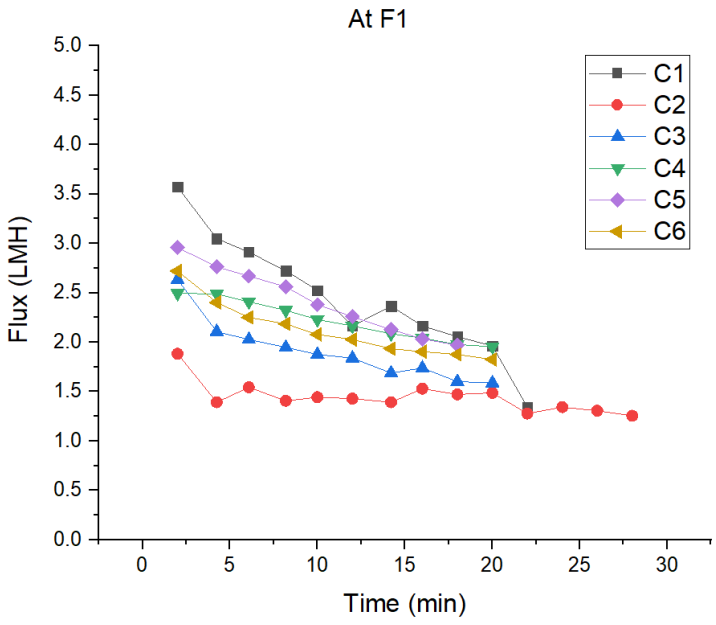

Figure 41 Variation of flux at F1 with changing concentration in T1-t1-PA nanofiber sample with time.

From figure 41, it can be noted that, by using C1 and C5 concentrations at flow rate F1, the sample showed better flux (2.5 L/m^{2}h) as compared to other concentrations. Out of the concentrations C1, C2, and C3, the concentration C1 showed highest flux, whereas out of the concentrations C4, C5, and C6, the concentration C5 showed higher flux. This is due the fact that the osmotic gradient is highest in this case (0 and 2 M), and hence the better flux. Overall, it can be noted that the best performance is observed using C1 concentration as it uses lesser salt (compared to C5) and also gets better flux. However, the most stable and consistent flux is observed in C4. The time period of the FO process extended between 20-23 mins and C2 taking 28 mins .

5.2.1.2 Varying concentration at Flow rate 2

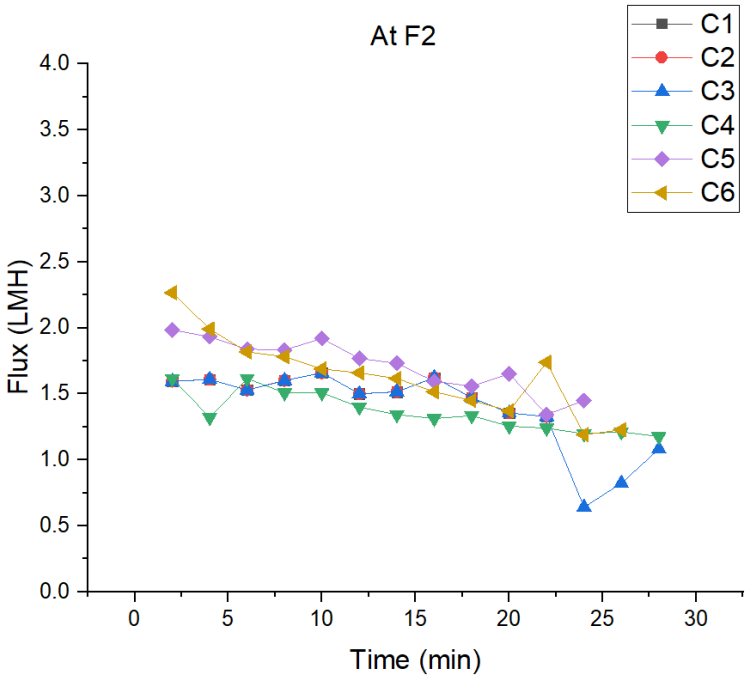

Figure 42: Variation of flux at F2 with changing concentration in T1-t1-PA nanofiber sample with time

From figure 42, it can be noted that when the flow rate F2 is used, the flux dropped

significantly. The flux range achieved was much higher using flow rate F1 (overall flux was between 2-3 L/m^2h) and by using flow rate F2, the flow rate at varying concentrations has dropped the flux between 0.8 to 2 L/m^2h . Here, the concentrations C5 and C6 showed better flux as compared to other concentrations. Using F2, the C1 (from 3 L/m^2h to 1.2 L/m^2h) and C4 (from 2.2 L/m^2h to 0.8 L/m^2h) flux dropped to almost half of what was achieved using F1. It can be noted that the concentrations C1 C2 C3 gave almost similar results as confirmed by the overlapping of the curves in figure 42. The sample C6 showed highest flux. Here, the best overall performance is observed using C5 concentration as it has the higher salt corresponding to higher osmotic gradient at this flow rate. The time period of the of the FO process extended between 25-30 mins which is higher than F1. Using flow rate very close to each other FS as 1250 ccm and DS at 1000 ccm yielded a decreased flux and takes more time leading to more energy consumption in running the experiment.

5.2.1.3 Varying concentration at Flow rate 3

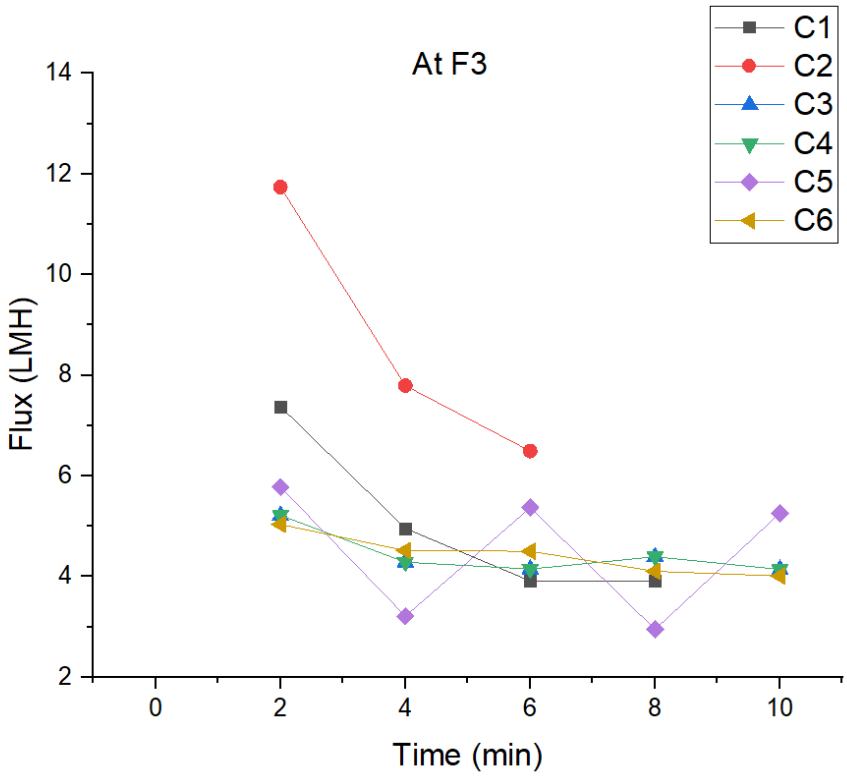

Figure 43: Variation of flux at F3 with changing concertation in T1-t1-PA nanofiber sample with time.

From figure 43, it can be noted that the flux achieved for all the concentrations is significantly much higher than the flow rates F1 and F2. Here, the concentrations C1 and C2 showed better flux as compared to other concentrations. There is a significant increased flux for C1 from 3 L/m^{2}h to an average of 5.5 L/m^{2}h, while C2 the flux jumped from 1.5 L/m^{2}h to avg of 8 L/m^{2}h while operating in F3. Similar increase in flux is seen in all other concentrations also when comparing figure 43 and figure 41. The time period of the of the FO process using F3 flow rate is one third of the time required for the experiment using F1 and F2 flow rates. Here, significantly higher flux was achieved when using C2, and this is due the fact that the DS flow rate is significantly lower and the and osmotic gradient is higher, which corresponds to

increased flux. Overall, the best performance is achieved for concertation C1 as the flux is higher while experiment run a bit longer than C2 giving a better stability and control on the experiment.

5.2.3 Flux and RSF at all flow rates for F1

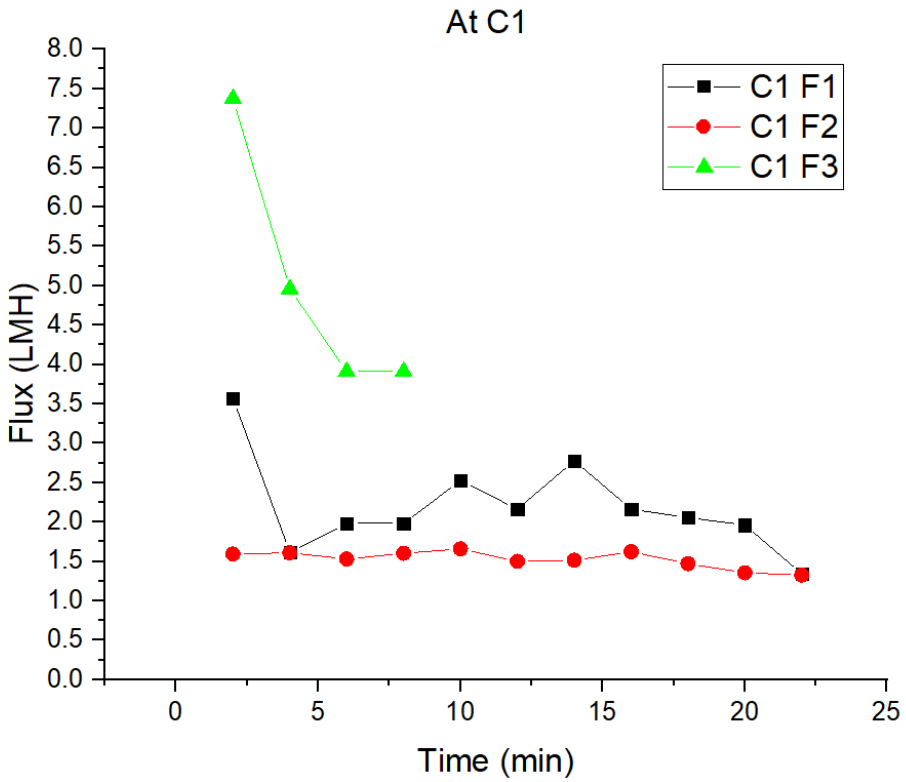

Figure 44 varying flux at C1 concertation for T1 t1 PA.

The figures 44 and 46 gives the overall picture when concentration C1 is used at different flow rates .

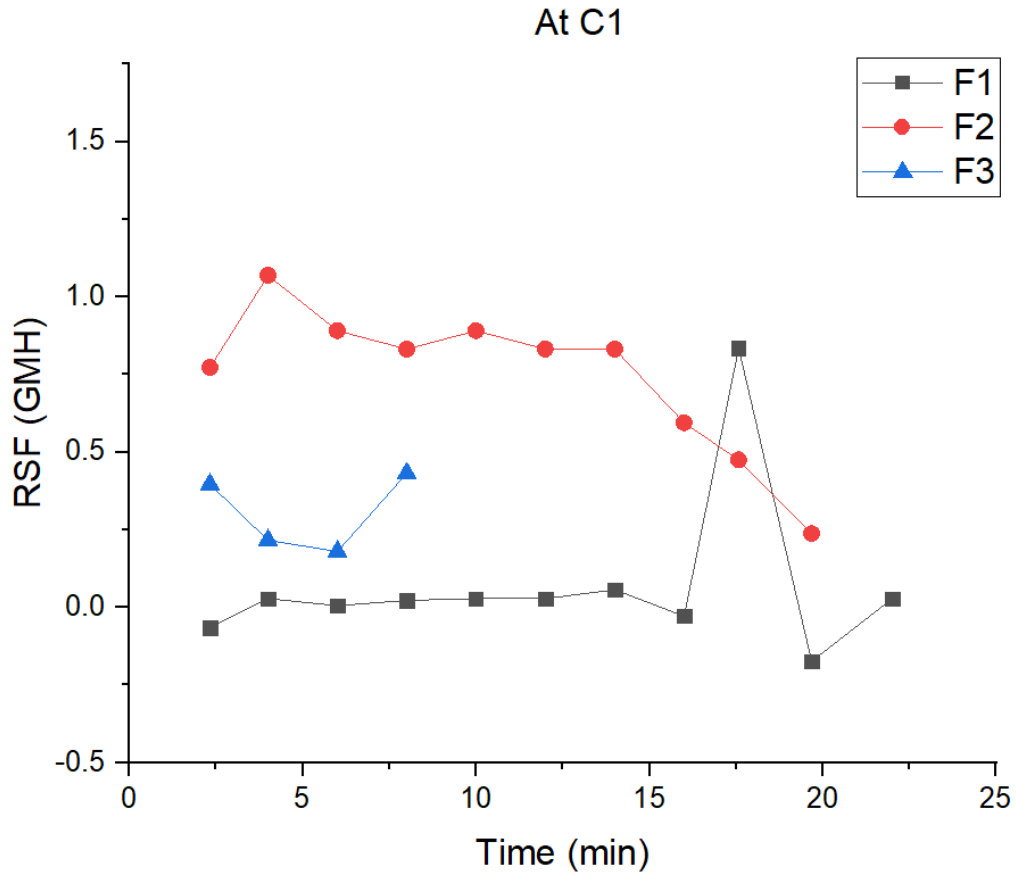

Figure 45 RSF for C1 at varying flow rates for t1 t1 pa

Here we it is clear from the graph that C1-F3 is having high flux but it has slightly higher RSF values which is still very good but as compared to C1-F1, the flux is much more stable and the RSF values are close to commercial membranes while having better flux. For the Flow F2, at concentration C1, the flux is lower and the RSF value is higher as compared to others. It is to be noted that even there is difference in performances, all the nano fiber membranes have performed very well as compared to some commercial membranes.

5.2.4 Variation in reverse solute flux with varying concentrations in sample-T1

In all the modified nanofiber samples prepared, it is evident that all of them have very low vales of reverse solute flux here in varying the concentration and flow rate. It was observed that the reverse solute flux has varied by a very small margin. These results showed that all the modified nanofiber membranes successfully limit the reverse solute flux while showing variation was observed in flux values and over all run time of the experiment.

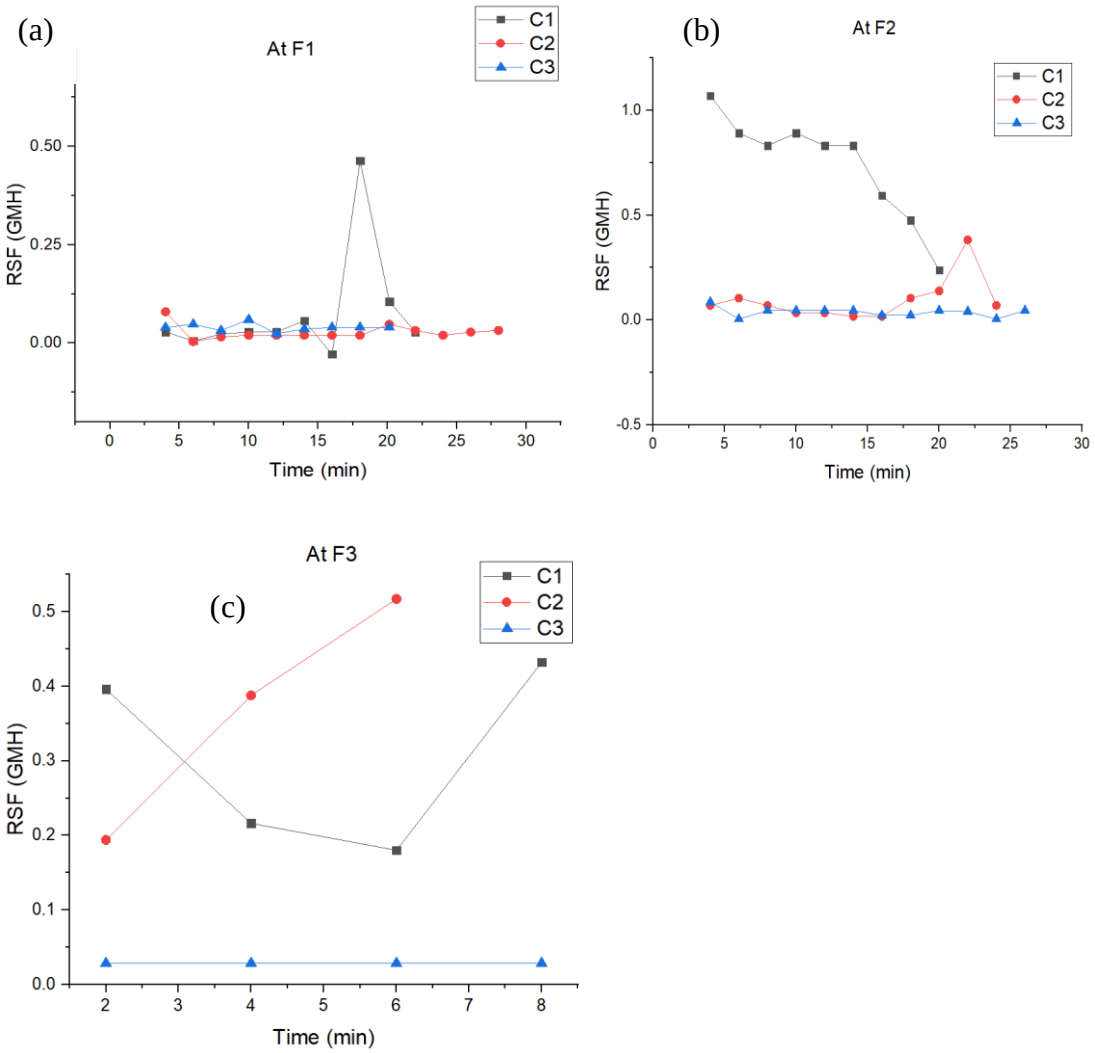

Figure 46 RSF values for varying concertation at (a) F1, (b) F2 and (c) F 3

In Figure 46 a, it can be noted that all the RSF values are overlapping each other showing very little change. The small change that is observed is only in C1 at F1 which is under 0.50 gm2/h. Similarly in figure 46 b, the C1 is having slightly higher RSF values while the C2 and C3 are almost same as F1 values. Similar trend is seen in flow F3 for RSF values .

5.2.5 Varying Flow rate F4 for flux and RSF

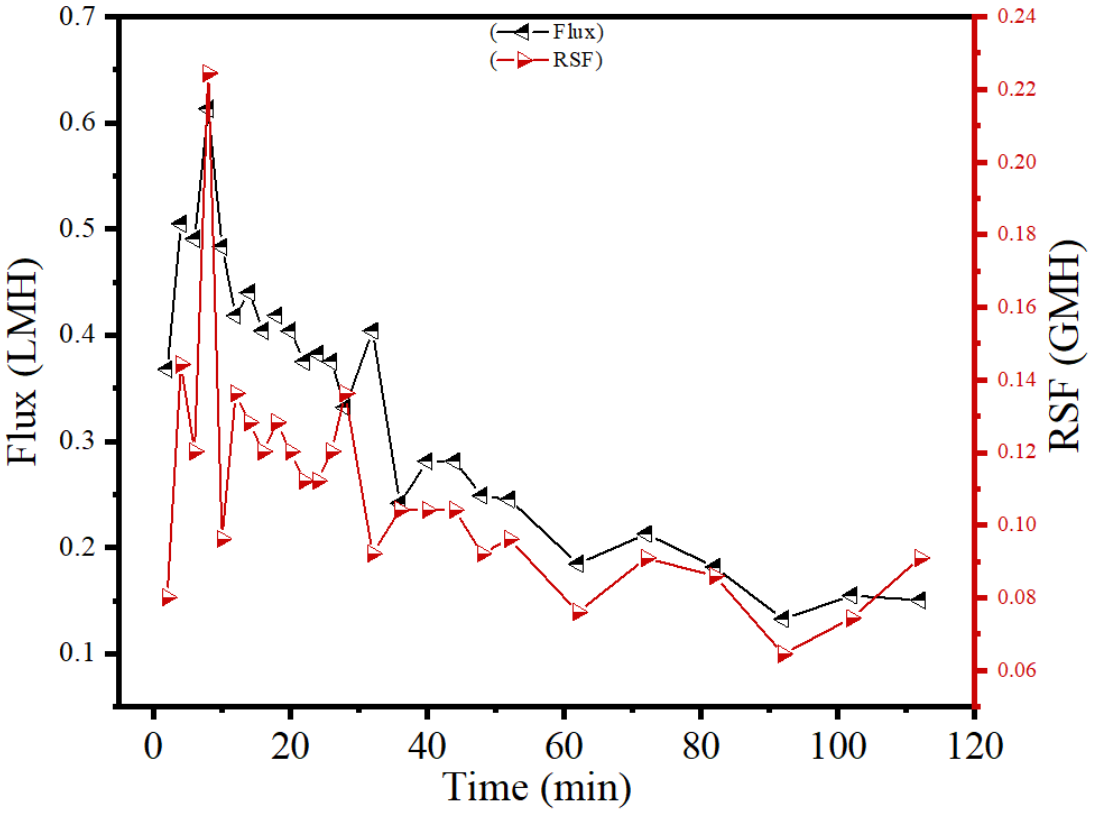

Figure 47 Same flow rate fs ds F4 for T1 t1 pa with time

From the figure47 , it can be concluded that running the experiment with equal FS and DS value with no pressure on the feed side results in very low flux values and the RSF value does not show any significant positive or negative trend. The RSF values shows the same trend as other readings.

5.2.6 Optimizing flow rate and Long term Experiments

5.2.6.1 Optimum Flow rate

Four flow rates were tested to study the effect of flow rate on newly developed and modified nano fiber membranes. It was found that the highest flux is achieved in Flow F3 ,whereas as the lower flux was observed in F2 as seen in 50, The lowest flux was observed in F4 which is seen 53. This is due to the fact these both have significantly higher flow rate for draw side. From literature we can note that the higher the flow rate in the draw side the more RSF higher value is obtained and lower flux. In all our samples the RSF was at minimum but the flux values achieved with higher DS flow rate is very low. It can be concluded that the closer feed side and draw side flow rate are the lower flux is obtained and the time period of the experiment significantly increases. In our experiment we find the optimum Flow rate is F1 as it has a better controlled flux throughout the experiment and over all time . The RSF values in all nano fiber modified membranes in this study do not change significantly with varying concentration and flow rates. Thus we can conclude that It doesn't have a significant effect on over all RSF values

5.2.6.2 Long term studies

Nano fiber samples T1 t1 PA and T1 t1 PA GO were used to test for long term performance. Two methods were adopted to do the required studies. For T1 t1 PA, 18 experiments were done with 20 mins back washing between each experiment. For this, 3 L feed and 1 L draw solutions were used. Parameters of the experiment are summarized in tables 7 and 8 . The membrane was found to perform well without any dip in performance throughout the experimental study. In total all the experiments were done at varying process parameters for in total of 10 hours and the results of which are discussed in the section above. After all the 18 experiments, there are no sign of possible

decrease in the performance and the overall experiments performed are presented in figure45 to figure 47 In total, 45 liters of feed solution was transferred via the T1 t1 PA membrane to the draw side in the 18 experiments.

Nano fiber sample T1 t1 PA Go was used to do a similar study at a set Flow rate F1 at concentration C1. In this experiment, the FS side 0 1. M in 20 liters in run 1 and 6 liter in run 2 , were the DS was having 1M two liter solutions for both the runs. These experiment were performed without back washing or any other change and the experiments were performed without any break.

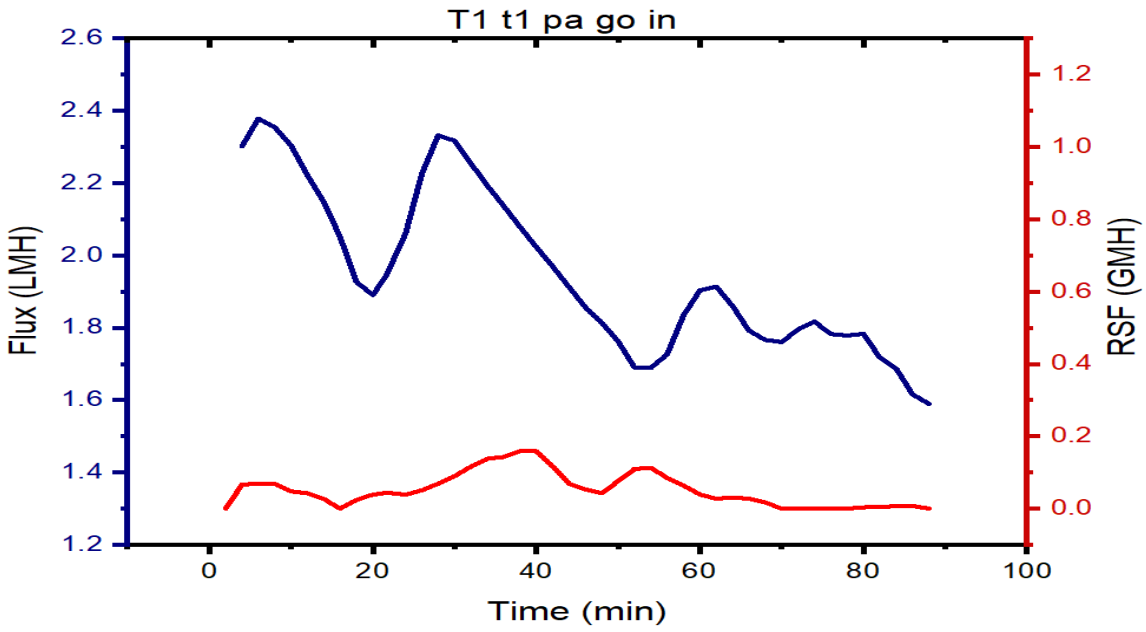

Figure 48: long term flux and rsf at F1 C1 for T1 t1 pa go membrane with time

Figure 48 shows the long term experiment performed were it can be seen the flux values are ranging between 1.6 ot 2.4 l/m^2 h and the RSF values below 0.2 g/m^2 h. This shows the superior performance of the nano fiber sample as it can go on for longer experiments also. The second run as show in figure 49

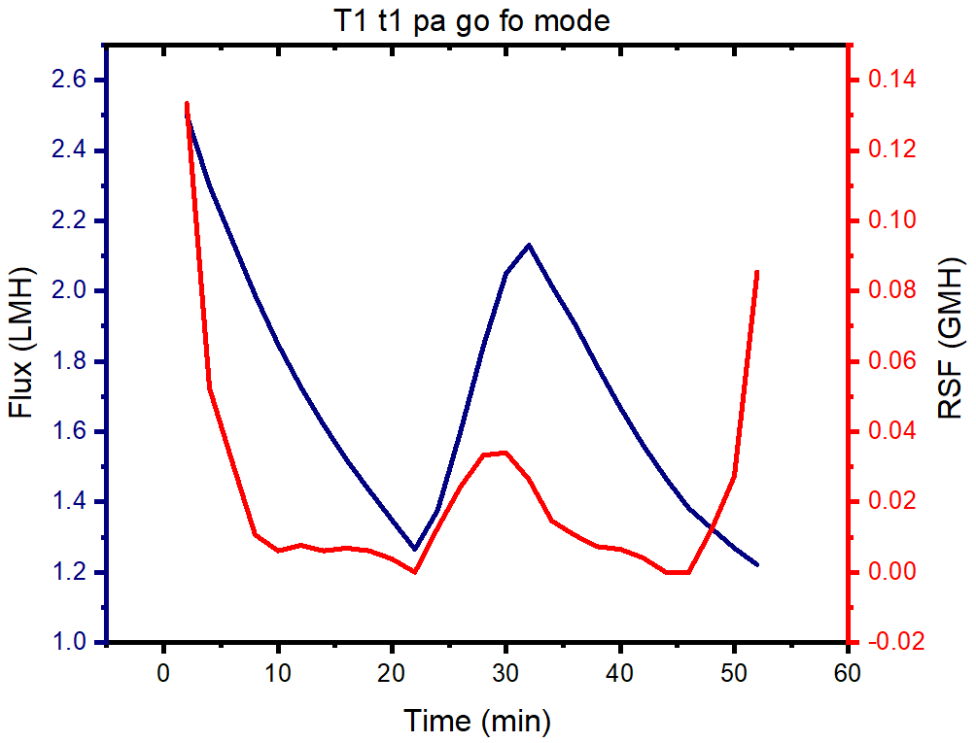

Figure 49 long term flux and RSF at F1 C1 for T1 t1 pa go membrane with time

The experiment was performed in a batch 3 liter FS solution and 1 liter ds solution at C1 concertation. After 28 minutes, both the FS and DS were changed. The trend is observed in both batches is similar to the trend observed in run 1 shown in figure 49 between range of 1.2 to 2. L /m^2 H. This confirms that there is no degradation in the performance after running the experiments for two runs with different volumes of water. The total water passed through the nano fiber membrane T1-t1-Pa-GO from feed to draw side is 26 liter in record total time of 160 min. In similar time, the commercial membranes performance is show in figure 50.

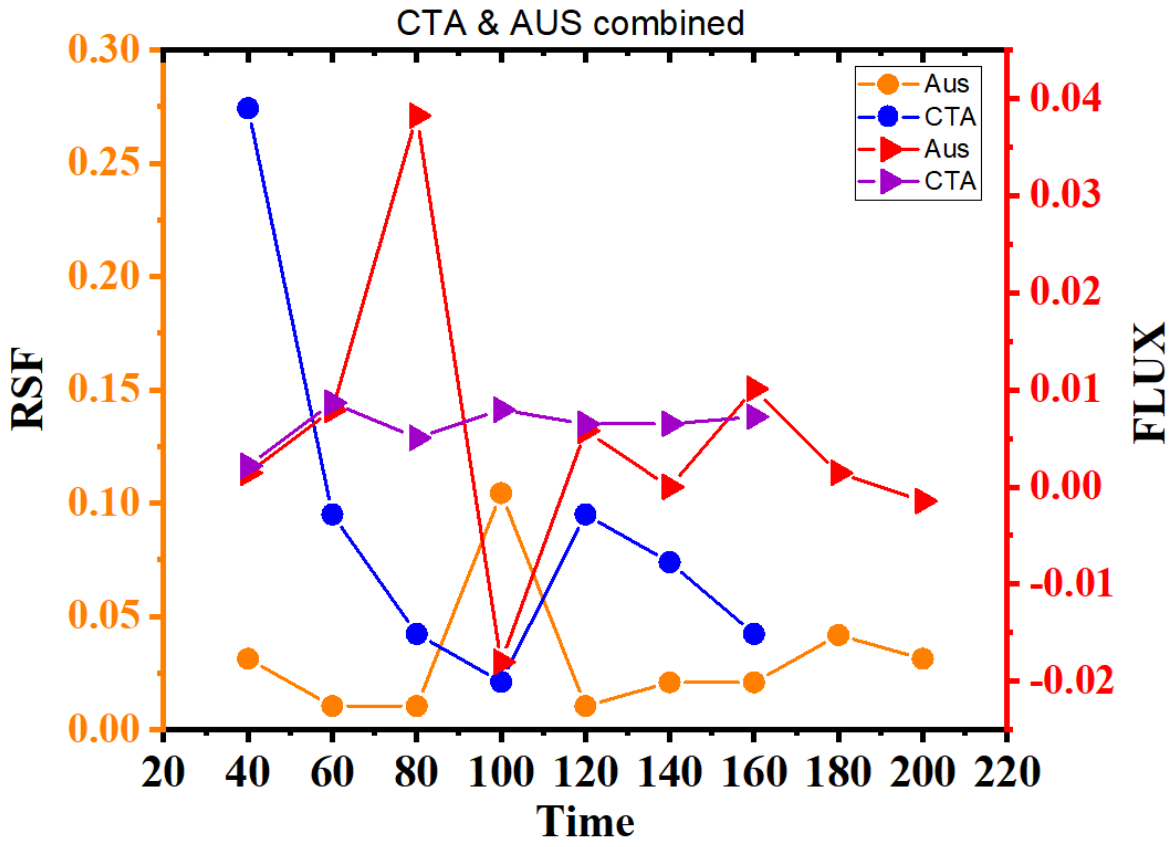

Figure 50: Commercial membrane RSF and flux

Commercial membranes were tested for FO mode in exact same F1 and C1 conditions in 3 L FS and 1 L DS solutions respectively. The results showed similar RSF values as achieved by our modified nano fiber samples were as it can be seen that the flux of the commercial membranes is significantly less, as shown by the right facing triangles in figure 50. The amount of water transferred from feed side to the draw side is 2 liters in 220 minutes. The membranes prepared by solution blow spinning technique in this work showed significant increase in overall performance and efficiency when compared to commercial TFC and CTA based membranes.

5.2.7 Salt Rejection for TFC Nano fibers

TFC nano fibers achieved salt rejection between 92 to 99 % using NsCl as the draw solution which was used as to be beneficial in water flux, less membrane fouling and high salt rejection . Base Nanofiber membranes fabricated step wise into TFC base membranes via interfacial polymerization technique and membrane prepare via this method often show high salt rejectin and high water permeability , this process of having a TFC membrane for desalination is extensively studied topic in RO and well established IN the field of RO membranes were similar results are achieved [109],

Our TFC nano fiber membranes show very low RSF values and high salt rejection values which on addition of nano particle only increase the salt rejection marginally which means the main driving force is of higher salt rejection is formation of heat treatment process and formation of PA layer this is similar to results achieved by dagchen ma et al during their experiments [110]

Salt concentration was monitored on both feed side and draw using HACH Multiparameter and these values were used to calculate the salt rejection [111, 112].

The equation used Shown in figure 51

$$R = \frac{C_f - C_p}{C_f} \times 100\%$$

$$C_p = \frac{C_t \times V_t - C_0 \times V_0}{V_t - V_0}$$

Figure 51 Equation For salt Rejection

Here the C_f and C_p are TDS (concentration) values of feed and permeate values C_o and C_t are initial and final salt concentrations of draw solutions respectively V_o V_t are volumes of the same .

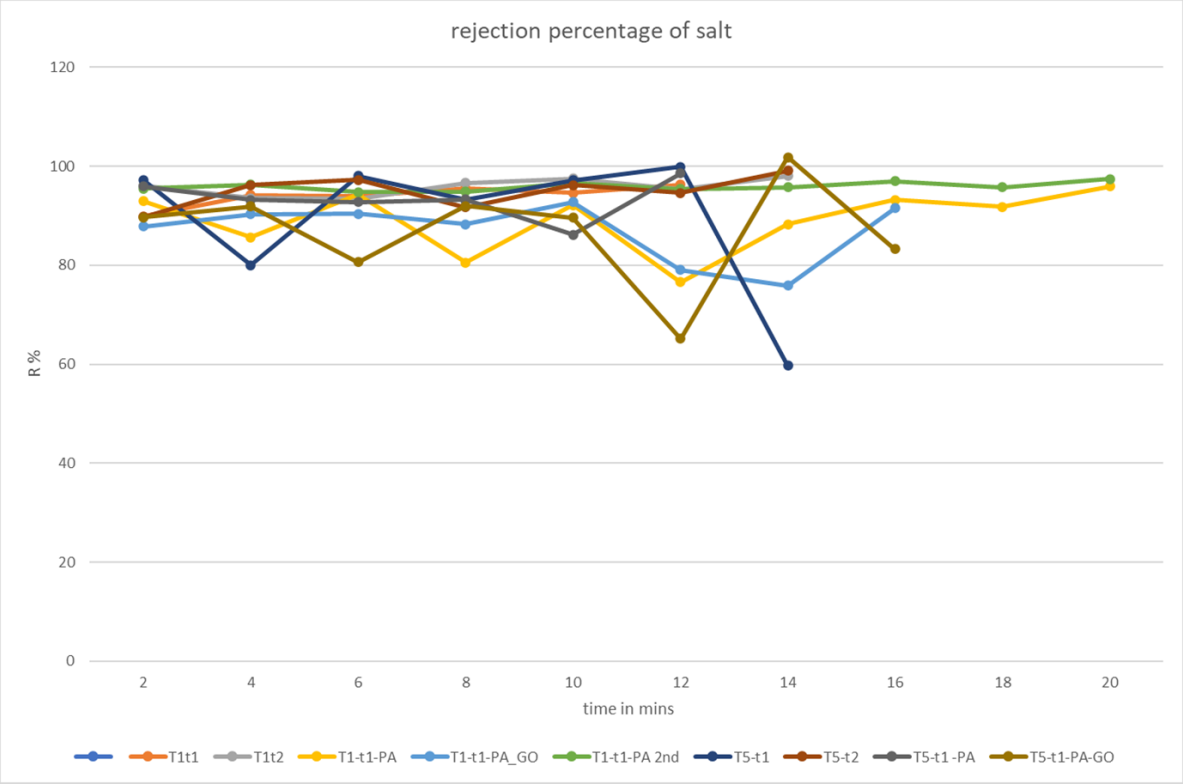

Figure 52 R % vs TIme for TFC nano Fibers

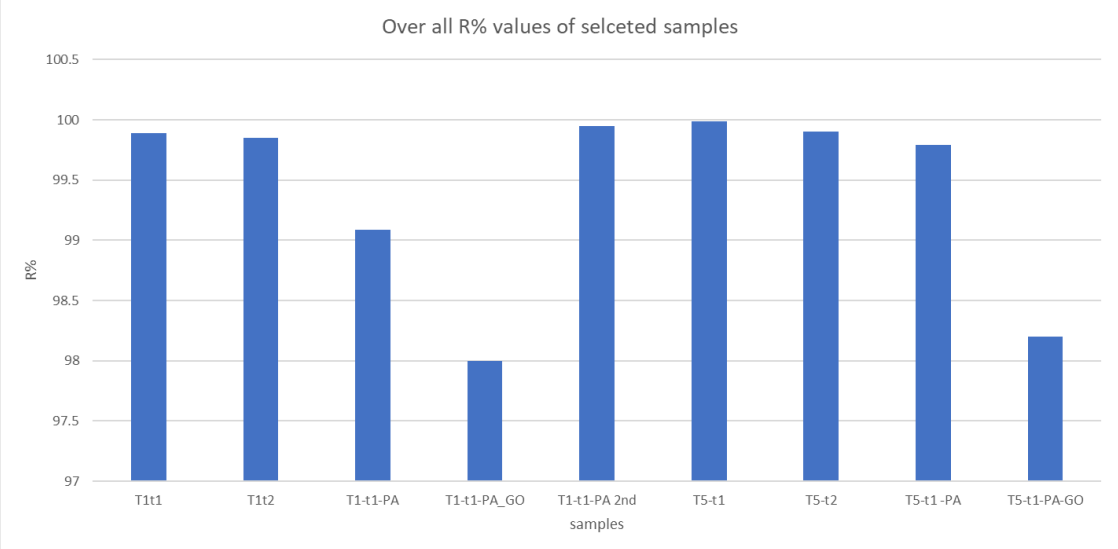

Figure 53 Over all R5 values of TFC Nano fibers.

T1 and T5 subsamples were selected to study Salt reject R % values of the newly fabricated and formed Nano fiber TFC membranes in this thesis work. our heat

processed TFC nano fibers exhibit excellent salt rejection . the lowest average rejection values are in the 80 % range and higher average is well above 95 % average salt reject values as show in figure 52 & 53. There is slight decrease in the salt rejection values in the TFC membranes with GO nano particles which is insignificant as these membranes also have higher flux when compared to the TFC nano fiber membranes with higher flux as the GO nano particles are super hydrophilic in nature which explains the increase in flux [113]. This increased flux is the reason for slight decrease in the salt rejection values .

To conclude we see the base heat processed nano fibers have highest salt rejection values but as shown in section 5.1 they have lower Flux and slightly higher RSF values where as TFC nano fiber with PA and TFC PA-GO have higher flux and RSF values and slightly lower salt rejection values.

5.3 Membrane Characterization and testing

5.3.1 Mechanical stability analysis .

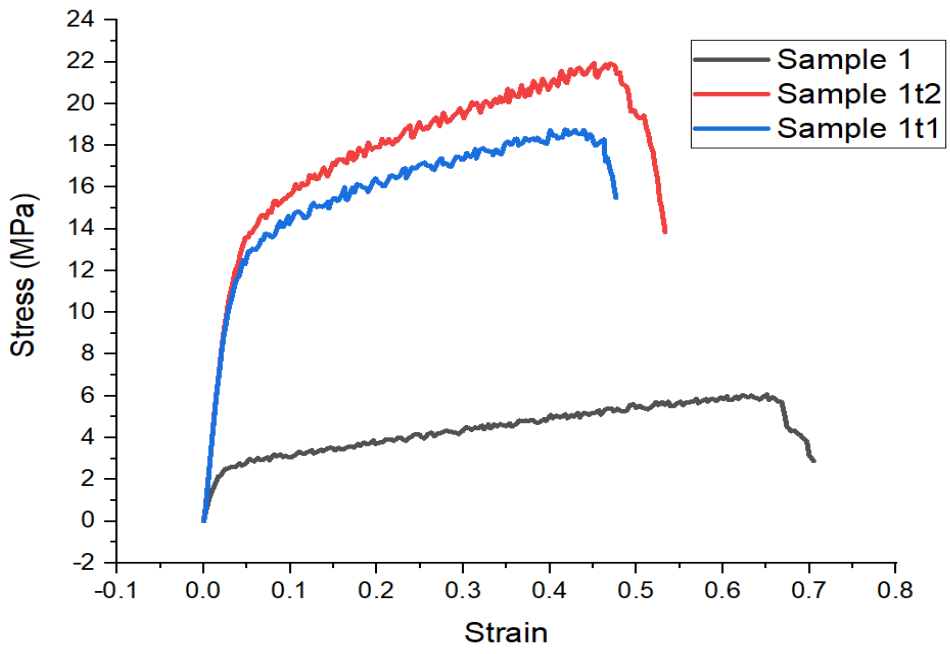

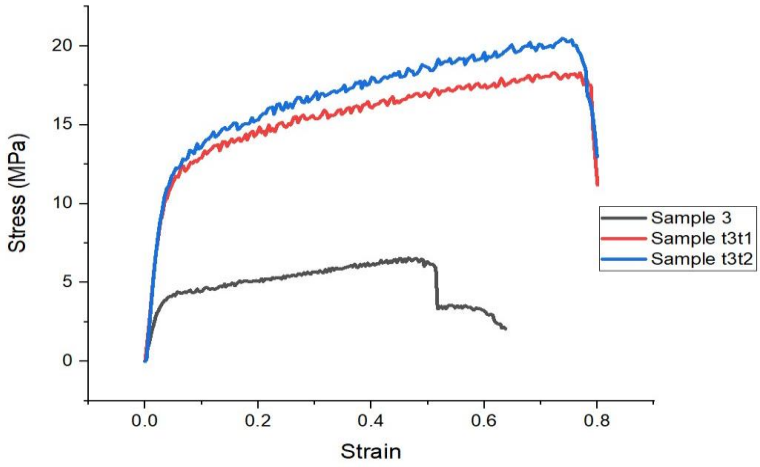

Figure 54 Strees Strain Curves of (a) sample 1 T1 at varring tempertaure ,(b) sample t3 at varrying temprature

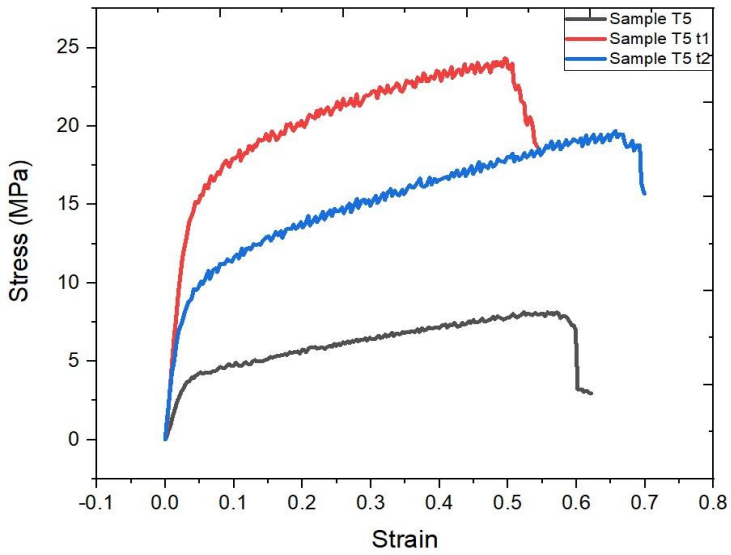

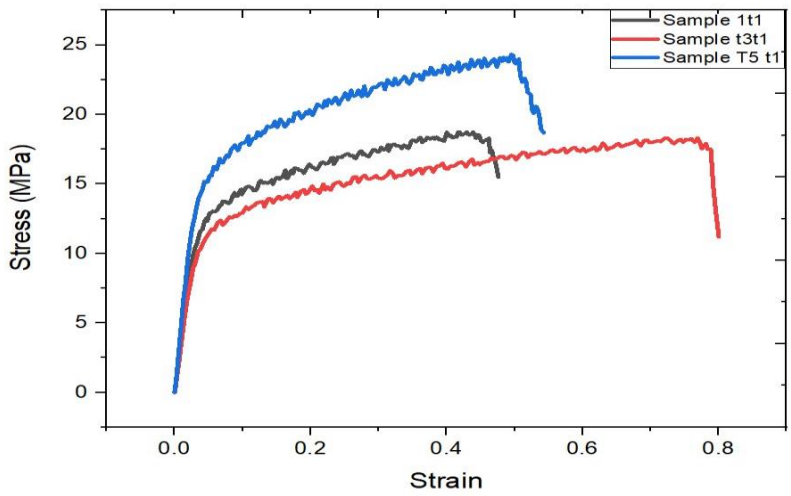

Figure 55 Strees Strain Curves of (a) sample 5 at varring tempertaure ,(b) All samples at T1 at varrying temprature

Mechanical stability is a very important characteristic for membranes used in any separation membranes' efficiency, as it should withstand high water flux. Table 8 represents the mechanical strength in terms of Young's modulus, tensile strength and elongation at break and stiffness for the PES(T1) and PSF(T3 and T5) samples before and after heat treatment . It is clear from the values that the mechanical properties are enhanced significantly after heat treatment [114, 115]. With the T1-showed increase in values of Young modulus by 3.1times and tensile strength by 3.4 times. This trend was repeated in sample 3 and 5 also which confirms that hot pressing at 0.5 tonnes at temperature of t1 &t2 significantly increases the strength of the fibers. This is due to fusing of the nano fiber on the top and bottom surfaces resulting in the strength gains [116, 117]. In our case, the at t1 the condition for hot pressed samples were 150^{o} c for 10 min at force of 0.5 tonne/m^{2}, For t2 the force was kept the same at 0.5 tonne /m^{2} and temperature was increased to 175^{o} C for 6 mins. It is also noticeable that increasing the temperature further at t2 improves the strength and stiffness of nano fiber samples. . This can be attributed to the increase in the toughening level attributed to the slight

melting of nanao fibers a this temperature is close to their tg value of the base polymer [118].the graphs can be observed in figure 54 and 55 above. Further details are summarized in table 9

Table 9 Mechanical properties of the PS and its nanocomposites before and after heat treatment

Samples	Tensile Strength (MPa)	Young's Modulus (MPa)	Elongation at break (%)	Stifness (N/mm)
T1	6.17± 0.50	172.10 ± 5.33	70.0 ± 2.15	49.08± 2.5
T1-t1	21.01± 0.56	536 ± 20.25	68.89 ± 2.80	62.39± 3.5
T1-t2	22.07± 0.53	574.95± 0.43	42.5 ± 0.95	64.62± 3.5
T3	6.63 ± 0.16	277.41 ± 0.92	64.5 ± 0.50	66.192±2.6
T3-t1	18.49 ± 1.16	577.04 ± 0.92	80.5 ± 0.50	72.192±0.5
T3-t2	14.56 ± 0.16	522.41 ± 0.92	61.5 ± 0.50	67.298±2.2
T5	8.2 ± 0.16	190.41 ± 0.92	62.5 ± 0.50	46.192±3.5
T5-t1	24.63 ± 0.16	867.41 ± 0.92	54.5 ± 0.50	86.192±1.2

5.3.2 Thermal stability of nano fibers (DSC AND TGA)

The thermal stability of the PSf and PES nanocomposites is illustrated in Figure. 56 It is clear from both the thermograms and derivative thermograms that the hot pressing sample at 150^{o} C for 10 min under 0.5 tonne /m^{2} enhanced the degradation temperature of T1 and T5 and thus the thermal stability. While the base T1(PES) and T5(PSF) decomposes at 436.78^{o} and , the heat treated T1-t1 and T5-t2 decomposes at 438.51^{o} and respectively . The inset of the figure marks the onset of degradation temperature, which also shows the higher thermal stability for the heat treated nanofibers.

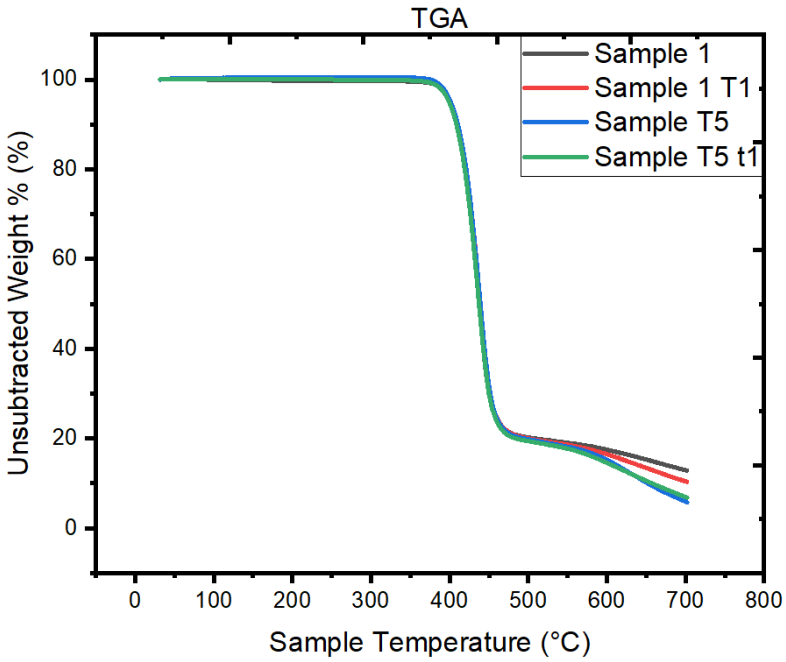

Figure 56 TGA curves of samples T1 and T5

The heat treated samples offered better dispersion and improved the interfacial interaction with the base samples. This is due to the combined heat resistance provided from the entailment of nanofibers and fusing with each other. This result is in agreement with the findings of various research mentioned above, where they also noticed an increased thermal stability while het treating the nano fibers. [119]. However, at higher temperatures and force greater than 0.5 tonne /m^2 may cause agglomerations within the polymer and cause more dense and less dense region with in the nanofiber samples which may cause loss of thermal stability due to the reduction in the uniform contact surface between the layers of the nanofiber polymer matrix .

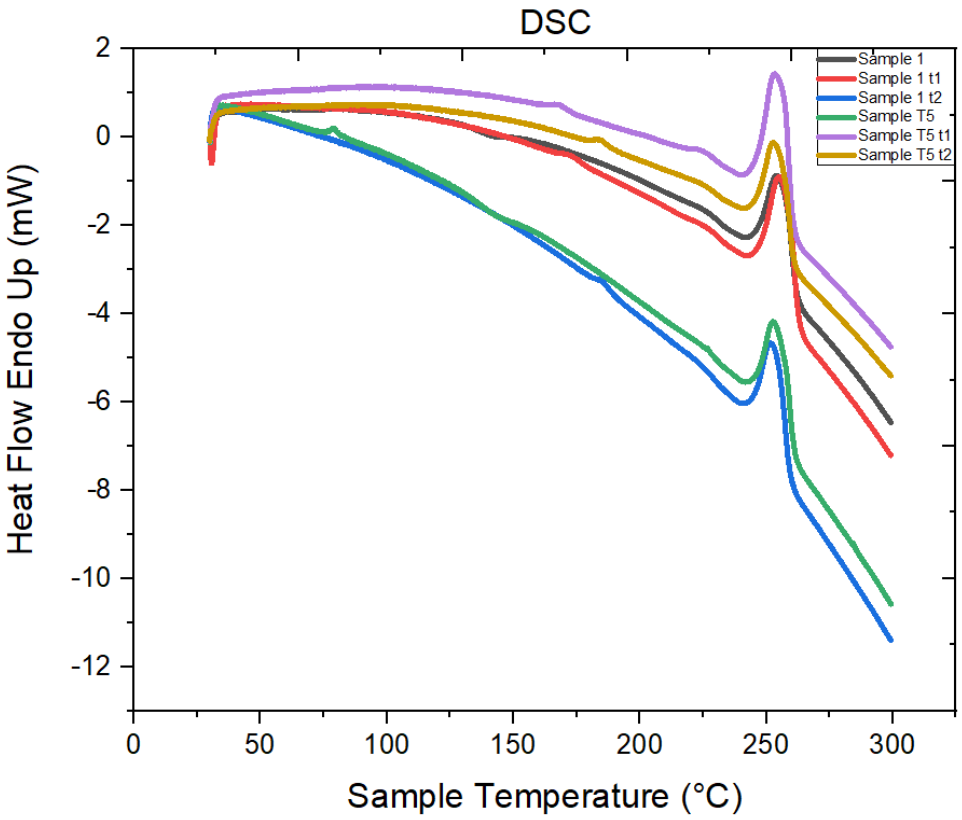

Figure 57 DSC curves of samples T1 and T5

The base T1 and T1-t1 nano fiber & heat treated nanofiber samples show a relatively large and s endothermic curve with a peak at 255.31 and 255.77 However, for T1-t2 nanofibers, the peak shifted towards slightly lower temperature at 250. It was observed that the peaks of the endothermic curves remains similar between base T1 and T1-t1 samples and there ΔHm values also saw an increase from 24.28 j/g to 28.19 J/g. This shows there is very little to no crystallization with heat treatment as this demonstrated that heat treating the polymers nano fibers have negligible effect for crystallization of the fiber. Where's as the T1-t2 shifted toward the lower temperature from 255 to 250 and the ΔHm values are observed at 26.09.Apart from this there are two peaks observed at 172 and 185.22 before the main peak in the dsc graphs , this corresponds to the solvent used in fabrication step or some other impurity undergoing a phase transition. All the peaks of samples tested for dsc are presented in Figure 57

5.3.3 XRD

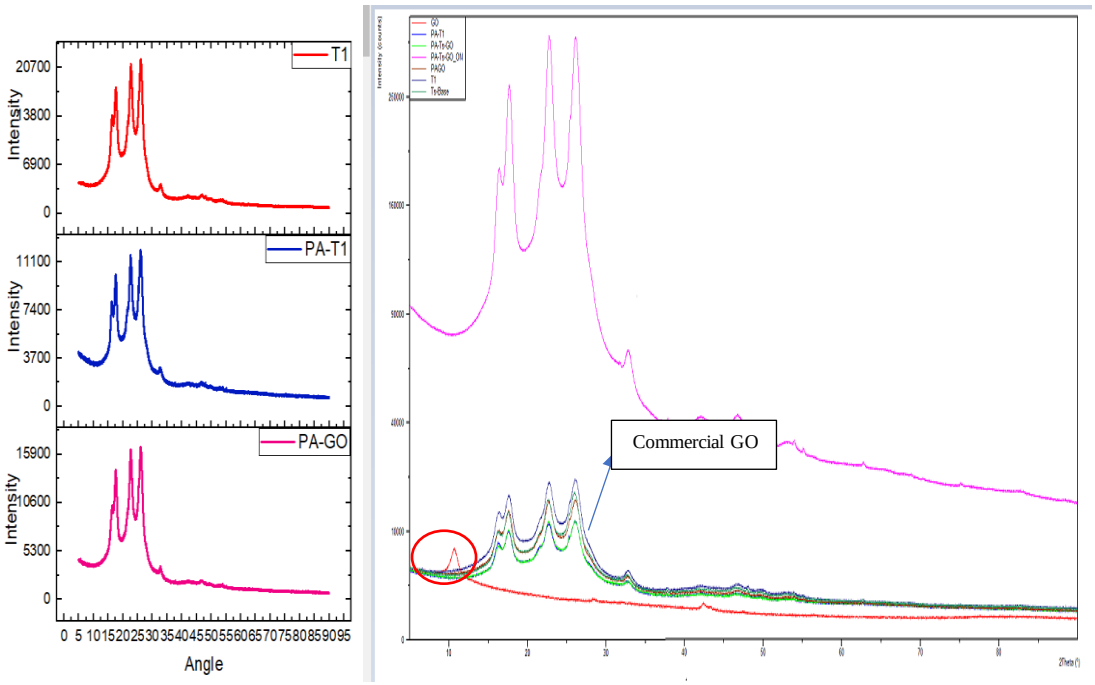

Figure 58 XRD Peaks

The nano fibers samples were characterized using XRD to find presence of GO and PA on samples .The finger print peak for Go is reported to be at 2θ =10 degree and for polyamide layer is at 21 degrees both these values are widely reported in literature [120, 121] .Figure 58 Shows XRD pattern of Sample T1, T-t1,& T1-t2 ,but the GO peak is not visible in the graph (a) .The encircled part of the graph b shows the XRD of commercially purchased GO with a distinct peak at 2θ=10 degrees ,the reason the peak did not show in XRD for our sample is the use of very small quantity of 0.006 wt % of GO was used whereas the ideal standard in fabricating and modification of membranes with GO generally use 0.1 wt % to 4 wt% in synthesis of there membranes [81, 121, 122]

Despite of very less quantity as compared to other studies membranes with go modification are performing with high flux values at near ideal behavior, the presence of Go is clearly confirmed by the peaks observed in FTIR analysis explained below

5.3.5 FTIR analysis

Figure 59 presents the FTIR spectra for all polymeric base samples and polymeric base with PA and GO modified samples used in this work. The absorption peaks ranging from 1500 cm^{-1} to 1700 cm^{-1} correspond to aromatic C-H stretching present in the polymeric matrix. The vibrational peaks ranging from 1300 cm^{-1} to 1500 cm^{-1} are mainly due to the aromatic C=C bond stretching in PA units in sample PA and PA GO samples(marked with black square) .Similar peaks for PA are widely reported in literature [123] .While the broad peak at 3442 cm^{-1} corresponds to the oxygen and carbon bond vibrations as it clearly shows the presence of graphene oxide in sample T5PA-GO (which is sample T5-t1-PA-GO), hence the broad peak corresponds to the vibration presents in the C-O bond, which is confirmed by its broad peak.[124, 125]. Other peaks that are visible are from PES from S=O the absorption peak is at 1025 cm^{-1} which is also widely seen in literature [126]The FTIR shows the presence of first modification on nano fibers which is the polyamide layer and also the second modification which is the incorporating GO in pa layer . by doing these two modification the nanofiber based fabricated membrane samples are performing very good .

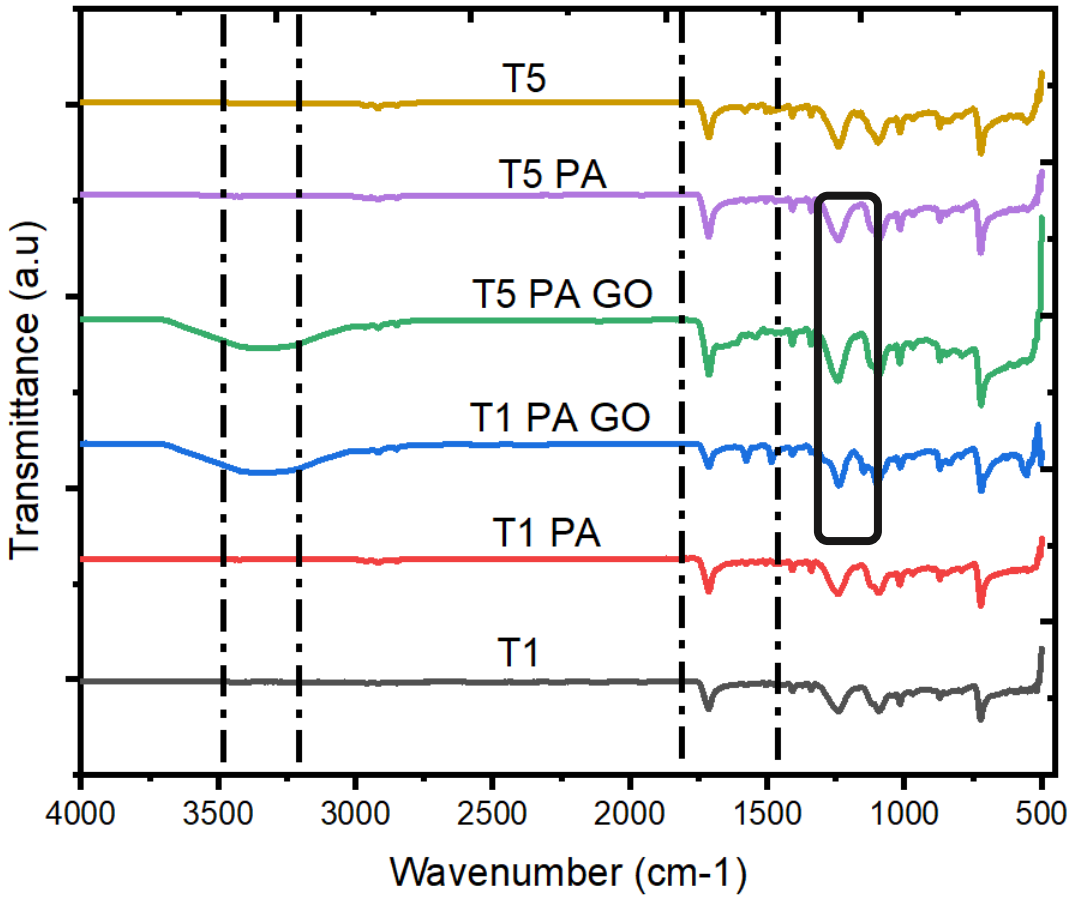

Figure 59 FTIR peaks of sample T1 all and T5

5.3.4 Atomic Force Microscopy

To further check the nanofiber surface morphologies, AFM analysis were carried out on nanofiber membrane in its original state and after heat treatment of the fibers at t1 and t2 respectively .From the surface roughness result summarized in table above it can be observed that the roughness trend between the heat treated and not treated sample is different .IN original condition the surface roughness is observed at 242.98 nm in sample T1 and 94 nm in sample T5. In hot treated samples the roughness value is much lower ranging between lowest of 49.60 to largest value of 159.114. The lower values of T1-t1 and T5-t1 means these surface are smooth and less fouling compared to others to which most of the experimental membrane testing work and modification work was

carried out on these two samples. The values in the range 50 nm is generally observed in most of commercial and lab synthesized polyamide membranes [122, 127]

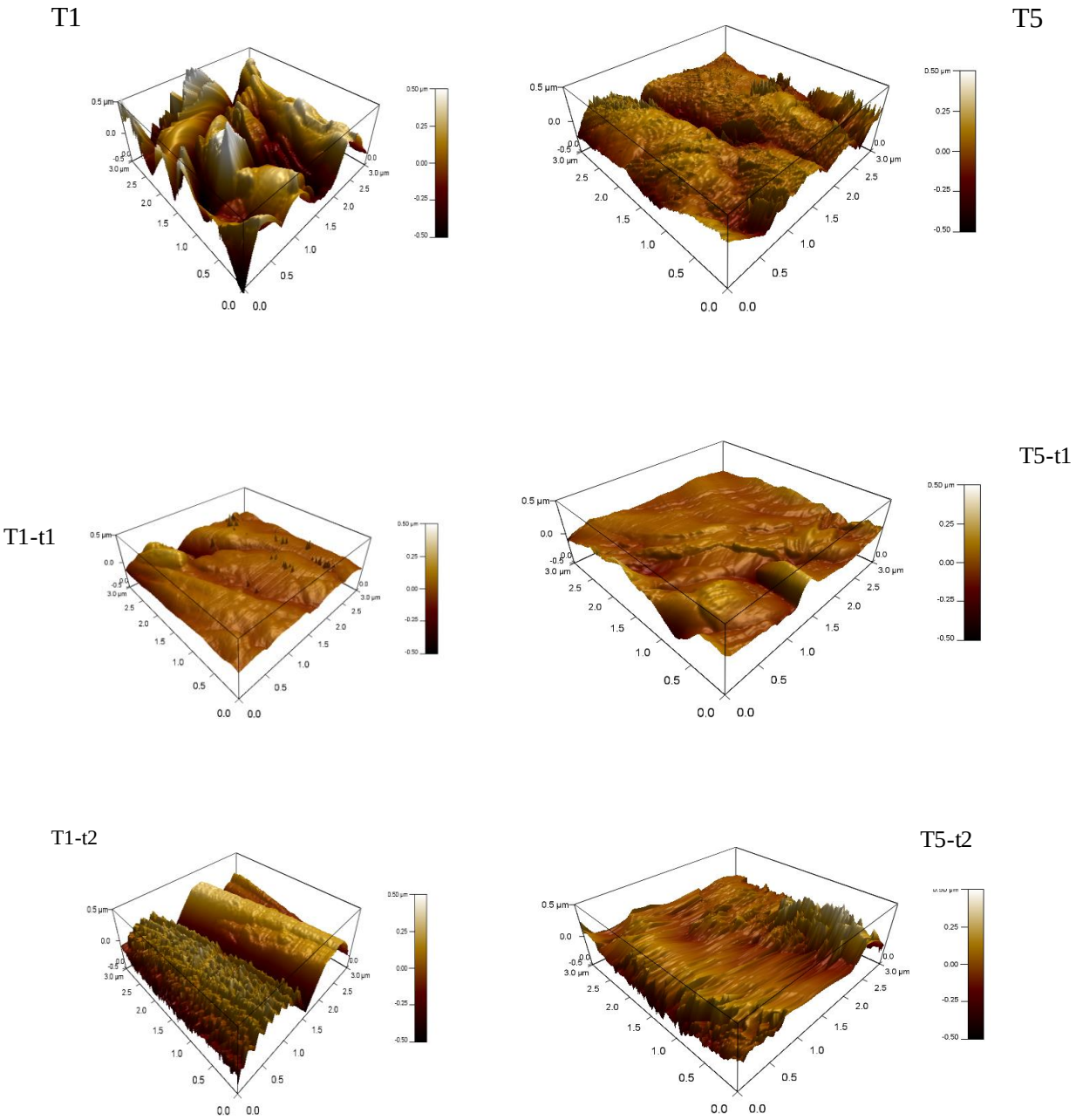

Figure 60 AFM 3D images of Sample T1 & T5 before and after heat tratment

Table 10 Roughnes values of samples T1 and T5

Membrane Name	**Material**	**R_{ms} (nm)**
T1	PES	242.986
T1-t1	PES	56.051
T1-t2	PES	159.114

T5	PSF	94.086
T5-t1	PSF	49.601
T5-t2	PSF	62.940

Previously many studies have reported that surface roughness is inversely proportional to water flux across the membranes .Eric .M et al [128] has reported similar trend in his study. This trend is observed in samples T1-t1 and T5-t1 of which values are reported in table.no 10 in these sample membranes with smooth surface morphology as seen by AFM images show in figure 60 significantly higher flux and vice versa .

5.3.6 SEM

SEM as represented in Figure 61 added morphology of the nanofibers with and without heat treatment s. It is clear from the figure that as the temperature of heat treatment increase more and more fibers start to fuse with each other . Furthermore from the SEM images (see figure 61 ,62) of sample T1 and T5 clearly illustrate the decrease in dimension difference in the pores size. This reduction in pore size is the reason for membranes are performing very well in FO bench scale experiments.

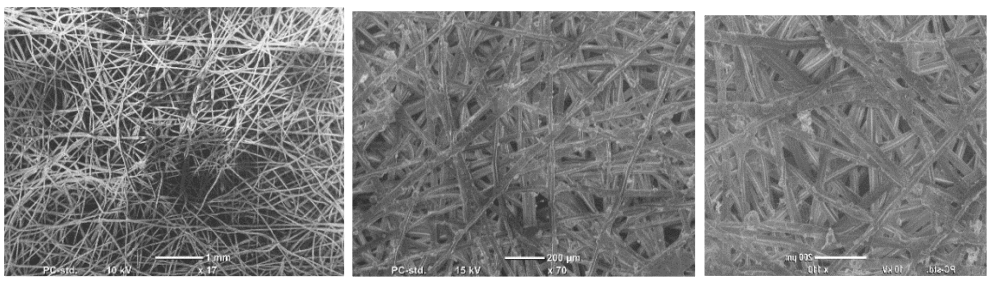

Figure 61 sample T1 ,T1-t1 ,T1-t2 surface micrographs

Hot pressing of nanofibers made from electrospinning were studied by hoyan wu et al. and yuan li et al. [129, 130] they also got decrease in pores size similar to our nanofibers. It is also noted as the temperature goes to T2 range of 175 ^{0}C the fiber size

start expanding as fibers start to flatten out . Further decreasing the pores as seen in figure 61 for sample T5-t2. It can also be seen from the images that the fiber start to infuse with each other this adds to the strength gains we observe in our tensile testing . Figure 62 shows sample porse covered by viscous thin film ,adding of this film reduces the contact angel thus increases the hydrophilicity of nano fibers .this PA layer always has a wave agglomeration kind of formation on its surface as seen in figure 63 [131].

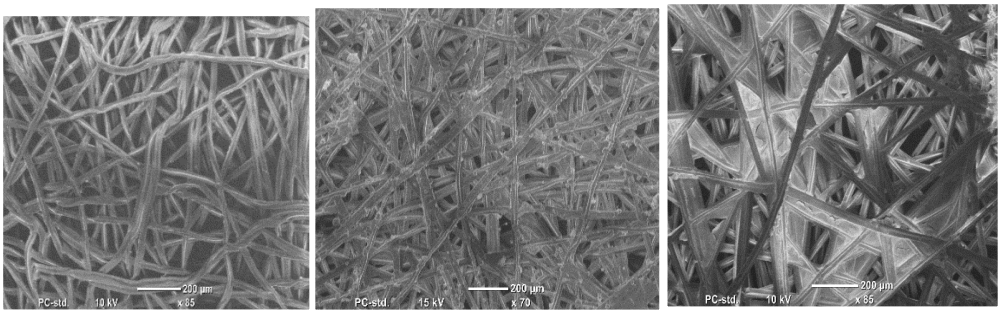

Figure 62 sample T5 ,T5-t1 ,T5-t2 surface micrographs

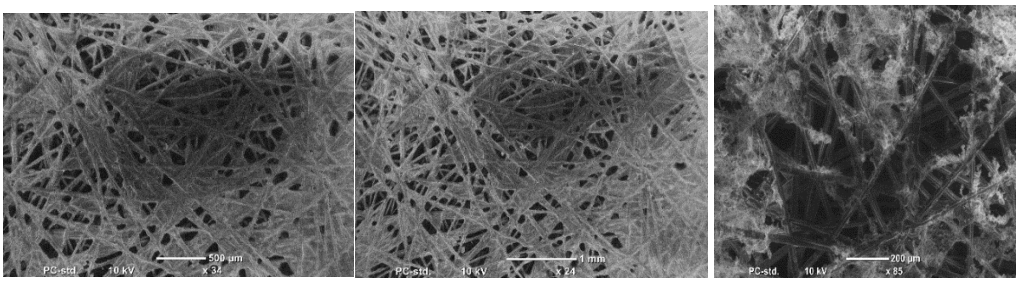

Figure 63 sample T5 -t1 -PA surface micrographs

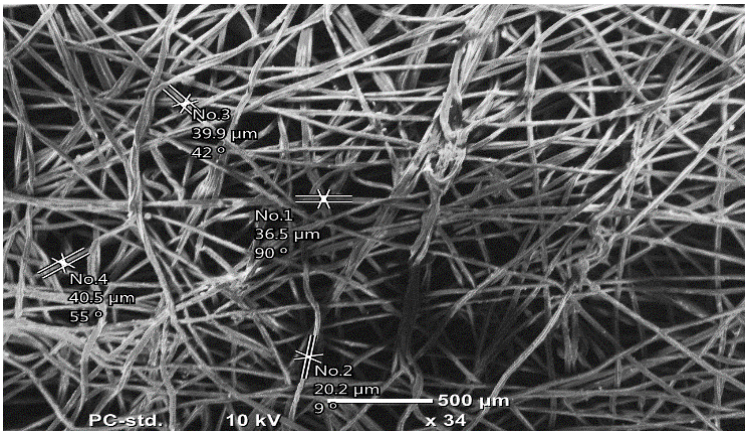

Figure 64SEM image showing fiber diameter of sample T1

5.3.6.1 SEM/TEM imaging of PS and PS individual nanofibers

Morphology of the nanofibers were investigated using the SEM The porous nature of the fibers are clearly observed(see figure64) . The pores formation on the surface of all fibers is mainly due to the non-solvent induced phase separation mechanism [119]. During the synthesis process, the PS undergoes phase separation as the non-solvent penetrates to the polymer structure. As this happens, electrospinning evaporates the solvent and decreases the surface temperature. During the solidification process, the composition reverts to its phase separation form, thus the porous structure is created.

5.3.7 Hydrophilicity and Hydrophobicity of Solution blown nano fiber membranes

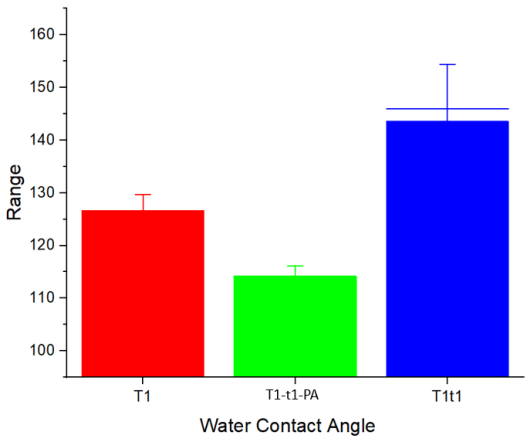

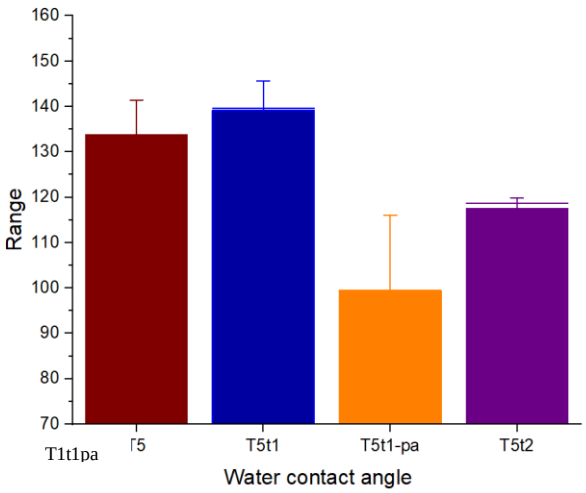

Figure 65 water conact angel of samples T1 and T5

The surface hydrophilicity/hydrophobicity is an important property for water purification membranes, as the selectivity of water absorption is a crucial property in the separating process. The solution blown nanofibers are tested for their water contact angle. The values are represented in Figure 65, in which the hydrophobicity increase can be clearly observed on the heat treated membranes . As the nano fiber membranes are heat treated, the contact angle value increased from 128.5º (base T1) to a maximum of 150.1º with heat treatment . This can be attributed to the encapsulation of pores with in polymeric base medium of nanofibers ,similar pattern is observed in sample T5 heat treatment increases the contact angel slightly from 135 º to 147 º, on further increase in temperature it drops to 120 º ,this drop is attributed to instability caused in the membrane from higher temperature of 175 º C in heat treatment process as this is close to the tg temperature of the polymer .The same is also observed from fig and fig which shows the all fabricated nanofiber membranes at t2 (T1-t2 and T5-t2) which means some part of the polymer start to melt forming a smooth layer possible large pores resulting in higher flux and RSF values. in addition to the increase in surface roughness on the nanoscale level, which is correlated with increase in surface area

provided by the nanomaterial inclusion [132-134]. The samples denoted with PA (polyamide layer) have lower contact angel values which shows these samples have become more hydrophilic which explains there better performance in over all flux and RSF values when compared to base samples. The sample T1 nanofiber are fabricated with PES which generally is more hydrophilic to sample T5 which is fabricated using polysulfone due to this reason the T1 modified with a thin PA layer and GO nano particles perform very well [135, 136].

5.3.8 Energy consumption of FO process

There is a significant difference in using commercial membranes and heat treated and modified nano fibers, the later consumes less energy .This due to high water flux and low RSF values when compared to exact same membrane testing conditions as commercial membranes. Further increasing the Flow rate on feed side while decreasing the draw side flow increases the water flux per watt of energy used significantly.

5.3.9 Post Experimental analysis

FTIR was used to determine the presence of GO nano particles post experiment to confirm the presence of the GO .FTIR analysis was carried out to determine the presence of GO from the hydroxyl functional group. Figure 66 presents the FTIR spectra for synthesized TFC nanofibers containing GO. As clearly observed from broad peak of blue spectrum line of hydroxyl group (O-H) around 3200-3600 spectral range infers the presence of GO functional group as reported in the literature. The presence of oxygen-containing functional group reveals GO. [137, 138]

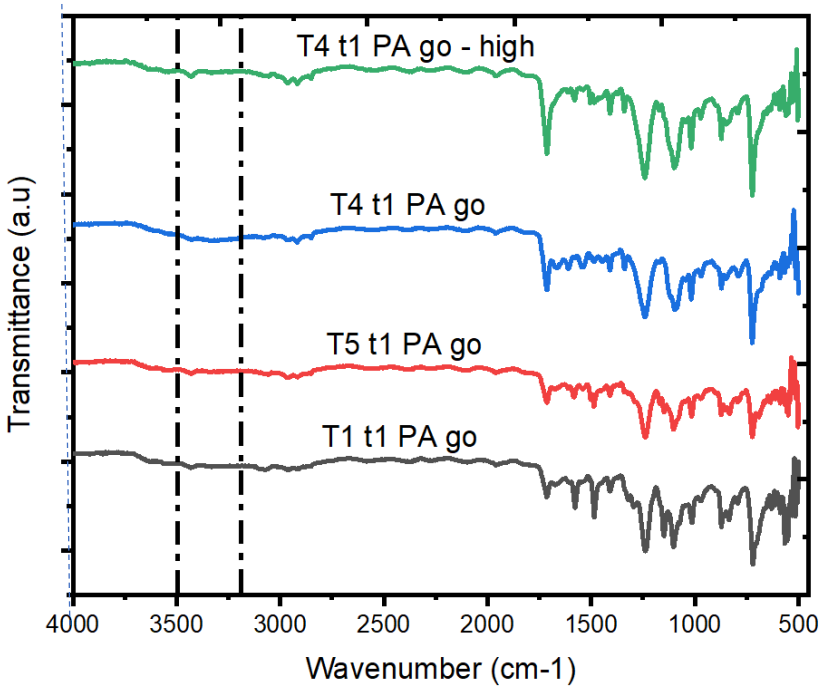

Figure 66 FTIR of TFC Nano fibers post experiment

The GO nano particles are added to the MPD aqueous solution as stated in section 4.3 and other details of MPD and go are provided in section 5.1.4.

When nano material is added before the IP step, it is permanently incorporated during the polymerization reaction which renders dislodging or wash away of the added GO nano particle during experimentation. Furthermore, our TFC nano fiber samples are performing consistently with no visible decline in water flux over multiple experiment also shows that TFC nano fiber has no affect during experimental procedure. These results are discussed extensively in section 5.2.1-5.2.4. where continuously 18 experiments were carried out with back washing between each of the experiment and no visible decline of membrane performance with respect. This proves PA layer formed On the TFC nano fiber is not deteriorating, Furthermore, the results discussed in detail in section 5.2.6 is for TFC nano fiber with GO nano particle incorporated in PA layer where the membrane was tested without backwashing between the experiments and similar trend is observed with no visible decline in any performance parameters of the membranes.

CHAPTER 6 CONCLUSION

In the current study, advanced nanofiber membranes fabricated using SBS technique were investigated and modified for improving its FO performance. The water flux was increased by two-fold while keeping the RSF values to less than 0.2 g/m^2h. The wettability and mechanical properties of these samples showed an improvement, which were confirmed by the experimental test runs as well as characterizations.

The major research findings from this study can be summarized as follows:

- Solution blow spinning technique can be successfully used in place of electro spinning due to its immense benefits such as better process control, easy operations, significantly lesser time ($1/5^{th}$ time as required for electro spinning), and better nanofiber distribution.
- The heat treatment on the nanofiber membrane showed FO performance along with an improved mechanical property.
- Also, applying polyamide layer with graphene oxide on hot-pressed sample by means of interfacial polymerization significantly improved its water flux properties.
- The tensile strength and Young's modulus of the prepared polymer nanocomposite is up to 2.4 times higher as compared to neat PES nanofibers, and 4.5 times higher as compared to pure PSF nanofibers.
- The addition of small amount of GO (0.006%) in the active layer has also increased the membrane FO performance significantly.
- The continuous FO testing carried out on the sample (T1-t1-PA), after intermittent backwashing, showed no drop in its performance in each of the twenty experiments.
- The sample T1-t1-PA-GO was continuously ran for four runs, and the flux

values repeatedly showed the same trend.

- The TFC nano fiber with PA and PA-GO layer have high salt rejection Values
- For T1-t1-PA sample, almost 45 L of feed solution was transferred to the draw side with minimal RSF values in 8.3 hours. Moreover, for T1-t1-PA-GO sample, 26 L of water was of feed solution was transferred to the draw side in just 3 hours with minimal RSF values. However, the commercial membranes transferred only 2 L of feed solution to draw solution in three hours. This clearly shows that the fabricated nanofiber membranes are superior to the commercial CTA and available TFC membranes.

REFERENCES

1. Elimelech, M. and W.A. Phillip, *The future of seawater desalination: energy, technology, and the environment.* Science, 2011. **333**(6043): p. 712-7.
2. Mekonnen, M.M. and A.Y. Hoekstra, *Four billion people facing severe water scarcity.* Science Advances, 2016. **2**(2): p. e1500323.
3. A. Shirazi, M.M. and A. Kargari, *A Review on Applications of Membrane Distillation (MD) Process for Wastewater Treatment.* Journal of Membrane Science and Research, 2015. **1**(3): p. 101-112.
4. Jones, E., et al., *The state of desalination and brine production: A global outlook.* Sci Total Environ, 2019. **657**: p. 1343-1356.
5. Shannon, M.A., et al., *Science and technology for water purification in the coming decades*, in *Nanoscience and technology: a collection of reviews from nature Journals*. 2010, World Scientific. p. 337-346.
6. Jamaly, S., et al., *A short review on reverse osmosis pretreatment technologies.* Desalination, 2014. **354**: p. 30-38.
7. Pearce, G.K., *UF/MF pre-treatment to RO in seawater and wastewater reuse applications: a comparison of energy costs.* Desalination, 2008. **222**(1): p. 66-73.
8. Van Voorthuizen, E.M., A. Zwijnenburg, and M. Wessling, *Nutrient removal by NF and RO membranes in a decentralized sanitation system.* Water Research, 2005. **39**(15): p. 3657-3667.
9. Zhao, S., et al., *Recent developments in forward osmosis: Opportunities and challenges.* Journal of Membrane Science, 2012. **396**: p. 1-21.
10. Al Hashemi, R., et al., *A Review of Desalination Trends in the Gulf Cooperation Council Countries.* International Interdisciplinary Journal of Scientific

Research, 2014. **1**(2): p. 72-96.

11. Al-mutaz, I., *Water desalination in the Arabian Gulf region.* 2017(January 2000).
12. Faizuddin, M., *water Desalination in Oman using Remote Sensing Technology Written for presentation at the 2017 ASABE Annual International Meeting Sponsored by ASABE.* 2017: p. 1-6.
13. Dawoud, M.A. and M.M. Al Mulla, *Environmental Impacts of Seawater Desalination: Arabian Gulf Case Study.* International Journal of Environment and Sustainability, 2012. **1**(3): p. 22-37.
14. Arab Emirates Abulllah Mohamed Al-Mutawa, U., et al., *Desalination in the GCC_History, present & Future_2014.* Report Prepared by Desalination Experts Group, Originating from the Water Resources Committee, 2014.
15. Abdul-Kareem Al-Sofi, M., *Seawater desalination - SWCC experience and vision.* Desalination, 2001. **135**(1-3): p. 121-139.
16. Baawain, M., et al., *Recent progress in desalination, environmental and marine outfall systems.* Recent Progress in Desalination, Environmental and Marine Outfall Systems, 2015: p. 1-347.
17. Elimelech, M. and W.A. Phillip, *The Future of Seawater Desalination: Energy, Technology, and the Environment.* 2011. **333**(August): p. 712-717.
18. Nair, M. and D. Kumar, *Water desalination and challenges: The Middle East perspective: A review.* Desalination and Water Treatment, 2013. **51**(10-12): p. 2030-2040.
19. Khawaji, A.D., I.K. Kutubkhanah, and J.M. Wie, *Advances in seawater desalination technologies.* Desalination, 2008. **221**(1-3): p. 47-69.
20. Villacorte, L.O., et al., *Seawater reverse osmosis desalination and (harmful)*

algal blooms. Desalination, 2015. **360**(March): p. 61-80.

21. Ahmed, M., et al., *Brine disposal from reverse osmosis desalination plants in Oman and the United Arab Emirates*. Desalination, 2001. **133**(2): p. 135-147.
22. International Water, S., *Energy Efficient Desalination.* 2018(January): p. 15.
23. Darwish, M., *Qatar water problem and solar desalination.* Desalination and Water Treatment, 2014. **52**(7-9): p. 1250-1262.
24. Darwish, M.A., H.K. Abdulrahim, and Y. Mohieldeen, *Qatar and GCC water security*. Desalination and Water Treatment, 2015. **55**(9): p. 2302-2325.
25. Gsdp, *Qatar National Vision 2030: Advancing Sustainable Development. Qatar's Second Human Development Report*. 2009.
26. Compain, P., *Solar energy for water desalination.* Procedia Engineering, 2012. **46**(0): p. 220-227.
27. Grubert, E.A., A.S. Stillwell, and M.E. Webber, *Where does solar-aided seawater desalination make sense? A method for identifying sustainable sites.* Desalination, 2014. **339**(1): p. 10-17.
28. Hamed, O.A., *Overview of hybrid desalination systems - Current status and future prospects.* Desalination, 2005. **186**(1-3): p. 207-214.
29. Amy, G., et al., *Membrane-based seawater desalination: Present and future prospects.* Desalination, 2017. **401**(January): p. 16-21.
30. Ghaffour, N., T.M. Missimer, and G.L. Amy, *Technical review and evaluation of the economics of water desalination: Current and future challenges for better water supply sustainability.* Desalination, 2013. **309**: p. 197-207.
31. Thomson, M. and D. Infield, *A photovoltaic-powered seawater reverse-osmosis without batteries.* 2002. **153**.
32. Al-Hajouri, A.A., A.S. Al-Amoudi, and A.M. Farooque, *Long term experience*

in the operation of nanofiltration pretreatment unit for seawater desalination at SWCC SWRO plant. Desalination and Water Treatment, 2013. **51**(7-9): p. 1861-1873.

33. Hilal, N., et al., *Nanofiltration of highly concentrated salt solutions up to seawater salinity*. Desalination, 2005. **184**(1-3): p. 315-326.

34. Zhang, S., et al., *Sustainable water recovery from oily wastewater via forward osmosis-membrane distillation (FO-MD)*. water research, 2014. **52**: p. 112-121.

35. Liu, Z., et al., *A low-energy forward osmosis process to produce drinking water.* Energy & Environmental Science, 2011. **4**(7): p. 2582-2585.

36. Achilli, A., et al., *The forward osmosis membrane bioreactor: a low fouling alternative to MBR processes*. Desalination, 2009. **239**(1-3): p. 10-21.

37. Flanagan, M.F. and I.C. Escobar, *Novel charged and hydrophilized polybenzimidazole (PBI) membranes for forward osmosis*. Journal of membrane science, 2013. **434**: p. 85-92.

38. Du, H., A. Thompson, and X. Wang, *Osmotically Driven Membrane Processes: Approach, Development and Current Status*. 2018: BoD–Books on Demand.

39. Haupt, A. and A. Lerch, *Forward osmosis application in manufacturing industries: A short review.* Membranes, 2018. **8**(3): p. 47.

40. McGovern, R.K. and J.H. Lienhard V, *On the potential of forward osmosis to energetically outperform reverse osmosis desalination.* Journal of Membrane Science, 2014. **469**: p. 245-250.

41. Chung, T.-S., et al., *Forward osmosis processes: Yesterday, today and tomorrow.* Desalination, 2012. **287**: p. 78-81.

42. Wang, K.Y., T.-S. Chung, and G. Amy, *Developing thin-film-composite forward osmosis membranes on the PES/SPSf substrate through interfacial*

polymerization. AIChE Journal, 2012. **58**(3): p. 770-781.

43. Shaffer, D.L., et al., *Forward osmosis: Where are we now?* Desalination, 2015. **356**: p. 271-284.

44. Mohanty, K. and M.K. Purkait, *Membrane technologies and applications*. 2011: CRC press.

45. Loeb, S. and S. Sourirajan, *Sea water demineralization by means of an osmotic membrane*. 1962, ACS Publications.

46. Taylor, J. and M. Wiesner, *Membranes Editor: Letterman RD. Water Quality and Treatment, 11.1-11.71*. 1999, New York, USA, McGraw Hill.

47. Montgomery, M.A. and M. Elimelech, *Water and sanitation in developing countries: including health in the equation.* Environmental science & technology, 2007. **41**(1): p. 17-24.

48. Subramani, A., et al., *Energy minimization strategies and renewable energy utilization for desalination: a review.* Water research, 2011. **45**(5): p. 1907-1920.

49. Qasim, M., et al., *Water desalination by forward (direct) osmosis phenomenon: A comprehensive review.* Desalination, 2015. **374**: p. 47-69.

50. Long, Q., et al., *Recent advance on draw solutes development in forward osmosis.* Processes, 2018. **6**(9): p. 165.

51. Li, Z., et al., *Graphene Oxide Incorporated Forward Osmosis Membranes With Enhanced Desalination Performance and Chlorine Resistance.* Front Chem, 2019. **7**: p. 877.

52. Ganesh, B.M., A.M. Isloor, and A.F. Ismail, *Enhanced hydrophilicity and salt rejection study of graphene oxide-polysulfone mixed matrix membrane.* Desalination, 2013. **313**: p. 199-207.

53. Li, P., et al., *Synergistic effect of polyvinyl alcohol sub-layer and graphene oxide condiment from active layer on desalination behavior of forward osmosis membrane.* Journal of the Taiwan Institute of Chemical Engineers, 2020. **112**: p. 366-376.

54. Amini, M., A. Rahimpour, and M. Jahanshahi, *Forward osmosis application of modified TiO2-polyamide thin film nanocomposite membranes.* Desalination and Water Treatment, 2015. **57**(30): p. 14013-14023.

55. Ahmed, F.E., B.S. Lalia, and R. Hashaikeh, *A review on electrospinning for membrane fabrication: Challenges and applications.* Desalination, 2015. **356**: p. 15-30.

56. Khorshidi, S., et al., *A review of key challenges of electrospun scaffolds for tissue-engineering applications.* Journal of Tissue Engineering and Regenerative Medicine, 2016. **10**(9): p. 715-738.

57. Strathmann, H. and K. Kock, *The formation mechanism of phase inversion membranes.* Desalination, 1977. **21**(3): p. 241-255.

58. Alayande, A.B., et al., *High-flux ultrafiltration membrane with open porous hydrophilic structure using dual pore formers.* Chemosphere, 2019. **227**: p. 662-669.

59. Hassan, M.A., et al., *Fabrication of nanofiber meltblown membranes and their filtration properties.* Journal of Membrane Science, 2013. **427**: p. 336-344.

60. Saleem, H., et al., *Recent advances in nanofibrous membranes: Production and applications in water treatment and desalination.* Desalination, 2020. **478**: p. 114178.

61. Liu, R.Q., et al., *Preparation of Nanofibrous PVDF Membrane by Solution Blow Spinning for Mechanical Energy Harvesting.* Nanomaterials (Basel),

2019. **9**(8).

62. Medeiros, E.S., et al., *Solution blow spinning: A new method to produce micro- and nanofibers from polymer solutions.* Journal of Applied Polymer Science, 2009. **113**(4): p. 2322-2330.

63. Daristotle, J.L., et al., *A Review of the Fundamental Principles and Applications of Solution Blow Spinning.* ACS Applied Materials & Interfaces, 2016. **8**(51): p. 34951-34963.

64. Vasireddi, R., et al., *Solution blow spinning of polymer/nanocomposite micro-/nanofibers with tunable diameters and morphologies using a gas dynamic virtual nozzle.* Scientific Reports, 2019. **9**(1): p. 14297.

65. You, Y., et al., *Thermal interfiber bonding of electrospun poly(l-lactic acid) nanofibers.* Materials Letters, 2006. **60**(11): p. 1331-1333.

66. Na, H., et al., *Effect of hot-press on electrospun poly(vinylidene fluoride) membranes.* Polymer Engineering & Science, 2008. **48**(5): p. 934-940.

67. Zhang, J., et al., *Impact of heat treatment on size, structure, and bioactivity of elemental selenium nanoparticles.* Int J Nanomedicine, 2012. **7**: p. 815-25.

68. Zou, S., M. Qin, and Z. He, *Tackle reverse solute flux in forward osmosis towards sustainable water recovery: reduction and perspectives.* Water research, 2019. **149**: p. 362-374.

69. Klaysom, C. and S. Shahid, *Zeolite-based mixed matrix membranes for hazardous gas removal*, in *Advanced Nanomaterials for Membrane Synthesis and its Applications*. 2019, Elsevier. p. 127-157.

70. Zornoza, B., et al., *Metal organic framework based mixed matrix membranes: An increasingly important field of research with a large application potential.* Microporous and Mesoporous Materials, 2013. **166**: p. 67-78.

71. Qadir, D., H. Mukhtar, and L.K. Keong, *Mixed matrix membranes for water purification applications.* Separation & Purification Reviews, 2017. **46**(1): p. 62-80.

72. Galizia, M., et al., *50th anniversary perspective: polymers and mixed matrix membranes for gas and vapor separation: a review and prospective opportunities.* Macromolecules, 2017. **50**(20): p. 7809-7843.

73. Saleem, H. and S.J. Zaidi, *Sustainable Use of Nanomaterials in Textiles and Their Environmental Impact.* Materials, 2020. **13**(22): p. 5134.

74. Park, M.J., et al., *Graphene oxide incorporated polysulfone substrate for the fabrication of flat-sheet thin-film composite forward osmosis membranes.* Journal of Membrane Science, 2015. **493**: p. 496-507.

75. Tian, M., Y.-N. Wang, and R. Wang, *Synthesis and characterization of novel high-performance thin film nanocomposite (TFN) FO membranes with nanofibrous substrate reinforced by functionalized carbon nanotubes.* Desalination, 2015. **370**: p. 79-86.

76. Mills, A. and S. Le Hunte, *An overview of semiconductor photocatalysis.* Journal of photochemistry and photobiology A: Chemistry, 1997. **108**(1): p. 1-35.

77. Emadzadeh, D., et al., *A novel thin film composite forward osmosis membrane prepared from PSf–TiO2 nanocomposite substrate for water desalination.* Chemical Engineering Journal, 2014. **237**: p. 70-80.

78. Sirinupong, T., et al., *Synthesis and characterization of thin film composite membranes made of PSF-TiO2/GO nanocomposite substrate for forward osmosis applications.* Arabian Journal of Chemistry, 2018. **11**(7): p. 1144-1153.

79. Shen, L., S. Xiong, and Y. Wang, *Graphene oxide incorporated thin-film*

composite membranes for forward osmosis applications. Chemical Engineering Science, 2016. **143**: p. 194-205.

80. Shokrgozar Eslah, S., et al., *Forward osmosis water desalination: Fabrication of graphene oxide-polyamide/polysulfone thin-film nanocomposite membrane with high water flux and low reverse salt diffusion.* Separation Science and Technology, 2018. **53**(3): p. 573-583.
81. Lim, S., et al., *Dual-layered nanocomposite substrate membrane based on polysulfone/graphene oxide for mitigating internal concentration polarization in forward osmosis.* Polymer, 2017. **110**: p. 36-48.
82. Lim, S., et al., *Defect-free outer-selective hollow fiber thin-film composite membranes for forward osmosis applications.* Journal of Membrane Science, 2019. **586**: p. 281-291.
83. Lim, S., et al., *Size-controlled graphene oxide for highly permeable and fouling-resistant outer-selective hollow fiber thin-film composite membranes for forward osmosis.* Journal of Membrane Science, 2020. **609**: p. 118171.
84. Akther, N., et al., *Recent advancements in forward osmosis desalination: A review.* Chemical Engineering Journal, 2015. **281**: p. 502-522.
85. Ge, Q., M. Ling, and T.-S. Chung, *Draw solutions for forward osmosis processes: Developments, challenges, and prospects for the future.* Journal of Membrane Science, 2013. **442**: p. 225-237.
86. Luo, H., et al., *A review on the recovery methods of draw solutes in forward osmosis.* Journal of Water Process Engineering, 2014. **4**: p. 212-223.
87. Valladares Linares, R., et al., *Forward osmosis niches in seawater desalination and wastewater reuse.* Water Research, 2014. **66**: p. 122-139.
88. She, Q., et al., *Membrane fouling in osmotically driven membrane processes: A*

review. Journal of Membrane Science, 2016. **499**: p. 201-233.

89. Altaee, A., A.A. Alanezi, and A.H. Hawari, *2 - Forward osmosis feasibility and potential future application for desalination*, in *Emerging Technologies for Sustainable Desalination Handbook*, V.G. Gude, Editor. 2018, Butterworth-Heinemann. p. 35-54.

90. Ben-Dov, E., et al., *Biofilm formation on RO membranes: the impact of seawater pretreatment*. Desalination and Water Treatment, 2015. **57**(11): p. 4741-4748.

91. http://en.wikipedia.org/wiki/Polysulfone.

92. Jian, S., et al., *Nanofibers with diameter below one nanometer from electrospinning*. RSC Advances, 2018. **8**(9): p. 4794-4802.

93. Stillman, D., L. Krupp, and Y.-H. La, *Mesh-reinforced thin film composite membranes for forward osmosis applications: The structure–performance relationship*. Journal of Membrane Science, 2014. **468**: p. 308-316.

94. Chen, H., et al., *Functionalized electrospun nanofiber membranes for water treatment: A review*. Science of The Total Environment, 2020. **739**: p. 139944.

95. Shokrollahzadeh, S. and S. Tajik, *Fabrication of thin film composite forward osmosis membrane using electrospun polysulfone/polyacrylonitrile blend nanofibers as porous substrate*. Desalination, 2018. **425**: p. 68-76.

96. Liu, Y., et al., *Solution Blown Nylon 6 Nanofibrous Membrane as Scaffold for Nanofiltration*. Polymers, 2019. **11**(2): p. 364.

97. Kaur, S., et al., *Hot pressing of electrospun membrane composite and its influence on separation performance on thin film composite nanofiltration membrane*. Desalination, 2011. **279**: p. 201-209.

98. Gopal, R., et al., *Electrospun nanofibrous filtration membrane*. Journal of

Membrane Science, 2006. **281**: p. 581-586.

99. Yao, M., et al., *Effect of heat-press conditions on electrospun membranes for desalination by direct contact membrane distillation.* Desalination, 2016. **378**: p. 80-91.

100. Duong, P.H.H., et al., *Highly Permeable Double-Skinned Forward Osmosis Membranes for Anti-Fouling in the Emulsified Oil–Water Separation Process.* Environmental Science & Technology, 2014. **48**(8): p. 4537-4545.

101. Ahmed, D.F., et al., *Graphene oxide incorporated cellulose triacetate/cellulose acetate nanocomposite membranes for forward osmosis desalination.* Arabian Journal of Chemistry, 2021. **14**(3): p. 102995.

102. Perreault, F., M.E. Tousley, and M. Elimelech, *Thin-Film Composite Polyamide Membranes Functionalized with Biocidal Graphene Oxide Nanosheets.* Environmental Science & Technology Letters, 2014. **1**(1): p. 71-76.

103. Choi, W., et al., *Layer-by-Layer Assembly of Graphene Oxide Nanosheets on Polyamide Membranes for Durable Reverse-Osmosis Applications.* ACS Applied Materials & Interfaces, 2013. **5**(23): p. 12510-12519.

104. Kim, S.G., et al., *Novel thin nanocomposite RO membranes for chlorine resistance.* Desalination and Water Treatment, 2013. **51**(31-33): p. 6338-6345.

105. Chae, H.-R., et al., *Graphene oxide-embedded thin-film composite reverse osmosis membrane with high flux, anti-biofouling, and chlorine resistance.* Journal of Membrane Science, 2015. **483**: p. 128-135.

106. Lee, S., *Exploring the Operation Factors that Influence Performance of a Spiral-Wound Forward Osmosis Membrane Process for Scale-up Design.* Membranes, 2020. **10**(3): p. 53.

107. Akther, N., S. Daer, and S. Hasan, *Effect of flow rate, draw solution*

concentration and temperature on the performance of TFC FO membrane, and the potential use of RO reject brine as a draw solution in FO-RO hybrid systems. Desalination and water treatment, 2018. **136**: p. 65-71.

108. Keir, G. and V. Jegatheesan, *A review of computational fluid dynamics applications in pressure-driven membrane filtration.* Reviews in Environmental Science and Bio/Technology, 2014. **13**(2): p. 183-201.

109. Mohammadifakhr, M., et al., *Forward Osmosis: A Critical Review.* 2020. **8**(4): p. 404.

110. Ma, D., et al., *Thin-Film Nanocomposite (TFN) Membranes Incorporated with Super-Hydrophilic Metal–Organic Framework (MOF) UiO-66: Toward Enhancement of Water Flux and Salt Rejection.* ACS Applied Materials & Interfaces, 2017. **9**(8): p. 7523-7534.

111. Wang, Y., et al., *Preparation of polyethersulfone/carbon nanotube substrate for high-performance forward osmosis membrane.* Desalination, 2013. **330**: p. 70-78.

112. Chen, X., et al., *Enhanced performance of cellulose triacetate membranes using binary mixed additives for forward osmosis desalination.* Desalination, 2017. **405**: p. 68-75.

113. Mouhat, F., F.-X. Coudert, and M.-L. Bocquet, *Structure and chemistry of graphene oxide in liquid water from first principles.* Nature Communications, 2020. **11**(1): p. 1566.

114. Ponnamma, D., et al., *Free-volume correlation with mechanical and dielectric properties of natural rubber/multi walled carbon nanotubes composites.* Composites Part A: Applied Science and Manufacturing, 2015. **77**: p. 164-171.

115. Devi, K.U., et al., *Enhanced morphology and mechanical characteristics of*

clay/styrene butadiene rubber nanocomposites. Applied clay science, 2015. **114**: p. 568-576.

116. Abdelrazeq, H., et al., *Recycled Polyethylene/Paraffin Wax/Expanded Graphite Based Heat Absorbers for Thermal Energy Storage: An Artificial Aging Study.* Molecules, 2019. **24**.

117. Ponnamma, D., et al., *Developing Polyaniline Filled Isoprene Composite Fibers by Electrospinning: Effect of Filler Concentration on the Morphology and Glass Transition.* Polymer Science, Series A, 2019. **61**: p. 194-202.

118. Lee, I., et al., *Interfacial toughening of solution processed Ag nanoparticle thin films by organic residuals.* Nanotechnology, 2012. **23**(48): p. 485704.

119. Wu, J., et al., *Electrospun porous structure fibrous film with high oil adsorption capacity.* ACS applied materials & interfaces, 2012. **4**(6): p. 3207-3212.

120. Mahdavi, H., et al., *Synthesis and performance study of amino functionalized graphene aerogel grafted with polyaniline nanofibers as an efficient supercapacitor material*. Journal of Materials Science: Materials in Electronics, 2017. **28**.

121. Idris, S.N.A., et al., *Graphene Oxide Incorporated Polysulfone Substrate for Flat Sheet Thin Film Nanocomposite Pressure Retarded Osmosis Membrane.* Membranes (Basel), 2020. **10**(12).

122. Lin, C.F., et al., *Enhancing the Efficiency of a Forward Osmosis Membrane with a Polydopamine/Graphene Oxide Layer Prepared Via the Modified Molecular Layer-by-Layer Method.* ACS Omega, 2020. **5**(30): p. 18738-18745.

123. Fathizadeh, M., A. Aroujalian, and A. Raisi, *Preparation and characterization of thin film composite reverses osmosis membranes with wet and dry support layer*. Desalination and water treatment, 2014. **2014**: p. 1-12.

124. Zhang, R., et al., *Effects of ultrasonication duration and graphene oxide and nano-zinc oxide contents on the properties of polyvinyl alcohol nanocomposites.* Ultrasonics Sonochemistry, 2019. **59**: p. 104731.

125. Bera, M., et al., *Facile One-Pot Synthesis of Graphene Oxide by Sonication Assisted Mechanochemical Approach and Its Surface Chemistry*. Journal of Nanoscience and Nanotechnology, 2018. **18**: p. 902-912.

126. Jacob, N., et al., *Sulfonated polyethersulfone-based membranes for metal ion removal via a hybrid process.* Journal of Materials Science, 2014. **49**.

127. Rastgar, M., A. Shakeri, and H. Salehi, *Study of polyamide thin film characteristics impact on permeability/selectivity performance and fouling behavior of forward osmosis membrane.* Environ Sci Pollut Res Int, 2019. **26**(2): p. 1181-1191.

128. erererervrijenhoek, E.M., S. Hong, and M. Elimelech, *Influence of membrane surface properties on initial rate of colloidal fouling of reverse osmosis and nanofiltration membranes.* Journal of Membrane Science, 2001. **188**(1): p. 115-128.

129. Liao, Y., et al., *Fabrication of polyvinylidene fluoride (PVDF) nanofiber membranes by electro-spinning for direct contact membrane distillation.* Journal of Membrane Science, 2013. **425-426**: p. 30-39.

130. Tijing, L.D., et al., *A novel dual-layer bicomponent electrospun nanofibrous membrane for desalination by direct contact membrane distillation.* Chemical Engineering Journal, 2014. **256**: p. 155-159.

131. Gao, Y., et al., *NGO/PA layer with disordered arrangement hybrid PPS composite membrane for desalination.* Desalination, 2019. **479**: p. 114211.

132. Tang, E. and S. Dong, *Preparation of styrene polymer/ZnO nanocomposite*

latex via miniemulsion polymerization and its antibacterial property. Colloid and Polymer Science, 2009. **287**(9): p. 1025-1032.

133. Montazer, M. and T. Harifi, *9 - Nanofinishes for self-cleaning textiles*, in *Nanofinishing of Textile Materials*, M. Montazer and T. Harifi, Editors. 2018, Woodhead Publishing. p. 127-143.

134. Wang, X., et al., *Engineering biomimetic superhydrophobic surfaces of electrospun nanomaterials*. Nano today, 2011. **6**(5): p. 510-530.

135. Chowdhury, M.R., L. Huang, and J.R. McCutcheon, *Thin Film Composite Membranes for Forward Osmosis Supported by Commercial Nanofiber Nonwovens*. Industrial & Engineering Chemistry Research, 2017. **56**(4): p. 1057-1063.

136. Singh, R., *Chapter 1 - Introduction to Membrane Technology*, in *Membrane Technology and Engineering for Water Purification (Second Edition)*, R. Singh, Editor. 2015, Butterworth-Heinemann: Oxford. p. 1-80.

137. Radzi Hanifah, M.F., et al., *Synthesis of Graphene Oxide Nanosheets via Modified Hummers' Method and Its Physicochemical Properties.* Jurnal Teknologi, 2015. **74 (1)**: p. 195-198.

138. Leaper, S., et al., *Flux-enhanced PVDF mixed matrix membranes incorporating APTS-functionalized graphene oxide for membrane distillation.* Journal of Membrane Science, 2018. **554**: p. 309-323.